An Exact Price-Cut-and-Enumerate Method for the Capacitated Multi-Trip Vehicle Routing Problem with Time Windows

Yu Yang
Department of Industrial and Systems Engineering, University of Florida, yu.yang@ise.ufl.edu

We consider the *capacitated multi-trip vehicle routing problem with time windows* (CMTVRPTW), where vehicles are allowed to make multiple trips. The ability to perform multiple trips is necessary for some real-world applications where the vehicle capacity, the trip duration, or the number of drivers or vehicles is limited. However, it substantially increases the solution difficulty in view of the additional trip scheduling aspect. We propose an *exact price-cut-and-enumerate method* (EPCEM) that solves a novel superstructure-based formulation inspired by Paradiso et al. (2020). The EPCEM obtains a tight lower bound by an alternating column and row generation method and computes a valid upper bound in the early stage of the algorithm. It obtains an optimal solution and further proves its optimality by a new multi-phase sift-and-cut method. Computationally, the EPCEM significantly outperforms the state-of-the-art exact method that only proves optimality for 9 of the 27 test instances with 50 customers. In particular, the EPCEM solves all test instances with up to 70 customers to optimality for the first time and obtains near-optimal solutions with an average optimality gap no more than 0.3% for instances with 80 to 100 customers. From a practical point of view, solving the CMTVRPTW by the EPCEM yields a solution that on average uses at least 45% fewer vehicles and increases the travel cost by no more than 7% compared with the solution to the standard CVRPTW.

Keywords: multi-trip vehicle routing · price-cut-and-enumerate · column-and-row generation

1. Introduction

Introduced in Dantzig and Ramser (1959), the *vehicle routing problem* (VRP) has been extensively researched for more than six decades due to its wide applications in practice and its notorious difficulty. Variants arising from different application scenarios have been proposed and studied, of which the *capacitated vehicle routing problem with time windows* (CVRPTW) attracts special attention since time is usually an indispensable element in real-world decision making. Toth and Vigo (2014), Golden et al. (2008), and Braekers et al. (2016) offer thorough reviews on the VRP and its variants. The readers are referred to Vidal et al. (2020) for a concise review. A vast majority of the research papers restrict each vehicle to perform no more than one trip, for which part of the reason is that the problem would have been more intractable without this constraint.

Recently, there has been a notable increase in publications addressing VRPs that allow multiple trips. To the best of our knowledge, Salhi (1987) was the first to solve a multi-trip VRP, which was

later formalized by Fleischmann (1990). Ever since then, various formulations and algorithms have been proposed. Interested readers are referred to Cattaruzza et al. (2016b) for a complete survey on this topic. In this paper, we consider the *capacitated multi-trip vehicle routing problem with time windows* (CMTVRPTW), which extends the well-known CVRPTW by allowing each vehicle to make more than one trip. The objective is to route a limited and homogeneous fleet of vehicles at the minimum travel cost. Meanwhile, every customer has to be served exactly once within their time window. The CMTVRPTW is of both practical and scientific interest for the following reasons.

1.1. Motivation

Practically, one of the main drives for the increased interest in allowing multiple trips results from the ever-increasing demand for package deliveries. Nowadays, urban centers usually impose a strict limit on heavy-duty trucks that causes severe air pollution, noise, and congestion (Janic 2007, Lyons et al. 2017). Because of their higher mobility and lower emission than trucks, small vans are routinely used for delivering packages in cities. Meanwhile, last-mile deliveries by electric vehicles (Amazon 2021, Pelletier et al. 2016) and autonomous robots (Figliozzi 2020) are around the corner. In addition, unmanned aerial vehicles or drones have shown promise in delivering essential goods, such as COVID-19 viral test, to potentially infected patients without direct human contact (Kunovjanek and Wankmüller 2021). However, those vehicles usually suffer from a relatively small capacity, rendering multiple trips necessary for a limited fleet size. For some applications, the trip duration has to be restricted due to regulations (Derigs et al. 2011, Benkebir et al. 2019) or the perishability of goods (Hernandez et al. 2014), which further necessitates multiple trips. Therefore, solving the CMTVRPTW exactly aids the decision-making in the aforementioned practical settings.

The trade-off between the flexibility in the vehicle or driver availability and the degradation in the solution quality in terms of the travel cost is also of great practical importance, especially when the labor costs or the fixed costs of vehicles are comparable with the operational costs. Although some attempts to quantify the trade-off when multiple trips are allowed have been made in Cattaruzza et al. (2014) and Dorling et al. (2016), the comparisons are performed between suboptimal solutions yielded by heuristics. Thus, it is unclear how much sacrifice in the optimal travel cost may occur as the number of vehicles available gradually decreases. This further motivates us to exactly solve larger CMTVRPTW instances to enable a systematic numerical analysis of this trade-off.

Allowing multiple trips on top of the CVRPTW increases the difficulty substantially, especially for exact methods that must prove optimality instead of merely obtaining suboptimal solutions. Besides the routing decisions, it introduces the additional scheduling aspect, i.e., deciding the set of trips and the temporally non-overlapping sequence of performing them for each vehicle, which escalates the combinatorial explosion. A straightforward two-stage heuristic may first solve the problem

as a CVRPTW with infinite fleet size. In the second stage, it tries to assign the obtained trips to the available vehicles by allowing multiple trips. Unfortunately, such a heuristic usually fails to obtain a feasible solution to the original problem, suggesting that the two sources of complexity cannot be easily decomposed. For the CVRPTW, the state-of-the-art branch-price-and-cut algorithms implemented in Pecin et al. (2017a) and Pessoa et al. (2020) can solve[1] all tested Solomon instances with 100 customers (Solomon 1987) and 51 and 56, respectively, of the 60 Gehring and Homberger instances with 200 customers (Homberger and Gehring 2005). By contrast, the best known exact method for solving the CMTVRPTW is the *exact solution framework* (ESF) from Paradiso et al. (2020), which can only prove optimality for 9 of the 27 type 2 Solomon instances with 50 customers. Such a wide gap in the capability of solving the CVRPTW and the CMTVRPTW exactly constitutes a major scientific motivation for this research.

Although the ESF achieves the best performance among all existing exact methods, it has several drawbacks that prevent it from solving larger instances. Firstly, it obtains a relatively weak initial lower bound (LB) by solving a relaxation without any cutting planes. The weakness of the LB can lead to an invalid upper bound (UB) because their initial UB is guessed by using the formula UB $= (1 + \text{gap}_{guess}) * \text{LB}$. Secondly, since the UB is guessed by using a fixed initial gap_{guess}, it may not be valid. If the guessed UB is invalid, i.e., smaller than the optimal value, the whole expensive optimization process has to be repeated with an adjusted UB. Such adjustment can happen several times, significantly hindering the efficiency. Lastly, not enough attention has been paid to dealing with the challenging integer program (IP) after all qualified columns[2] are enumerated. For some difficult instances, the IP can contain millions of integer variables and usually cannot be solved in a reasonable amount of time. This is one of the main reasons why the ESF fails to solve large instances. These drawbacks open up opportunities for enhancement and motivate us to introduce new ideas for solving the CMTVRPTW to optimality faster.

1.2. Contributions and Outline

This paper proposes an *exact price-cut-and-enumerate method* (EPCEM) for solving the CMTVRPTW and its four variants (see Section 2.1). It makes the following contributions.

- *From the modeling perspective, we introduce a novel superstructure-based formulation that is both theoretically and computationally effective.* The proposed superstructure concept helps to significantly reduce the number of superstructure feasibility cuts added in the solution process without sacrificing the strength of the root LP relaxation. The underlying idea is general and

[1] In this paper, a problem can be solved means it can be solved to optimality.

[2] Columns, variables, structures, and superstructures, if applicable, are used interchangeably in this paper due to their correspondence.

can be applied to the branch-and-price type of algorithms with lazy cuts for handling side constraints. For example, the concept of fragment introduced in Alyasiry et al. (2019) can be generalized to "superfragment" similarly to reduce both the number of variables in the formulation and the lazy cuts needed for solving the *pickup and delivery problem with time windows and last-in-first-out loading*.

- *From the algorithmic perspective, we propose to obtain tight bounds before enumerating all qualified columns and smartly manage the generated columns to achieve and prove optimality faster.* A tight LB is computed by an alternating column and row generation method. A valid UB is obtained by solving an IP with an enhanced separator for generating lazy cuts. In addition, a new auxiliary problem is derived to reduce columns. Finally, an optimal solution is computed, and its optimality is proved via a new multi-phase sift-and-cut (MPSC) method.
- *From the practical perspective, we explore the trade-off between the optimal travel cost and the number of vehicles needed.* The EPCEM enables us to perform a numerical analysis of this trade-off, which provides useful managerial guidance for industry practitioners. In particular, we found that a relatively small sacrifice (no more than 7%) in the travel cost can bring in significant savings (more than 45%) in the number of vehicles needed.
- *From the computational perspective, we conduct an extensive numerical study, demonstrating that our EPCEM considerably outperforms the state-of-the-art method, the ESF, consistently.* The EPCEM is the first exact method that solves all CMTVRPTW (type 2 Solomon) instances with up to 70 customers to optimality. Meanwhile, it obtains near-optimal solutions with an average optimality gap no more than 0.3% for instances with 80 to 100 customers. In addition, it is easily adapted to solve four CMTVRPTW variants and achieves exceptional performance. The compiled standalone C++ library for solving new instances of the CMTVRPTW and its four variants has been made publicly available at `https://github.com/Yu1423/CMTVRPTW`.
- *From the implementation perspective, our EPCEM eliminates the need to branch and maintain the branch-and-bound tree by users compared with the ESF.* A major implementation difficulty for branch-and-price algorithms is to make branching decisions when necessary and keep track of the branch-and-bound process by a tree. Thanks to the tight bounds obtained and the enumeration procedures in the EPCEM, such difficulty can be circumvented, facilitating the practical usage of the EPCEM. It is worth mentioning that the idea of route enumeration was first introduced in the seminal work Baldacci et al. (2008).

The rest of the paper is organized as follows. In Section 2, we review some recent progress about the CMTVRPTW. In Section 3, we formally define the CMTVRPTW and present the novel superstructure-based formulation. We describe formulations used to obtain lower and upper bounds in Section 4. Section 5 provides an overview of the EPCEM, where the major enhancements are

highlighted. The EPCEM is elaborated step by step in Section 6. In Section 7, we present the results of four sets of numerical experiments. Finally, concluding remarks are made, and some future directions are pointed out in Section 8. All the proofs, some implementation details, and detailed numerical results are included in the e-companion.

2. Literature Review

In this section, we review some academic extensions, applications, and recent advancements in exact solution methods of the CMTVRPTW and its variants. We consider problems that are most relevant to the scope of this paper. Thus, all the problems reviewed share the two defining features, i.e., multiple trips and time windows, with the CMTVRPTW.

2.1. Academic Extensions

The CMTVRPTW has been intensively researched in the past two decades. Many academic extensions motivated by practical applications have been proposed, and their features are summarized in Table 1 at the end of this section.

Hernandez et al. (2016) extend the CMTVRPTW to the CMTVRPTW *with loading times* (CMTVRPTW-LT) by including a service-dependent loading time at the depot. The loading time is computed as a percentage (usually 20%) of the total service time of all customers visited in the route. Motivated by a last-mile delivery problem where operations start from the city distribution center (CDC), Cattaruzza et al. (2016a) add release dates, i.e., times at which the goods requested by the customers become available at the depot, to the CMTVRPTW. It models the situation where goods may not necessarily be available at the CDC at the beginning of the planning horizon. The resulting problem is called the CMTVRPTW *with release dates* (CMTVRPTW-R).

When perishable goods are transported, there is usually a limit on the duration of each route. Hernandez et al. (2014) and François et al. (2019) study a limited duration version of the CMTVRPTW-LT, named the CMTVRPTW *with limited trip duration* (CMTVRPTW-LD), which requires the last customer to be served in a route within $t_{\max}$ time units of the route start time. Azi et al. (2010), Macedo et al. (2011), Azi et al. (2014), and Wang et al. (2014) consider the case when it may not be possible to serve all customers. Therefore, serving customers brings profits and the objective is to maximize the number of served customers within the time horizon of interest and, for the same number of served customers, to minimize the total distance. For convenience, we call this problem the CMTVRPTW *with profit* (CMTVRPTW-P). In view of the substantial variance in the travel times of peak and off-peak hours in the urban areas, Sun et al. (2019) and Pan et al. (2021) propose to modify the constant travel times of the CMTVRPTW-LD to be time-dependent and obtain

the *multi-trip time-dependent* VRPTW (MT-TDVRPTW). It is worth noting that the duration is computed as the difference between the arrival and departure times at the depot.

As an alternative to traditional vehicles for package delivery, drones have been studied heavily recently due to their potential to shorten the delivery time and reduce the emission and operating cost. Cheng et al. (2020) propose the *drone routing problem* (DRP), which extends the CMTVRPTW by including the battery constraint and the energy cost. More specifically, the drone relies on its battery which has a limited capacity, and each trip has to be completed before the battery dies. In addition, the battery consumption depends not only on the distance traveled but also on the load carried, which adds to the solution difficulty.

In this paper, we focus on solving the basic CMTVRPTW and four of the aforementioned variants: the CMTVRPTW-LT, the CMTVRPTW-R, the CMTVRPTW-LD, and the DRP faster. These problems are the basis for modeling and solving problems with similar features and problem-specific side constraints.

Table 1 The CMTVRPTW and some academic extensions.

Reference	Problem	Loading time	Limited trip duration	Profit	Release date	Battery constraint	Time-dependent travel time
Paradiso et al. (2020) This Paper	CMTVRPTW						
Hernandez et al. (2016)	CMTVRPTW-LT	✓					
Cattaruzza et al. (2016a)	CMTVRPTW-R				✓		
Hernandez et al. (2014) François et al. (2019)	CMTVRPTW-LD	✓	✓				
Sun et al. (2019) Pan et al. (2021)	MT-TDVRPTW	✓	✓				✓
Azi et al. (2010) Macedo et al. (2011) Azi et al. (2014) Wang et al. (2014)	CMTVRPTW-P	✓	✓	✓			
Cheng et al. (2020)	DRP					✓	

2.2. Applications

The CMTVRPTW and its variants have seen a wide spectrum of real-world applications. Derigs et al. (2011) solve a CMTVRPTW variant under the EU regulations for drivers arsing in the air cargo road feeder service business. The primary objective is to minimize the number of required vehicles. Their proposed heuristic methods are currently applied in practice. In a closely related work, Benkebir et al. (2019) consider the CMTVRPTW with European and French driver regulations. Their proposed method significantly improves the previous software developed by a company specialized in solving large-scale real-world CMTVRPTW. He and Li (2019) consider the CMTVRPTW variant arising in the harvesting and transportation system where grain, harvested by combine-harvesters, is then

transported by transporters from disperse farmlands to the depot. The proposed method can help agricultural production to implement optimal harvesting operations.

Tang et al. (2015) apply a pickup and delivery variant of the CMTVRPTW to model the pickup and delivery of customers to the airport service provided by some airline ticket sales agencies in China. Lim et al. (2017) model the non-emergency ambulance transfer service, i.e., transportation service for disabled or elderly patients between their residences and clinics, for Hong Kong public hospitals as a multi-trip pickup and delivery problem with time windows and manpower planning. Their proposed method is demonstrated to be effective for real-world instances.

Choi et al. (2019) propose to apply the maximum-flight-time-constrained CMTVRPTW model to small unmanned aircraft systems (sUAVs) based urban delivery. They explore the use case of a sUAVs delivery system in a model of downtown San Diego, which is created from airborne light detection and ranging (LiDAR) sensor data and predefined restricted airspace. Motivated by the fact that some companies in Singapore have already used mobile robots to transport materials in the factories and mobile robots have been heavily used in Amazon's warehouse, the CMTVRPTW is used by Liu et al. (2017) to model a single robot transporting materials/parts from a warehouse to feeders of production lines.

Although our research is not tied to a specific application, it generates results that can provide managerial guidance for related applications. More specifically, our research tries to deepen the understanding of the trade-off between the flexibility in the vehicle or driver availability and the degradation in the solution quality in terms of the travel cost, which is practically important when deciding the fleet size. The trade-off is analyzed by comparing the solution quality of the CMTVRPTW and the standard single-trip CVRPTW, which has never been done before for exact methods.

2.3. Exact Methods

Exact methods have attached interest from many researchers despite the fact that the CMTVRPTW and its variants are mostly solved by heuristics in practice. Azi et al. (2007) solve a single-vehicle variant of the CMTVRPTW-P via a two-stage method. In the first stage, all non-dominated feasible trips are generated, and the second stage seeks to select some of them to form a deliverable sequence. Their experiments on Solomon instances with up to 100 customers show that the number of feasible trips generated differs sharply across different instances, which results in completely different solution difficulties. Azi et al. (2010) use a set packing formulation of the CMTVRPTW-P, which is solved by a branch-and-price algorithm. Each column corresponds to an ordered sequence of trips that can be performed by a single vehicle. The numerical study demonstrates that Solomon instances with 25 customers can be routinely solved but some instances with 40 customers cannot

be solved in six hours. Macedo et al. (2011) propose a new pseudo-polynomial network flow model for the CMTVRPTW-P, where the variables represent feasible vehicle trips. An iteratively refining of discretization is applied until a feasible solution is produced. According to the numerical results, their algorithm can solve more instances with shorter computational times than that presented in Azi et al. (2010).

Hernandez et al. (2014) propose a two-stage algorithm for the CMTVRPTW-LD, which enumerates all qualified trips in the first stage and then applies a branch-and-price algorithm to solve a set covering formulation. Experiments on Solomon instances with 25 and 40 customers demonstrate that their method is on average better than that developed in Azi et al. (2010) and outperforms the method in Macedo et al. (2011) on some instances. Hernandez et al. (2016) remove the limit on the trip duration and consider the CMTVRPTW-LT. Two formulations, *scheduling in subproblem* (SSP) and *scheduling in master problem* (SMP), are solved by a two-stage algorithm. Experiments on Solomon instances with 25 customers show that the SSP is much better. Cheng et al. (2020) introduce two formulations strengthened by valid inequalities for the DRP. Two branch-and-cut algorithms are developed and tested on instances with up to 50 customers. The more compact formulation is reported to outperform the other in terms of the number of instances solved and computing time.

Paradiso et al. (2020) propose an exact solution framework (ESF) for solving the CMTVRPTW and it can be tailored to solve four variants: the CMTVRPTW-LT, the CMTVRPTW-LD, the CMTVRPTW-R, and the DRP. It considers a novel structure-based formulation, of which two relaxations are introduced to obtain lower bounds. Their numerical study shows that the ESF can solve almost all type 2 Solomon instances with 40 customers and 9 out of the 27 instances with 50 customers. The ESF has also been tested on instances from Hernandez et al. (2014, 2016), Cattaruzza et al. (2016a), and Cheng et al. (2020), and can achieve significant performance gains.

We try to mitigate the drawbacks of the ESF (mentioned at the end of Section 1.1) and develop a more effective exact method. We especially focus on obtaining tight bounds and thus a small gap before enumerating all qualified columns. Route enumeration has been successfully applied to accelerating various exact methods for solving routing problems (see Costa et al. 2019) since it was first introduced in Baldacci et al. (2008). Instead of using a hybrid approach that attempts (possibly restricted) route enumeration frequently and resorts to branching upon failure (e.g., Pecin et al. 2017a,b), we perform route enumeration once in the main Algorithm 1 when the gap is sufficiently small, which is similar to the ESF in Paradiso et al. (2020). While the ESF separates the cuts by a branch-and-price method, our EPCEM performs an enumeration in the cut separator and thus does not need to branch for the whole solution process. In addition, we introduce several new ideas to remove unnecessary columns that have been enumerated and solve the final large IP faster.

3. Problem Statement and the Superstructure-Based Formulation

3.1. Problem Statement

Before formally describing the CMTVRPTW, we first define the notation used throughout the rest of the paper. There are n customers, denoted by $N := \{1, 2, \cdots, n\}$, to be served by a fleet of m identical vehicles of capacity Q. Let $V := N \cup \{0\}$ be the set of nodes, where 0 represents the depot. Each node $i \in V$ has a demand quantity q_i and a service time r_i and requires the service to be started in the time window $[a_i, b_i]$. For all $i, j \in V$ such that $i \neq j$, t_{ij} and c_{ij} are the travel time and travel cost from node i to j, respectively. Without loss of generality, we assume $\forall i \in V$, $0 \leq q_i \leq Q$, $r_i \geq 0$, $b_i \geq a_i \geq a_0$. In particular $q_0 = r_0 = 0$, $b_0 \geq \max\{b_i : i \in N\}$. The triangle inequality $t_{ij} \leq t_{ik} + t_{kj}$ is assumed to hold, which is a standard assumption for the CVRPTW. For convenience, let $t'_{ij} := t_{ij} + r_i$ and define a directed graph $G = (V, A)$, with arc set $A := \{(i, j) : a_i + t'_{ij} \leq b_j,\, i, j \in V,\, i \neq j\}$.

Following the convention of Paradiso et al. (2020), let c_s be the cost of a structure s (defined in the second paragraph of Section 4 in Paradiso et al. 2020), and $[e_s, \ell_s]$ be the associated departure time interval, where e_s and ℓ_s are the earliest and latest times, respectively, to start s such that the minimum duration d_s is achieved. We refer to a trip as a structure with a fixed departure time from the depot and refer to a journey as a sequence of temporally non-overlapping trips assigned to the same vehicle. The CMTVRPTW asks to find no more than m journeys that jointly serve each customer exactly once and meanwhile the total travel cost is minimized.

Three formulations have been proposed to solve the CMTVRPTW exactly: the trip-based formulation (i.e., the SMP formulation in Hernandez et al. 2014, 2016), the journey-based formulation (i.e., the SSP formulation in Hernandez et al. 2016), and the structure-based formulation (3a)-(3d) in Paradiso et al. (2020), denoted by $\mathrm{F}^{\mathcal{S}}$, where $\mathcal{S}$ is the set of all structures. All three formulations have an exponential number of variables.

3.2. The Superstructure-Based Formulation $\mathrm{F}^{\mathcal{U}}$

We propose to generalize the concept of structure to superstructure as follows. A superstructure u comprises a set of structures that satisfy the conditions: (i) they visit the same set of customers; (ii) they have the same cost and duration; (iii) their associated departure time intervals can be combined into a continuous interval. That means they differ only in the order of visiting the given set of customers and possibly their associated departure time intervals. Essentially, we can view a superstructure as an artificial structure with a wider associated departure time window, and it can be used to replace all its component structures. The conditions required to combine a set of structures into a superstructure may seem restrictive. In reality, they can be satisfied relatively easily when the customers have wide time windows because reversing the sequence of visiting the same

customers is likely to produce a feasible structure with the same cost and duration. Furthermore, the example in Figure 1 suggests that different sequences other than a reversed order may also satisfy the conditions. It is worth mentioning that instances with wide time windows are generally more challenging to solve, and the new formulation shows its strength especially for them.

The example in Figure 1 is generated in the process of solving the instance RC202 with 25 customers (see Section 7). Observe that $N_{s_1} = N_{s_2} = \{1,5,6,8,12\}$, $c_{s_1} = c_{s_2} = 176.8$, $d_{s_1} = d_{s_2} = 126.8$, $[e_{s_1}, \ell_{s_1}] \cap [e_{s_2}, \ell_{s_2}] = [254.5, 369.3] \cap [294.3, 409.1] \neq \emptyset$. We can combine s_1 and s_2 into a superstructure $u := \{s_1, s_2\}$ with the set of visited customers $N_u = N_{s_1} = \{1,5,6,8,12\}$, cost $c_u = c_{s_1} = 176.8$, duration $d_u = d_{s_1} = 126.8$, and the associated departure time interval $[e_u, \ell_u] = [e_{s_1}, \ell_{s_1}] \cup [e_{s_2}, \ell_{s_2}] = [254.5, 409.1]$.

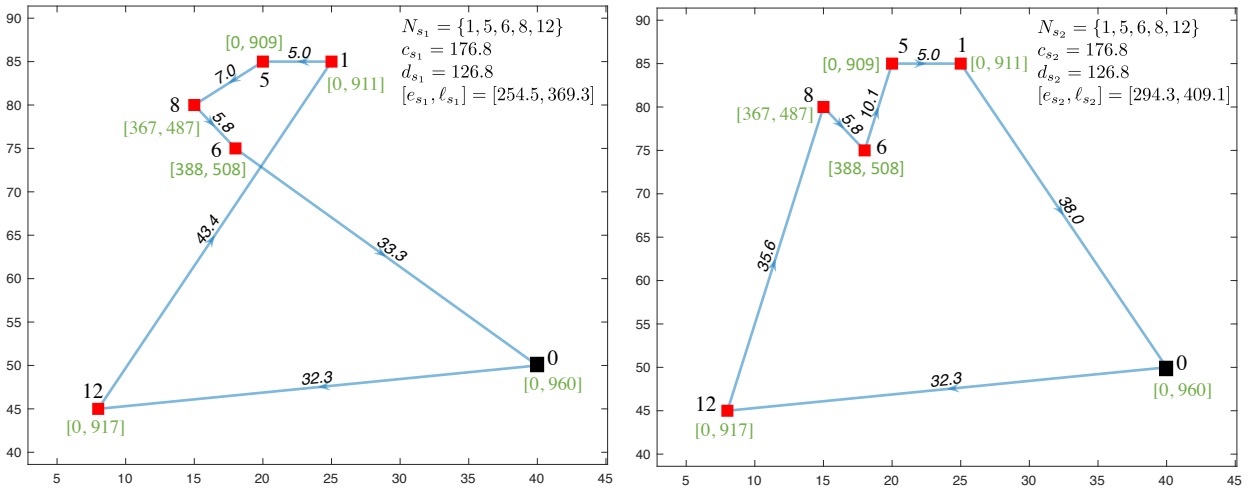

Figure 1 An illustration of the superstructure that contains two structures s_1 and s_2. We have $N_{s_1} = N_{s_2}$, $c_{s_1} = c_{s_2}$, $d_{s_1} = d_{s_2}$, $[e_{s_1}, \ell_{s_1}] \cap [e_{s_2}, \ell_{s_2}] \neq \emptyset$. The example comes from the instance RC202 with 25 customers where 0 is the depot, the number on each arc is the travel time (also the travel cost), and the text in green denotes the time window of each customer.

Let $\mathcal{U}$ be the set of all superstructures. A binary variable x_u is used to decide if u should be included in an optimal solution. In addition, for each subset $\overline{\mathcal{U}} \subseteq \mathcal{U}$, constant $\zeta_m(\overline{\mathcal{U}})$ is the maximum number of superstructures in $\overline{\mathcal{U}}$ that can be converted into no more than m journeys. Formulation $\mathrm{F}^{\mathcal{U}}$ with an exponential number of variables and constraints is shown below.

$$(\mathrm{F}^{\mathcal{U}}) \qquad z^{\mathcal{U}} = \min \sum_{u \in \mathcal{U}} c_u x_u \tag{1}$$

$$\text{s.t.} \sum_{u \in \mathcal{U}} \alpha'_{iu} x_u = 1, \qquad \forall i \in N, \tag{2}$$

$$\sum_{u \in \overline{\mathcal{U}}} x_u \leq \zeta_m(\overline{\mathcal{U}}), \qquad \forall \overline{\mathcal{U}} \subseteq \mathcal{U}, \tag{3}$$

$$x_u \in \{0,1\}, \qquad \forall u \in \mathcal{U},$$

where $\alpha'_{iu} \in \{0,1\}$ indicates if customer i is served by u. The objective function (1) to be minimized computes the total cost of selected superstructures. Constraints (2) force each customer to be visited exactly once. Constraints (3) are called *superstructure feasibility constraints* (SSFCs). Similar to the *structure feasibility constraints* (SFCs), i.e., constraints (3c) in Paradiso et al. (2020), they are applied to guarantee that the superstructures selected can be carried out by the m available vehicles.

The main motivation for combining qualified structures into a superstructure is that they correspond to "almost duplicate" columns in the structure-based formulation $\mathrm{F}^{\mathcal{S}}$ due to their identical objective coefficients and coefficients of constraints (2) in $\mathrm{F}^{\mathcal{S}}$. As a result, there is potentially an exponential number of equivalent (not necessarily feasible) solutions. To test their feasibility, the SFC separator has to be called frequently, slowing down the solution process significantly. However, we cannot simply eliminate such "duplication" from $\mathrm{F}^{\mathcal{S}}$ because the SFCs are added in a cutting-plane fashion. Working with superstructures instead of structures removes such "duplication" and thus reduces the frequency of calls to the separator. In addition, the superstructure-based formulation $\mathrm{F}^{\mathcal{U}}$ is superior to the structure-based formulation $\mathrm{F}^{\mathcal{S}}$ because it has fewer binary variables and the formulation tightness in terms of its LP relaxation is not sacrificed.

THEOREM 1. *$\bar{z}^{\mathcal{U}} = \bar{z}^{\mathcal{S}}$, where $\bar{z}^{\mathcal{U}}$ and $\bar{z}^{\mathcal{S}}$ are the optimal values of the root LPs of the superstructure-based and the structure-based formulations, respectively.*

The proof of Theorem 1 is included in Section EC.1.1 of the e-companion. It relies on the following Lemma 1. For ease of presentation, we introduce some notation. The set of superstructures $\mathcal{U}$ is generated from $\mathcal{S}$ by the procedure described in Section 6.6. Let $\Psi : \mathcal{S} \to \mathcal{U}$ be the resulting mapping, and Ψ is an onto mapping. For convenience, let $\Psi^{-1}(u) := \{s \in \mathcal{S} : \Psi(s) = u\}$ for each $u \in \mathcal{U}$ and thus $\{\Psi^{-1}(u) : u \in \mathcal{U}\}$ defines a partition of $\mathcal{S}$, i.e., for any $u, u' \in \mathcal{U}$ and $u \neq u'$, we have $\Psi^{-1}(u) \cap \Psi^{-1}(u') = \emptyset$ and $\cup_{u\in\mathcal{U}} \Psi^{-1}(u) = \mathcal{S}$. For any $\overline{\mathcal{S}} \subseteq \mathcal{S}$ and $\overline{\mathcal{U}} \subseteq \mathcal{U}$, let $\Psi(\overline{\mathcal{S}}) := \cup_{s\in\overline{\mathcal{S}}} \Psi(s)$ and $\Psi^{-1}(\overline{\mathcal{U}}) := \cup_{u\in\overline{\mathcal{U}}} \Psi^{-1}(u)$. Let $2^{\mathcal{U}} := \{\overline{\mathcal{U}} : \overline{\mathcal{U}} \subseteq \mathcal{U}\}$ and $2^{\mathcal{S}} := \{\overline{\mathcal{S}} : \overline{\mathcal{S}} \subseteq \mathcal{S}\}$ be the power sets of $\mathcal{U}$ and $\mathcal{S}$, respectively. The constants $\zeta_m(\overline{\mathcal{U}})$ and $\eta_m(\overline{\mathcal{S}})$ for $\overline{\mathcal{U}} \subseteq \mathcal{U}$ and $\overline{\mathcal{S}} \subseteq \mathcal{S}$ induce two functions $\zeta_m : 2^{\mathcal{U}} \to \mathbb{Z}_+$ and $\eta_m : 2^{\mathcal{S}} \to \mathbb{Z}_+$. Note that ζ_m is a non-decreasing submodular function. Because for any $\mathcal{U}^1, \mathcal{U}^2 \subseteq \mathcal{U}$ with $\mathcal{U}^1 \subseteq \mathcal{U}^2$ and $u \in \mathcal{U} \setminus \mathcal{U}^2$, we have $\zeta_m(\mathcal{U}^1 \cup \{u\}) - \zeta_m(\mathcal{U}^1) \geq \zeta_m(\mathcal{U}^2 \cup \{u\}) - \zeta_m(\mathcal{U}^2)$. Similarly, η_m is a non-decreasing submodular function. Let P_{ζ_m} and P_{η_m} be the polymatroids defined by ζ_m and η_m, respectively, i.e., $P_{\zeta_m} := \{y \in \mathbb{R}^{\mathcal{U}}_+ : \sum_{u\in\overline{\mathcal{U}}} y_u \leq \zeta_m(\overline{\mathcal{U}}), \forall \overline{\mathcal{U}} \subseteq \mathcal{U}\}$ and $P_{\eta_m} := \{x \in \mathbb{R}^{\mathcal{S}}_+ : \sum_{s\in\overline{\mathcal{S}}} x_s \leq \eta_m(\overline{\mathcal{S}}), \forall \overline{\mathcal{S}} \subseteq \mathcal{S}\}$.

LEMMA 1. *For any $\hat{y} \in P_{\zeta_m}$, the intersection $P_{\eta_m} \cap \{x \in \mathbb{R}^{\mathcal{S}} : \sum_{s\in\Psi^{-1}(u)} x_s = \hat{y}_u, \forall u \in \mathcal{U}\} \neq \emptyset$.*

Observe that functions ζ_m and η_m satisfy the following properties.

- P1. For any $u \in \mathcal{U}$ and $\overline{\mathcal{S}} \subseteq \Psi^{-1}(u)$ such that $\overline{\mathcal{S}} \neq \emptyset$, $\zeta_m(u) = \eta_m(\overline{\mathcal{S}}) = 1$ and $\zeta_m(\emptyset) = \eta_m(\emptyset) = 0$;

- P2. For any $\mathcal{U}^1 \subseteq \mathcal{U}^2 \subseteq \mathcal{U}$ and $\mathcal{S}^1 \subseteq \mathcal{S}^2 \subseteq \mathcal{S}$, $\zeta_m(\mathcal{U}^1) \leq \zeta_m(\mathcal{U}^2)$ and $\eta_m(\mathcal{S}^1) \leq \eta_m(\mathcal{S}^2)$;
- P3. For any $\overline{\mathcal{S}} \subseteq \mathcal{S}$, $\eta_m(\overline{\mathcal{S}}) \leq \zeta_m(\Psi(\overline{\mathcal{S}})) \leq |\Psi(\overline{\mathcal{S}})| \leq |\overline{\mathcal{S}}|$;
- P4. For any $\overline{\mathcal{U}} \subseteq \mathcal{U}$, there exists $\overline{\mathcal{S}} \subseteq \Psi^{-1}(\overline{\mathcal{U}})$ such that $\eta_m(\overline{\mathcal{S}}) = |\overline{\mathcal{S}}| = \zeta_m(\overline{\mathcal{U}})$.

Proving Lemma 1 is not trivial because for any $\overline{\mathcal{S}} \subseteq \mathcal{S}$, we only have $\eta_m(\overline{\mathcal{S}}) \leq \zeta_m(\Psi(\overline{\mathcal{S}}))$. In some cases, $\eta_m(\overline{\mathcal{S}})$ can be much smaller than $\zeta_m(\Psi(\overline{\mathcal{S}}))$. It is worth mentioning that $\overline{\mathcal{S}}$ can be significantly different for different $\overline{\mathcal{U}}$ in Property P4. In particular, for $\overline{\mathcal{U}} \subseteq \widetilde{\mathcal{U}} \subseteq \mathcal{U}$ and $\overline{\mathcal{S}} \subseteq \Psi^{-1}(\overline{\mathcal{U}})$ such that $\eta_m(\overline{\mathcal{S}}) = |\overline{\mathcal{S}}| = \zeta_m(\overline{\mathcal{U}})$, it is not guaranteed that there exists $\widetilde{\mathcal{S}}$ such that $\eta_m(\widetilde{\mathcal{S}}) = |\widetilde{\mathcal{S}}| = \zeta_m(\widetilde{\mathcal{U}})$ and $\overline{\mathcal{S}} \subseteq \widetilde{\mathcal{S}}$. The proof of Lemma 1 is included in Section EC.1.2 of the e-companion.

4. Formulations for Bounding

This section presents formulations employed to compute lower and upper bounds that help to narrow the search space substantially and thus prove optimality faster. The following formulation $\overline{\mathrm{F}}^{\mathcal{S}}$ (i.e., formulation (7a) - (7e) in Paradiso et al. 2020) is a relaxation of the structure-based formulation $\mathrm{F}^{\mathcal{S}}$, where (4) is the *relaxed structure feasibility constraints* (RSFCs), and (5) is the well-known *subset-row inequalities* (SRIs) (Jepsen et al. 2008, Pecin et al. 2017a). Let $\mathcal{C} := \{(i,j,k) : i,j,k \in N, i<j<k\}$ be the set of all combinations of three different customers in N, and define its subset $\mathcal{C}_s := \{(i,j,k) \in \mathcal{C} : \alpha_{is} + \alpha_{js} + \alpha_{ks} \geq 2\}$.

$$
\begin{aligned}
(\overline{\mathrm{F}}^{\mathcal{S}}) \qquad \bar{z}^{\mathcal{S}} \;=\; \min \quad & \sum_{s\in\mathcal{S}} c_s x_s && \\
\text{s.t.} \quad & \sum_{s\in\mathcal{S}} \alpha_{is} x_s = 1, && \forall i \in N, \\
& \sum_{s\in\mathcal{S}} \mathbb{1}_{\,[\ell_s, e_s+d_s)}(t)\, x_s \leq m, && \forall t \in [a_0, b_0], \qquad (4)\\
& \sum_{s\in\mathcal{S}} \mathbb{1}_{\,\mathcal{C}_s}((i,j,k))\, x_s \leq 1, && \forall (i,j,k) \in \mathcal{C}, \qquad (5)\\
& x_s \geq 0, && \forall s \in \mathcal{S},
\end{aligned}
$$

where α_{is} is the number of times customer i is served by structure s, and the notation $\mathbb{1}_{\,X}(x)$ denotes the indicator function that equals 1 if $x \in X$ and 0 otherwise. Although the starting time of a structure s can be any number in the interval $[e_s, \ell_s]$, s must be active in $[\ell_s, e_s + d_s)$ when $\ell_s < e_s + d_s$, meaning that the corresponding vehicle is on the way or waiting at a customer. In practice, interval $[a_0, b_0]$ is discretized in the computation. Constraints (5) are a special case of the SRI class, which require that for each possible combination $(i,j,k) \in \mathcal{C}$, no more than one structure can be selected from those visiting at least two of customers i, j, and k. Its validity can be shown straightforwardly by the pigeonhole principle.

The number of inequalities in (4) and (5) can be hundreds of thousands when the end time b_0 and the number of customers n are relatively large. Including all of them can make the above linear program (LP) difficult to solve, especially when the number of variables is exponentially large. We

obtain the first lower bound by a partial solution (early terminated when the limit on the number of cuts added is reached) of $\overline{\mathrm{F}}^{\mathcal{S}}$ via the *alternating column and row generation* (ACRG) to be described in Section 6.1.

Let $\mathcal{H} \subseteq [a_0, b_0]$, $\mathcal{I} \subseteq \mathcal{C}$ be two index subsets corresponding to the generated RSFCs and SRIs when the ACRG terminates. Define $\overline{\mathrm{F}}^{\mathcal{S}}_{\mathcal{H},\mathcal{I}}$ to be the formulation with $[a_0, b_0]$ and $\mathcal{C}$ in $\overline{\mathrm{F}}^{\mathcal{S}}$ replaced by $\mathcal{H}$ and $\mathcal{I}$, respectively. We use $\bar{z}^{\mathcal{S}}_{\mathcal{H},\mathcal{I}}$ to denote its optimal value. Obviously, $\overline{\mathrm{F}}^{\mathcal{S}}_{\mathcal{H},\mathcal{I}}$ is a weaker relaxation than $\overline{\mathrm{F}}^{\mathcal{S}}$ and thus $\bar{z}^{\mathcal{S}}_{\mathcal{H},\mathcal{I}} \leq \bar{z}^{\mathcal{S}}$. But it has the following benefits. Due to the tailing-off effect commonly seen in cutting-plane methods, little improvement is achieved per cut added when the incumbent solution is close to the optimum. Therefore, an early termination produces a tight enough LB within a reasonable time. Meanwhile, it avoids ending up with many rows. Both RSFCs and SRIs are so-called non-robust cuts (see Pecin et al. 2017b), which usually considerably hinder the solution of subsequent pricing subproblems if too many are present.

Let $\mathcal{S}_1$ be the set of structures generated by the ACRG at termination, which is further taken advantage of to compute a valid UB. To this end, we replace the set $\mathcal{S}$ in $\mathrm{F}^{\mathcal{S}}$ with $\mathcal{S}_1$ and use $\mathrm{F}^{\mathcal{S}_1}$ to denote the resulting formulation. In contrast to the potentially exponential size of $\mathcal{S}$, $\mathcal{S}_1$ is usually moderate-sized (its size is usually no more than 50,000 for instances with 50 or fewer customers and no more than 100,000 for instances with 70 or more customers). Therefore, $\mathrm{F}^{\mathcal{S}_1}$ is an IP that can be solved relatively fast in practice. If an optimal solution to $\mathrm{F}^{\mathcal{S}_1}$ cannot be obtained within a predetermined time limit, but a feasible solution has been found, we still have a valid UB.

5. The EPCEM

5.1. Overview of the EPCEM

We outline the EPCEM in Algorithm 1, whose seven steps are detailed subsequently in Section 6. It computes an initial LB by the ACRG in *Step 1* and a valid UB in *Step 2*, which help to narrow the search space substantially. In particular, we only need to consider columns with reduced costs no larger than UB−LB, which are enumerated in *Step 3*. The LB is then tightened in *Step 4*, and an auxiliary LP is solved in *Step 5* to further remove unnecessary columns. Structures corresponding to the remaining columns are subsequently combined into superstructures in *Step 6*. Finally, in *Step 7*, the superstructure-based formulation is solved to obtain an optimal solution. Note $\overline{\mathrm{F}}^{\mathcal{S}_2}$ and $\mathrm{F}^{\mathcal{U}_3}$ represent the formulations with $\mathcal{S}$ in $\overline{\mathrm{F}}^{\mathcal{S}}$ replaced by $\mathcal{S}_2$ and $\mathcal{U}$ in $\mathrm{F}^{\mathcal{U}}$ replaced by $\mathcal{U}_3$, respectively.

The EPCEM takes its name from the three major components: pricing (column generation in *Step 1*), cutting planes (*Steps 1, 2*, and *7*), and structure enumeration (*Step 3*). In contrast to most state-of-the-art exact methods, branching is not performed explicitly (although it is automatically performed within the IP solver), and thus, "branch" does not appear in the name. By convention,

when a column generation method is used to solve an LP that has an exponential number of variables, the restricted master problem (RMP) is referred to as the LP with all columns generated so far. The subproblem solved to generate new columns is called the pricing subproblem.

Algorithm 1: The EPCEM for Solving the CMTVRPTW

Step 1. Initial LB Computation: Solve $\overline{\mathrm{F}}^{\mathcal{S}}$ partially by the ACRG and obtain the initial LB, $\mathcal{S}_1$, $\mathcal{H}$, and $\mathcal{I}$. Let π^* be the corresponding optimal dual solution at termination.

Step 2. Initial UB Computation: Solve $\mathrm{F}^{\mathcal{S}_1}$ by an IP solver with our enhanced SFC separator and obtain the initial UB. ***If*** LB equals UB, ***then*** optimality is achieved, **stop**.

Step 3. Structure Enumeration: Enumerate the set, denoted by $\mathcal{S}_2$, of all structures with reduced costs no larger than UB−LB with respect to π^*.

Step 4. LB Tightening: Solve $\overline{\mathrm{F}}^{\mathcal{S}_2}$ and update LB. ***If*** LB equals UB, ***then*** optimality is achieved, **stop**.

Step 5. Structure Pruning: Solve an auxiliary problem to update the reduced cost of each variable. Remove columns with reduced costs greater than UB−LB and obtain the set of structures corresponding to the remaining columns, denoted by $\mathcal{S}_3$.

Step 6. Superstructure Generation: Generate the set of superstructures $\mathcal{U}_3$ from $\mathcal{S}_3$.

Step 7. Optimal Solution Computation: Solve $\mathrm{F}^{\mathcal{U}_3}$ via the MPSC method.

5.2. Advantages of the EPCEM over the ESF

The state-of-the-art exact method for solving the CMTVRPTW is the ESF (see Section 6 of Paradiso et al. 2020). Our EPCEM significantly outperforms the ESF due to the following six major enhancements.

E1. Instead of solving a linear relaxation with only set-partitioning constraints by column generation in Step 2 of the ESF, we partially solve a stronger relaxation by a new ACRG to obtain a tighter initial LB in our *Step 1*. The dominance rule is modified to tackle dual variables associated with the non-robust cuts.

E2. We solve a restricted problem with early termination to obtain a valid UB in our *Step 2* in contrast to guessing an initial UB in Step 2 of the ESF. It not only significantly simplifies the subsequent enumeration but also eliminates the potential need to adjust the guessed UB gradually.

E3. We take advantage of the reduced costs in several aspects. Firstly, the reduced cost fixing (RCF; see, e.g., Desaulniers et al. 2020, Irnich et al. 2010) is applied to remove redundant columns whenever a bound is updated in our *Steps 4* and *7*. Secondly, we propose to solve an auxiliary problem to update the reduced costs, which facilitates RCF in our *Step 5*. Finally, we come up with the *reduced cost cut* (RCC) that helps to close the gap faster for some large Solomon instances if applied in our *Step 7*.

E4. We propose a novel concept, superstructure, leading to the superstructure-based formulation that is superior to the structure-based formulation. The new formulation reduces the combinatorial complexity and helps prove optimality faster.

E5. We introduce the MPSC method in our *Step 7* that incrementally uses the columns enumerated (see Section 6.7.1). For extremely difficult instances with millions of columns in the pool, the new method can yield high-quality solutions and even proven optimality sometimes.

E6. We propose an effective algorithm to separate the (super)structure feasibility cut (used in our *Steps 2* and *7*), whose computational time is negligible compared with the total solution time.

6. Detailed Description of Every Step of the EPCEM

6.1. *Step 1*: Initial LB Computation

Step 1 in the EPCEM serves the same function of computing the initial LB as Step 2 in the ESF. The ESF computes the CVRPTW-LB from the relaxation with only set-partitioning constraints. In contrast, the EPCEM solves a tighter relaxation with RSFCs and SRIs to obtain the initial LB. Since new rows (cuts) are added gradually, the column generation used in the ESF is no longer applicable. We modify the labeling algorithm in the ESF to handle the non-robust cuts and combine it with a row generation subroutine into the ACRG.

The ACRG has two major parts: the *dynamic column generation via backward labeling* (DCGBL) is responsible for generating new columns with negative reduced costs; the *row generation* (RG) identifies RSFCs and SRIs violated by the current solution. The DCGBL and the RG are performed alternatively until a predetermined limit on the total number of new rows generated is reached. Before termination, the DCGBL is applied once more to guarantee that $\overline{\mathrm{F}}^{\mathcal{S}}_{\mathcal{H},\mathcal{I}}$ is solved to optimality for some index sets $\mathcal{H}$ and $\mathcal{I}$.

6.1.1. The DCGBL in the ACRG. The DCGBL generates qualified structures with negative reduced costs by a two-stage labeling algorithm. Labeling-type methods are widely used in solving the *elementary shortest path problem with resource constraints* (Feillet et al. 2004, Irnich and Desaulniers 2005, Righini and Salani 2006, 2008). They have been adapted to generate columns in most exact methods for solving the CVRPTW and its variants (Azi et al. 2007, 2010, Hernandez et al. 2014, 2016, Tilk and Irnich 2017). In the first stage, the backward labeling method (BLM) is used, which is based on the labeling algorithm in Paradiso et al. (2020) and is modified to be compatible with the newly generated non-robust cuts. In the second stage, it switches to the BLM with *completion bounds* (see Baldacci et al. 2012; BLMCB).

6.1.1.1. *The BLM in the DCGBL.* Let $\mathcal{b}=(i_0,i_1,\cdots,i_{k_\mathcal{b}})$ be an elementary backward path that starts from the depot $i_0=0$, serves each customer in $N^\mathcal{b}=\{i_1,\cdots,i_{k_\mathcal{b}}\}$ exactly once in their required time windows, can leave customer $i^\mathcal{b}:=i_{k_\mathcal{b}}$ at any time in $[e^\mathcal{b},\ell^\mathcal{b}]$, and meanwhile achieves the minimum duration $d^\mathcal{b}$. Let $\pi:=(\pi^N,\pi^\mathcal{H},\pi^\mathcal{I})$ be the corresponding optimal dual solution to the RMP, where $\pi^N=(\pi_i)_{i\in N}$, $\pi^\mathcal{H}=(\pi_t)_{t\in\mathcal{H}}$, and $\pi^\mathcal{I}=(\pi_{ijk})_{(i,j,k)\in\mathcal{I}}$ correspond to the partition constraints and the added cuts (4) and (5), respectively. Note that $\forall t\in\mathcal{H}$, $\forall(i,j,k)\in\mathcal{I}$, $\pi_t\le 0$, $\pi_{ijk}\le 0$. Let $\beta^\mathcal{b}$ and $\gamma^\mathcal{b}$ be the partial and full reduced costs of $\mathcal{b}$ with respect to π, separately, which are computed as follows.

$$\beta^\mathcal{b}=\sum_{g=0}^{k_\mathcal{b}-1}\bar{c}_{i_{g+1}i_g},\quad \gamma^\mathcal{b}=\beta^\mathcal{b}-\sum_{t\in\mathcal{H}}\mathbb{1}_{[\ell^\mathcal{b},e^\mathcal{b}+d^\mathcal{b})}(t)\,\pi^\mathcal{H}_t-\sum_{(i,j,k)\in\mathcal{I}}\mathbb{1}_{C^\mathcal{b}}((i,j,k))\,\pi^\mathcal{I}_{(i,j,k)}, \tag{6}$$

where $C^\mathcal{b}=\{(i,j,k)\in C:|N^\mathcal{b}\cap\{i,j,k\}|\ge 2\}$, and $\bar{c}_{i_{g+1}i_g}=\begin{cases}c_{i_{g+1}i_g}-\pi_{i_{g+1}}/2, & \text{if } i_g=0,\\ c_{i_{g+1}i_g}-(\pi_{i_g}+\pi_{i_{g+1}})/2, & \text{if } i_g\ne 0, i_{g+1}\ne 0,\\ c_{i_{g+1}i_g}-\pi_{i_g}/2, & \text{if } i_{g+1}=0.\end{cases}$

The label $L^\mathcal{b}$ associated with path $\mathcal{b}$ is defined to be a 8-tuple $L^\mathcal{b}:=(N^\mathcal{b},q^\mathcal{b},e^\mathcal{b},\ell^\mathcal{b},d^\mathcal{b},i^\mathcal{b},\beta^\mathcal{b},\gamma^\mathcal{b})$, where $e^\mathcal{b}$ and $\ell^\mathcal{b}$ are the earliest and latest times, respectively, to depart from the depot such that the minimum duration $d^\mathcal{b}$ can be achieved, and $q^\mathcal{b}:=\sum_{i\in N^\mathcal{b}}q_i$ is the total demand of the customers visited. $L^\mathcal{b}$ is feasible if

$$q^\mathcal{b}\le Q,\qquad \ell^\mathcal{b}\ge a_{i^\mathcal{b}},\qquad e^\mathcal{b}+d^\mathcal{b}\le b_0. \tag{7}$$

Generating structures with negative reduced costs is equivalent to generating feasible backward paths (labels) with $i^\mathcal{b}=0$ and $\gamma^\mathcal{b}<0$, which is accomplished by the BLM. In particular, $L^\mathcal{b}$ can be extended to $L^{\mathcal{b}'}=(N^{\mathcal{b}'},q^{\mathcal{b}'},e^{\mathcal{b}'},\ell^{\mathcal{b}'},d^{\mathcal{b}'},i^{\mathcal{b}'},\beta^{\mathcal{b}'},\gamma^{\mathcal{b}'})$ by the following update rule, where $\mathcal{b}':=(i_0,i_1,\cdots,i_{k_\mathcal{b}},j)$ for $j\in V\setminus N^\mathcal{b}$.

$$\begin{cases} N^{\mathcal{b}'}=\begin{cases}N^\mathcal{b}\cup\{j\}, & \text{if } j\in N,\\ N^\mathcal{b}, & \text{if } j=0,\end{cases} \quad q^{\mathcal{b}'}=q^\mathcal{b}+q_j,\quad e^{\mathcal{b}'}=\begin{cases}b_j, & \text{if } e^\mathcal{b}>b_j+t'_{ji^\mathcal{b}},\\ e^\mathcal{b}-t'_{ji^\mathcal{b}}, & \text{if } a_j+t'_{ji^\mathcal{b}}\le e^\mathcal{b}\le b_j+t'_{ji^\mathcal{b}},\\ a_j, & \text{otherwise,}\end{cases}\\ \ell^{\mathcal{b}'}=\min\{\ell^\mathcal{b}-t'_{ji^\mathcal{b}},b_j\},\quad d^{\mathcal{b}'}=d^\mathcal{b}+\max\{t'_{ji^\mathcal{b}},e^\mathcal{b}-b_j\},\quad i^{\mathcal{b}'}=j,\\ \beta^{\mathcal{b}'}=\beta^\mathcal{b}+\bar{c}_{ji^\mathcal{b}},\quad \text{compute } \gamma^{\mathcal{b}'} \text{ by (6).}\end{cases} \tag{8}$$

The following equality can be easily verified.

$$e^{\mathcal{b}'}+d^{\mathcal{b}'}=\max\{e^\mathcal{b}+d^\mathcal{b},\,a_j+t'_{ji^\mathcal{b}}+d^\mathcal{b}\}. \tag{9}$$

Proposition 1 is applied as a dominance rule to accelerate the BLM, whose proof is presented in Section EC.1.3 of the e-companion.

PROPOSITION 1. *$L^{\mathcal{b}_1}=(N^{\mathcal{b}_1},q^{\mathcal{b}_1},e^{\mathcal{b}_1},\ell^{\mathcal{b}_1},d^{\mathcal{b}_1},i^{\mathcal{b}_1},\beta^{\mathcal{b}_1},\gamma^{\mathcal{b}_1})$ and $L^{\mathcal{b}_2}=(N^{\mathcal{b}_2},q^{\mathcal{b}_2},e^{\mathcal{b}_2},\ell^{\mathcal{b}_2},d^{\mathcal{b}_2},i^{\mathcal{b}_2},\beta^{\mathcal{b}_2},\gamma^{\mathcal{b}_2})$ are two feasible labels. $L^{\mathcal{b}_1}$ dominates $L^{\mathcal{b}_2}$ if the following six relations are satisfied:* (i) $i^{\mathcal{b}_1}=i^{\mathcal{b}_2}$, (ii) $N^{\mathcal{b}_1}\subseteq N^{\mathcal{b}_2}$, (iii) $\ell^{\mathcal{b}_1}\ge\ell^{\mathcal{b}_2}$, (iv) $e^{\mathcal{b}_1}+d^{\mathcal{b}_1}\le e^{\mathcal{b}_2}+d^{\mathcal{b}_2}$, (v) $d^{\mathcal{b}_1}\le d^{\mathcal{b}_2}$, *and* (vi) $\beta^{\mathcal{b}_1}\le\beta^{\mathcal{b}_2}$.

6.1.1.2. *The BLMCB in the DCGBL.* When the BLM takes more than a predetermined number of iterations to converge, the BLMCB will be activated and used in the DCGBL to generate new columns until the termination of the ACRG. The BLMCB differs from the BLM in two places. Firstly, for any $i \in N$ and $0 \leq q \leq Q$, it computes a lower bound (completion bound) on the partial reduced cost, denoted by $\bar{\omega}(i,q)$ (see Section EC.2.1 of the e-companion). Secondly, every time a new label $L^{\mathscr{b}'}$ is generated, the completion bounds are used to check whether or not $L^{\mathscr{b}'}$ can be discarded by the following Proposition 2. Unfortunately, computing the completion bounds can be time-consuming, which is the reason why the BLM is first applied in the DCGBL. When the number of iterations of the BLM exceeds the predetermined limit, the BLMCB may outperform the BLM by discarding some unpromising labels early and thus is activated thereafter.

PROPOSITION 2. *Given a label $L^{\mathscr{b}}$, if $\bar{\omega}(i^{\mathscr{b}}, Q + q_{i^{\mathscr{b}}} - q^{\mathscr{b}}) \neq +\infty$ and $\gamma^{\mathscr{b}} + \bar{\omega}(i^{\mathscr{b}}, Q + q_{i^{\mathscr{b}}} - q^{\mathscr{b}}) \geq 0$, then $\mathscr{b}$ cannot generate a structure with a negative reduced cost, and thus the label $L^{\mathscr{b}}$ can be discarded.*

The proof of Proposition 2 can be found in Section EC.1.4 of the e-companion.

6.1.2. The RG in the ACRG. The violated RSFCs and SRIs are identified by enumeration, and some implementation details are included in Section EC.2.2 of the e-companion.

6.2. *Step 2*: Initial UB Computation

The gap UB−LB is crucial because it significantly impacts the number of columns enumerated and thus the difficulty of the final IP solved in *Step 7*. Guessing a UB in Step 2 of the ESF can be problematic because a conservative guess leads to a large gap that fails the algorithm, and an aggressive guess can result in additional iterations, increasing the computational time significantly. Instead of guessing a UB, we solve a restricted version of the structure-based formulation. More specifically, we solve $\mathrm{F}^{\mathcal{S}_1}$ to obtain a valid UB, which is usually very tight according to our experimental observations and thus yields a small gap.

To solve $\mathrm{F}^{\mathcal{S}_1}$, we resort to the state-of-the-art general IP solver Gurobi (Gurobi Optimization, LLC 2021) with the *enhanced SFC separator* (ESFCS) implemented as a lazy callback function to add violated SFCs, if any. That means whenever an integer solution is computed in the solution process, the lazy callback (ESFCS) function will be called to check its feasibility.

6.2.1. The ESFCS. Basically, the separator needs to decide if $\eta_m(\overline{\mathcal{S}}) \geq |\overline{\mathcal{S}}|$ for a given integer solution $\hat{\boldsymbol{x}} := (x_s)_{s \in \mathcal{S}_1}$, where $\overline{\mathcal{S}} = \{s \in \mathcal{S}_1 : \hat{x}_s = 1\}$ and $\eta_m(\overline{\mathcal{S}})$ is the maximum number of structures in $\overline{\mathcal{S}}$ that can be combined into no more than m journeys. We modify the SFC separator in Paradiso et al. (2020) which solves a *team orienteering problem with time windows* (TOPTW) (Vansteenwegen et al. 2009, Labadie et al. 2012). We also solve the same TOPTW. The main difference is that

their separator solves the formulation (11a)-(11d) in Paradiso et al. (2020), denoted by $\text{SEP}^{\overline{\mathcal{S}}}$, via a branch-and-price method that generates new columns and requires customized branching rules, while our ESFCS (see Algorithm 2) performs an enumeration in Step 2 and solves an IP with all enumerated columns directly by Gurobi. Let $\overline{\text{SEP}}^{\overline{\mathcal{S}}}$ denote the LP relaxation of $\text{SEP}^{\overline{\mathcal{S}}}$ when the integer requirement is relaxed, $\bar{\eta}_m(\overline{\mathcal{S}})$ be its optimal value, and $\tilde{\mathcal{R}}$ be the set of all feasible journeys.

Algorithm 2: The ESFCS.

Step 1. Solve $\overline{\text{SEP}}^{\overline{\mathcal{S}}}$ and obtain $\bar{\eta}_m(\overline{\mathcal{S}})$. **If** $\bar{\eta}_m(\overline{\mathcal{S}}) < |\overline{\mathcal{S}}|$, **then** cut off $\hat{\boldsymbol{x}}$ by the inequality $\sum_{s\in\overline{\mathcal{S}}} x_s \le \lfloor \bar{\eta}_m(\overline{\mathcal{S}}) \rfloor$, **stop**.

Step 2. Enumerate all journeys with reduced cost no less than $|\overline{\mathcal{S}}| - \bar{\eta}_m(\overline{\mathcal{S}})$ to form the set $\bar{\mathcal{R}}$.

Step 3. Solve $\text{SEP}^{\overline{\mathcal{S}}}$ directly with $\tilde{\mathcal{R}}$ replaced by $\bar{\mathcal{R}}$ and obtain $\eta_m(\overline{\mathcal{S}})$. **If** $\eta_m(\overline{\mathcal{S}}) \ge |\overline{\mathcal{S}}|$, **then** $\hat{\boldsymbol{x}}$ is feasible, **otherwise** cut off $\hat{\boldsymbol{x}}$ by the inequality $\sum_{s\in\overline{\mathcal{S}}} x_s \le \eta_m(\overline{\mathcal{S}})$.

6.2.2. Remarks. According to our numerical study, the set $\bar{\mathcal{R}}$ computed in Step 2 is small-sized, and thus the formulation $\text{SEP}^{\overline{\mathcal{S}}}$ in Step 3 can be solved fast by Gurobi. Our implementation of the ESFCS is so effective that the total time spent in separation is negligible. In our experiments, we have never encountered cases where $\text{F}^{\mathcal{S}_1}$ is infeasible. Still, if it does happen, we have to add more columns, which can be generated by the enumeration scheme described in the following Section 6.3. On the contrary, it is often the case that we have more columns than needed. Since our goal in this step is to compute a good enough UB, too many columns will slow down the computation. If $|\mathcal{S}_1| > n'$ (a constant), we only keep the smallest n' columns in terms of reduced costs.

The ESFCS can be used to separate SSFCs directly since superstructures and structures are represented in the same way, i.e., as nodes in the supported graph (Figure 1 in Paradiso et al. 2020) when the TOPTW is solved. In other words, a superstructure can be viewed as a structure with an extended associated departure time window that is the union of those of its element structures. As a result, the ESFCS is applied to solve the final superstructure-based formulation $\text{F}^{\mathcal{U}_3}$ in a similar fashion to solving $\text{F}^{\mathcal{S}_1}$.

6.3. *Step 3*: Structure Enumeration

This step is similar to Step 3 in the ESF. The BLMCB with a modified dominance rule (Proposition 3) is applied to enumerate all structures with reduced costs no larger than UB-LB with respect to π^*. Let $|\mathcal{L}|$ be the set of labels generated in the pool so far. Since $|\mathcal{L}|$ can be large, checking dominance for each newly generated $L^{\mathscr{b}'}$ can be computationally excruciating. Thus, every time a path $\mathscr{b}$ is extended to a new feasible label $L^{\mathscr{b}'}$, we check if it can be discarded by the completion bounds. If not, we consider the following two cases. When $i^{\mathscr{b}'} \neq 0$, the dominance check is skipped

and the new label $L^{\flat'}$ is added to the pool. When $i^{\flat'}=0$, we check whether $L^{\flat'}$ is dominated by any $L\in\mathcal{L}$. For a backward path $\flat=(i_0,i_1,\cdots,i_{k_\flat})$, its cost is defined to be $c^\flat:=\sum_{g=0}^{k_\flat-1}c_{i_{g+1}i_g}$.

PROPOSITION 3. *$L^{\flat_1}=(N^{\flat_1},q^{\flat_1},e^{\flat_1},\ell^{\flat_1},d^{\flat_1},i^{\flat_1},\beta^{\flat_1},\gamma^{\flat_1})$ and $L^{\flat_2}=(N^{\flat_2},q^{\flat_2},e^{\flat_2},\ell^{\flat_2},d^{\flat_2},i^{\flat_2},\beta^{\flat_2},\gamma^{\flat_2})$ are two feasible labels. $L^{\flat_1}$ dominates $L^{\flat_2}$ if the following six relations hold.* (i) $i^{\flat_1}=i^{\flat_2}$, (ii) $N^{\flat_1}=N^{\flat_2}$, (iii) $\ell^{\flat_1}\geq\ell^{\flat_2}$, (iv) $e^{\flat_1}+d^{\flat_1}\leq e^{\flat_2}+d^{\flat_2}$, (v) $d^{\flat_1}\leq d^{\flat_2}$ *if* $e^{\flat_1}\leq\ell^{\flat_2}$, *and* (vi) $c^{\flat_1}\leq c^{\flat_2}$.

Proposition 3 is proved in Section EC.1.5 of the e-companion.

6.4. *Step 4*: LB Tightening

This step essentially combines Steps 4 and 5 in the ESF. We start with formulation $\overline{\mathrm{F}}^{\mathcal{S}_2}_{\mathcal{H},\mathcal{I}}$, obtained from $\overline{\mathrm{F}}^{\mathcal{S}}_{\mathcal{H},\mathcal{I}}$ by replacing $\mathcal{S}$ with $\mathcal{S}_2$, and apply RG iteratively until no new violated cuts can be identified. After each RG iteration, we update the LB to the optimal value of the current LP and remove variables with reduced costs (with respect to the dual optimal solution to the current LP) larger than UB$-$LB. It accelerates the computation significantly since we can remove a large proportion of columns in the first several RG iterations, resulting in much smaller-sized LPs to be solved in subsequent iterations.

6.5. *Step 5*: Structure Pruning

Step 5 is new and is motivated by the fact that the following $\overline{\mathrm{F}}^{\mathcal{S}_2}$ usually has multiple dual optimal solutions, and the reduced cost of a column may be different with respect to different optimal dual values. In other words, the optimal solution to the dual $\overline{\mathrm{DF}}^{\mathcal{S}_2}$ is not unique, and we would like to find one that helps to remove as many columns as possible.

$$
\begin{aligned}
(\overline{\mathrm{F}}^{\mathcal{S}_2}) \qquad \bar{z}^{\mathcal{S}_2} \;=\; \min \quad & \sum_{s\in\mathcal{S}_2} c_s x_s & & \\
\text{s.t.} \quad & \sum_{s\in\mathcal{S}_2} \alpha_{is} x_s = 1, & & \forall i\in N,\\
& \sum_{s\in\mathcal{S}_2} \mathbb{1}_{[\ell_s,e_s+d_s)}(t)\, x_s \leq m, & & \forall t\in[a_0,b_0],\\
& \sum_{s\in\mathcal{S}_2} \mathbb{1}_{\mathcal{C}_s}((i,j,k))\, x_s \leq 1, & & \forall (i,j,k)\in\mathcal{C},\\
& x_s\geq 0, & & \forall s\in\mathcal{S}_2.
\end{aligned}
$$

$$
\xRightarrow{Dual}
\begin{cases}
(\overline{\mathrm{DF}}^{\mathcal{S}_2}) \qquad \max & \displaystyle\sum_{i\in N}\pi_i + \sum_{t\in[a_0,b_0]} m\pi_t + \sum_{(i,j,k)\in\mathcal{C}} \pi_{ijk} & \\
\text{s.t.} & \displaystyle\sum_{i\in N}\alpha_{is}\pi_i + \sum_{t\in[a_0,b_0]} \mathbb{1}_{[\ell_s,e_s+d_s)}(t)\,\pi_t + \sum_{(i,j,k)\in\mathcal{C}} \mathbb{1}_{\mathcal{C}_s}((i,j,k))\,\pi_{ijk}\leq c_s, & \forall s\in\mathcal{S}_2,\\
& \pi_t\leq 0,\ \forall t\in[a_0,b_0], & \\
& \pi_{ijk}\leq 0,\ \forall (i,j,k)\in\mathcal{C}. &
\end{cases}
$$

Note that the reduced cost of each variable x_s is computed by $\bar{c}_s = c_s - (\sum_{i\in N}\alpha_{is}\pi_i + \sum_{t\in[a_0,b_0]}\mathbb{1}_{[\ell_s,e_s+d_s)}(t)\,\pi_t + \sum_{(i,j,k)\in\mathcal{C}}\mathbb{1}_{\mathcal{C}_s}((i,j,k))\,\pi_{ijk})$. To remove more variables, we try to increase

the number of variables with reduced costs larger than the current gap UB−LB. To this end, we maximize $\sum_{s\in\mathcal{S}_2}\bar{c}_s$, the sum of the reduced costs of all the variables. Meanwhile, we ensure that the resulting solution is an optimal dual solution to $\overline{\mathrm{F}}^{\mathcal{S}_2}$, which can be achieved by solving the following LP, denoted by $\widetilde{\mathrm{DF}}^{\mathcal{S}_2}$, or equivalently its dual LP, denoted by $\widetilde{\mathrm{F}}^{\mathcal{S}_2}$.

$$
\begin{aligned}
(\widetilde{\mathrm{DF}}^{\mathcal{S}_2}) \quad \max \quad & \sum_{s\in\mathcal{S}_2}\left(c_s-\sum_{i\in N}\alpha_{is}\pi_i-\sum_{t\in[a_0,b_0]}\mathbb{1}_{[\ell_s,e_s+d_s)}(t)\,\pi_t-\sum_{(i,j,k)\in\mathcal{C}}\mathbb{1}_{\mathcal{C}_s}((i,j,k))\,\pi_{ijk}\right)\\
\text{s.t.} \quad & \sum_{i\in N}\alpha_{is}\pi_i+\sum_{t\in[a_0,b_0]}\mathbb{1}_{[\ell_s,e_s+d_s)}(t)\,\pi_t+\sum_{(i,j,k)\in\mathcal{C}}\mathbb{1}_{\mathcal{C}_s}((i,j,k))\,\pi_{ijk}\le c_s, && \forall s\in\mathcal{S}_2,\\
& \sum_{i\in N}\pi_i+\sum_{t\in[a_0,b_0]}m\pi_t+\sum_{(i,j,k)\in\mathcal{C}}\pi_{ijk}=\bar{z}^{\mathcal{S}_2},\\
& \pi_t\le 0,\ \forall t\in[a_0,b_0],\\
& \pi_{ijk}\le 0,\ \forall (i,j,k)\in\mathcal{C}.
\end{aligned}
$$

$$
\xRightarrow{Dual}
\begin{cases}
(\widetilde{\mathrm{F}}^{\mathcal{S}_2}) \quad \min & \displaystyle\sum_{s\in\mathcal{S}_2}c_s x_s+\bar{z}^{\mathcal{S}_2}y\\
\text{s.t.} & \displaystyle\sum_{s\in\mathcal{S}_2}\alpha_{is}x_s+y=-\sum_{s\in\mathcal{S}_2}\alpha_{is}, && \forall i\in N,\\
& \displaystyle\sum_{s\in\mathcal{S}_2}\mathbb{1}_{[\ell_s,e_s+d_s)}(t)\,x_s+my\le-\sum_{s\in\mathcal{S}_2}\mathbb{1}_{[\ell_s,e_s+d_s)}(t), && \forall t\in[a_0,b_0],\\
& \displaystyle\sum_{s\in\mathcal{S}_2}\mathbb{1}_{\mathcal{C}_s}((i,j,k))\,x_s+y\le-\sum_{s\in\mathcal{S}_2}\mathbb{1}_{\mathcal{C}_s}((i,j,k)), && \forall (i,j,k)\in\mathcal{C},\\
& x_s\ge 0, && \forall s\in\mathcal{S}_2.
\end{cases}
$$

In our experiments, we found $\widetilde{\mathrm{F}}^{\mathcal{S}_2}$ is easier to solve than $\widetilde{\mathrm{DF}}^{\mathcal{S}_2}$. Actually, $\widetilde{\mathrm{F}}^{\mathcal{S}_2}$ resembles the original $\overline{\mathrm{F}}^{\mathcal{S}_2}$, with only one additional decision variable and different right hand side of the constraints, and can be resolved efficiently. Let $(\pi_i^*,\pi_t^*,\pi_{ijk}^*)$ be an optimal dual solution to $\widetilde{\mathrm{F}}^{\mathcal{S}_2}$. The reduced cost of each variable x_s in $\overline{\mathrm{F}}^{\mathcal{S}_2}$ is computed by $c_s-(\sum_{i\in N}\alpha_{is}\pi_i^*+\sum_{t\in[a_0,b_0]}\mathbb{1}_{[\ell_s,e_s+d_s)}(t)\,\pi_t^*+\sum_{(i,j,k)\in\mathcal{C}}\mathbb{1}_{\mathcal{C}_s}((i,j,k))\,\pi_{ijk}^*)$, which coincides with that of $\widetilde{\mathrm{F}}^{\mathcal{S}_2}$. Thus, we can obtain the desired reduced costs directly after solving $\widetilde{\mathrm{F}}^{\mathcal{S}_2}$. Subsequently, structure pruning is performed to remove columns with updated reduced costs more than UB−LB. Let $\mathcal{S}_3$ be the set of structures remained after this process.

6.6. *Step 6*: Superstructure Generation

The set of superstructures $\mathcal{U}_3$ is generated from $\mathcal{S}_3$ by a very straightforward and effective procedure as follows. We start from $\mathcal{U}_3=\emptyset$ and partition $\mathcal{S}_3$ into subsets $\mathcal{G}_1,\cdots,\mathcal{G}_p$, where each subset consists of structures that visit the same set of customers and have the same cost and duration.

For any $\mathcal{G}\in\{\mathcal{G}_1,\cdots,\mathcal{G}_p\}$, suppose $\mathcal{G}=\{s_{i_1},s_{i_2},\cdots,s_{i_k}\}$. We first sort the structures in a non-decreasing order according to the left endpoints of the associated departure time intervals $e_{s_{i_1}},\cdots,e_{s_{i_k}}$. Without loss of generality, suppose $e_{s_{i_1}}\le e_{s_{i_2}}\le\cdots\le e_{s_{i_k}}$. Due to the dominance rule, we have $\ell_{s_{i_1}}\le\ell_{s_{i_2}}\le\cdots\le\ell_{s_{i_k}}$, otherwise some structures could have been dominated. Find the largest $1\le k'\le k$ such that $\ell_{s_{i_1}}\ge e_{s_{i_2}}$, $\ell_{s_{i_2}}\ge e_{s_{i_3}}$, $\cdots$, and $\ell_{s_{i_{k'-1}}}\ge e_{s_{i_{k'}}}$ hold. In particular,

if $\ell_{s_{i_1}} < e_{s_{i_2}}$, we have $k' = 1$. Then, we generate a new superstructure $u := \{s_{i_1}, s_{i_2}, \cdots, s_{i_{k'}}\}$ with the associated departure time interval $[e_u, \ell_u] := [e_{s_1}, \ell_{s_{k'}}]$. After that, we update $\mathcal{U}_3 \leftarrow \mathcal{U}_3 \cup \{u\}$ and $\mathcal{G} \leftarrow \mathcal{G} \setminus \{s_{i_1}, s_{i_2}, \cdots, s_{i_{k'}}\}$. This process is conducted recursively until $\mathcal{G} = \emptyset$ for all $\mathcal{G} \in \{\mathcal{G}_1, \cdots, \mathcal{G}_p\}$, and we obtain the desired $\mathcal{U}_3$ at termination.

6.7. *Step 7*: Optimal Solution Computation

For instances with 70 or more customers, $\mathcal{U}_3$ obtained in *Step 6* can have millions of elements, resulting in IPs with millions of binary variables that are usually intractable. Instead of solving $\mathrm{F}^{\mathcal{U}_3}$ directly in the same way as solving the final formulation in Step 6 of the ESF, we propose the MPSC solution scheme that incrementally uses the columns in the pool.

6.7.1. The MPSC for Solving $\mathrm{F}^{\mathcal{U}_3}$. When $|\mathcal{U}_3|$ is larger than a predetermined constant n_7^1, we sort the columns non-increasingly according to their reduced costs γ_u for $u \in \mathcal{U}_3$. In the first phase, let $\overline{\mathcal{U}}_1$ be the set of superstructures corresponding to the n_7^1 columns with the smallest reduced costs. Then, we solve $\mathrm{F}^{\overline{\mathcal{U}}_1}$, obtained from $\mathrm{F}^{\mathcal{U}}$ with $\mathcal{U}$ replaced by $\overline{\mathcal{U}}_1$, similarly to solving $\mathrm{F}^{\mathcal{S}_1}$ in *Step 2*. The current UB is set as a cutoff value. If a new feasible solution is found, we update the UB and remove all superstructures u from $\mathcal{U}_3$ with $\gamma_u > \mathrm{UB}-\mathrm{LB}$. In case more than n_7^1 elements are left in $\mathcal{U}_3$ after the removal, we continue to the next phase. Otherwise, the solution obtained is optimal, and we can stop here. For each of the subsequent phases except the last one, we add the next n_7^2 smallest (in terms of reduced costs) columns to the current IP. After solving each new IP, we update the UB and $\mathcal{U}_3$ as appropriate. In the last phase, we use all columns corresponding to the remaining elements in $\mathcal{U}_3$. In this case, the lower bound reported by the solver is valid for the original problem. It can be used to decide the quality of our current best feasible solution if optimality is not proved upon termination due to the time or machine limit.

6.7.2. The RCC. Inspired by the well-known RCF, we propose the RCC. To the best of our knowledge, RCC is new while its special case, RCF, has been widely used (see e.g., Desaulniers et al. 2020, Irnich et al. 2010). For each superstructure $u \in \mathcal{U}_3$, let γ_u be its reduced cost. We define RCC as follows.

$$\sum_{u \in \mathcal{U}_3} \mathbb{1}_{\left\{\gamma : \gamma > \frac{\mathrm{UB}-\mathrm{LB}}{k}\right\}}(\gamma_u)\, x_u \le k-1, \qquad \forall k \in \{1, 2, \cdots\}. \tag{10}$$

It requires that for each positive integer number k, the number of superstructures with reduced costs larger than $\frac{\mathrm{UB}-\mathrm{LB}}{k}$ in any optimal solution should be no larger than $k-1$. When $k = 1$, it is essentially RCF. The validity of (10) is stated in the following Proposition 4, whose proof is available in Section EC.1.6 of the e-companion.

Proposition 4. *Inequality* (10) *is valid for* $\mathrm{F}^{\mathcal{U}_3}$.

RCC is dense cut and may slow down the solver despite its effectiveness in shrinking the feasible region of the relaxation. It has been observed in our experiments that RCC deteriorates the performance for most cases but is effective in closing the gap faster for some large Solomon instances with 100 customers. In particular, without any RCC, the optimality gaps of the three 100-customer instances, i.e., C202, C203, and R202, are 0.29%, 0.61%, and 0.79%, respectively. The numbers decrease to 0.19%, 0.58%, and 0.74%, respectively, when the RCC is added. Thus, the RCC is disabled by default in our implementation but can be turned on manually.

7. Numerical Results

In this section, we present four sets of numerical experiments. The first one is to demonstrate the strength of our EPCEM compared with the ESF. All the results of the ESF presented in Paradiso et al. (2020) are computed in the single-thread mode by a Windows server running at 2.59GHz with 16GB of RAM. For a fair comparison, we run all the experiments in Section 7.1 in the single-thread mode on Machine 1, a personal computer running Ubuntu 18.04 with very similar hardware: a 2.60GHz CPU and 16GB of RAM. The major differences (enhancements) between our EPCEM and the ESF have been highlighted in Section 5.2. To reveal their effectiveness separately, we carefully design the second set of experiments where some difficult instances are solved. The third set of experiments analyzes the trade-off between the optimal travel cost and the number of vehicles needed. The last one serves the function of further demonstrating the potential of the EPCEM. To this end, we solve substantially larger (more difficult) instances. The last three sets of experiments are run on Machine 2, a workstation running Red Hat Enterprise Linux 8.2 with Intel(R) Core(TM) i9-10900K CPU @ 3.70GHz and 128GB of RAM, using 8 threads to take advantage of the multiple cores available.

The EPCEM is implemented in C++ language and compiled into a library by g++ 8.3.1. Gurobi 9.1.1 is used as an LP and IP solver. Following the convention in Paradiso et al. (2020), for *Step 7*, we disable the presolve phase and the ESFCS is embedded in the lazy callback; all other parameters are set to default. The time limit for solving each instance is set to 3 hours, and all input values of travel time and cost are truncated to one decimal digit. The compiled C++ library and all the test instances are available at `https://github.com/Yu1423/CMTVRPTW`.

7.1. Comparison with the ESF

In this section, we compare our EPCEM with the ESF, the best existing exact method, for solving the CMTVRPTW and its variants. Modifications required for the EPCEM to solve the four variants are included in Sections EC.3.1 to EC.3.4 of the e-companion. The results of the EPCEM applied to

solving much larger instances are postponed to Section 7.4. For each problem type, we consider the same instances as Paradiso et al. (2020). For the sake of completeness, we describe the instances in each subsection. Figure 2 summarizes the results, and more details can be found in Section EC.4 of the e-companion. The following information is included: the number of instances solved within the 3-hour per instance time limit (Solved), and the average computing time (in seconds) of instances solved (CPU). All the numbers for the ESF are copied directly from Paradiso et al. (2020).

7.1.1. Comparison on the CMTVRPTW This test set contains 81 instances derived from the type 2 Solomon instances. More specifically, there are three groups of type 2 instances, which are C, R, and RC, with 8, 11, and 8 instances, separately, and thus 27 in total. For each instance, we consider three cases, i.e., the first 25, 40, and 50 customers, which results in 81 instances. For instances with 25 customers, there are two vehicles available. When there are 40 or 50 customers, we allow four vehicles. The vehicle capacity Q is set to 100 for all the instances.

As shown in Figure 2, our EPCEM solves all 81 instances within the 3-hour per instance time limit, while the ESF can only solve 60 of them. In particular, the ESF cannot solve any instance from group R with 50 customers. Compared with the ESF, the EPCEM reduces the computing time by more than 91% for the 60 instances that can be solved by the ESF.

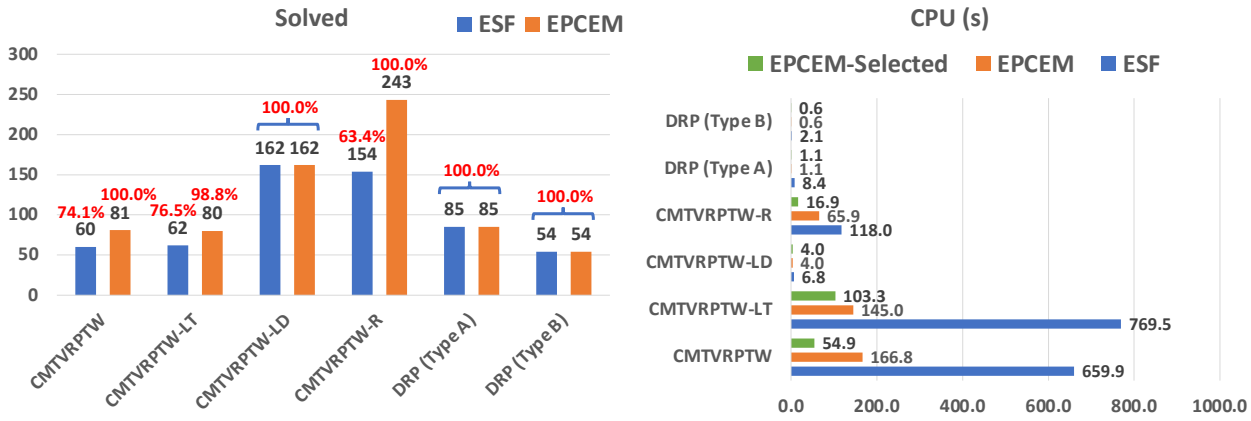

Figure 2 Comparison on the number of instances solved and the average computing time (in seconds) for the CMTVRPTW and its four variants. Each number in red in the left figure denotes the corresponding percentage of instances solved. For the right figure, the numbers beside the orange (EPCEM) and green (EPCEM-Selected) bars represent the average times of the EPCEM over all instances that can be solved by the EPCEM and the ESF, respectively.

7.1.2. Comparison on the CMTVRPTW-LT For the CMTVRPTW-LT, each vehicle spends a loading time, computed as the sum of the loading time lt_i for each customer i visited in this trip, at the depot before it can start the trip, where lt_i is the time needed to load goods for customer $i \in N$. The test set for the CMTVRPTW-LT consists of the same instances as in Section 7.1.1.

Following the procedure introduced in Hernandez et al. (2016), the loading time of each customer $i \in N$ is set to $\mathrm{lt}_i = 0.2r_i$, i.e., 20% of the service time.

The EPCEM can solve all but one instance (80 instances), while the ESF can only solve 62 of them. In terms of computing time, the EPCEM is much faster. As shown in Figure 2, the average CPU of the EPCEM over all instances solved by the ESF is reduced by more than 86% compared with that of the ESF. Thus, we conclude that the EPCEM is also significantly more effective than the ESF in solving the CMTVRPTW-LT.

7.1.3. Comparison on the CMTVRPTW-LD We test 162 CMTVRPTW-LD instances, obtained from the 81 instances in Section 7.1.2 by assigning two different trip duration values $\bar{d}$ to each instance. As suggested in Azi et al. (2010), we use $\bar{d} \in \{220, 250\}$ for instances in group C and $\bar{d} \in \{75, 100\}$ for groups R and RC. In this case, the vehicle capacity Q is no longer universally set to 100. Instead, $Q = 700$ for instances in group C and $Q = 1000$ for groups R and RC.

Since the CMTVRPTW-LD is expected to be much easier to solve compared with the previous two problems due to the presence of the duration limit, we disable the completion bounds in the BLMCB, i.e., we use purely the BLM for *Steps 1* and *3*. The experiments confirm our intuition that CMTVRPTW-LD is indeed much easier to solve. From Figure 2, we can see that both the EPCEM and the ESF can solve all 162 instances fast. The average solution time is less than ten seconds. Still, the EPCEM is much faster than the ESF.

7.1.4. Comparison on the CMTVRPTW-R For the CMTVRPTW-R, each customer $i \in N$ has an associated release date rd_i, and each vehicle cannot depart the depot earlier than any of the release dates of the customers visited in the trip. Neither the loading time nor the limited duration is considered in this case. The CMTVRPTW-R instances are derived from the Solomon instances via the procedure described in Cattaruzza et al. (2016a). This test set consists of 243 instances, obtained by considering the first 25, 40, and 50 customers with release date parameter $\kappa \in \{0.25, 0.5, 0.75\}$. That means, for each of the 27 instances, there are 9 combinations of the number of customers and the release date, making it 243 in total. Similar to the CMTVRPTW, instances with 25 customers have two vehicles, and instances with 40 or 50 customers have four vehicles. The vehicle capacity is set to 100.

As shown in Figure 2, the EPCEM can solve all the instances, while ESF can only solve less than 64% of them (154 out of the 243). In addition, the average computing time of the EPCEM over instances solved by the ESF is less than 15% of that spent by the ESF. The EPCEM again outperforms the ESF substantially in terms of both the number of instances solved and computational time.

7.1.5. Comparison on the DRP We use two test sets for the DRP. One of them is created according to the framework presented in Solomon (1987) and Dorling et al. (2016), denoted by Set A. The other one, called Set B, is derived from Solomon instances. The details on how to generate these instances can be found in Cheng et al. (2020). Set A has 85 instances which are further divided into groups A1 and A2. Both groups have instances with 10, 15,$\cdots$, 45 customers, and A2 additionally has instances with 50 customers. The difference between Sets A1 and A2 lies in the depot location. Set B has 54 instances with the first 25 or 40 customers.

Similar to the CMTVRPTW-LD, we turn off the completion bounds in the BLMCB since the DRP instances are also very easy to solve. Figure 2 reports the results of the two sets of DRP instances. All instances in Sets A and B can be solved by the EPCEM and the ESF very fast. Our EPCEM completes the computation in a much shorter time than the ESF.

7.2. Effectiveness of the Enhancements

We design five experiments, denoted by Exp1 to Exp5, to demonstrate the isolated effectiveness of the first five enhancements listed in Section 1. For each of them, we either replace it by the counterpart from the ESF, if any, or disable it if it is entirely new. One of the reasons why we skip showing the effectiveness of E6, the ESFCS, directly is because implementing the SFC separator in the ESF is highly non-trivial. Meanwhile, it cannot be disabled since it may yield wrong results. Its high effectiveness can be concluded based on our observation from the numerical study that the computational time cost by the ESFCS is negligible compared with the total solution time.

For E1, we run Exp1 with the RG disabled. In this case, the ACRG essentially reduces to a pure column generation method and the formulation solved in *Step 1* is the same as that solved in Step 2 of the ESF. For E2, instead of solving $\mathrm{F}^{\mathcal{S}_1}$ to compute a valid UB, we run Exp2 with a guessed initial UB (5% gap) as is done in the ESF. For E3, we would like to demonstrate the benefits of solving the auxiliary problem to prune unnecessary structures. Thus, Exp3 is run with *Step 5* skipped. For E4, we skip *Step 6* in our Exp4 and solve the structure-based formulation as in the ESF. Lastly, for E5, instead of applying our MPSC, all columns in the pool are used to construct the IP solved directly in Exp5. As a baseline, Exp0 is run in the default setting, i.e., all seven steps shown in Algorithm 1 are turned on. We test 27 difficult CMTVRPTW instances derived from type 2 Solomon instances with 70 customers and six vehicles, and the vehicle capacity Q is set to 100.

For each of the five experiments, i.e., Exp1 to Exp5, we report the number of instances solved within the 3-hour time limit (Solved) and the average computing time (in seconds) of all the 27 instances (Time). The time of an unsolved instance is set to 10,800 seconds (3 hours). As shown in Figure 3, Exp1 and Exp2 can only solve 15 and 9 of the 27 instances, respectively. Thus, we conclude that enhancements E1 and E2, i.e., solving $\overline{\mathrm{F}}^{\mathcal{S}}$ partially by the ACRG and computing the initial UB

by solving $F^{\mathcal{S}_1}$, bring the most performance gains. In addition, although Exp3 and Exp4 can also solve all 27 instances, the solutions speed is significantly slower. More precisely, Exp3 and Exp4 take 20.5% and 25.8%, respectively, more time than the baseline Exp0. According to Exp5, the MPSC seems to boost the performance the least in terms of computational time. Actually, for even more challenging instances, e.g., the eight instances derived from group C (type 2 Solomon instances) with 100 customers and eight vehicles, the default setting can solve five out of the eight (see Table 2 in Section 7.4.1), but only one of them can be solved if the MPSC is disabled. In addition, the MPSC adds columns incrementally and uses any updated UB to further remove unnecessary columns in the pool. Consequently, the final IP solved has a much smaller size and thus requires significantly less memory, which is especially important for machines with relatively limited memory.

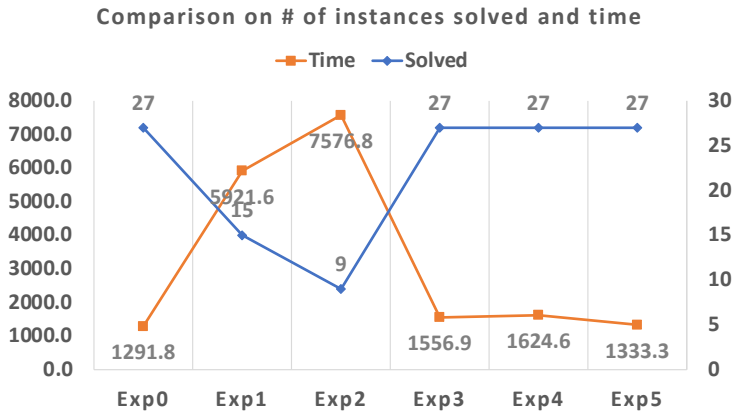

Figure 3 Comparison on the number of instances solved and the average computing time (in seconds) when one enhancement is disabled each time.

7.3. Numerical Analysis on the Trade-off

Allowing multiple trips reduces the number of vehicles needed, but in the meantime, the total travel cost will increase if fewer vehicles are available. In this section, we perform a numerical analysis of this trade-off by repeatedly solving a set of instances while gradually decreasing the number of available vehicles. After the solution is obtained, we perform the post-processing for a fair comparison, which computes the minimum number of vehicles needed to perform the trips in the solution. In other words, we assign the trips to as few vehicles as possible, which can be accomplished by calling the ESFCS several times. For example, if the solution obtained has ten trips, we first call the ESFCS with $m = 1$ and see if all the ten trips can be made by using only one vehicle. If not, we increase m to 2 and call the ESFCS again. We stop until the ESFCS confirms that all the ten trips can be made by using the m vehicles, and the value of m is the minimum number of vehicles needed for this solution. Evidently, this process can be accelerated using bisection.

We first apply the EPCEM to solve a set of instances as the CVRPTW with infinite fleet size. This can be accomplished by a minor change that sets the ESFCS to return the value $|\overline{\mathcal{S}}|$ for any input subset of structures, $\overline{\mathcal{S}}$ (or $|\overline{\mathcal{U}}|$ for any subset of superstructures $\overline{\mathcal{U}}$). Let v^* be the optimal value, x^* be the optimal solution, and n_t be the number of trips in x^*. We compute the minimum number of vehicles needed, denoted by n_v, to conduct these n_t trips if we allow each vehicle to make multiple trips. After that, we solve the same instances as the CMTVRPTW, i.e., allowing multiple trips in the solution process, with the number of available vehicles m set to $\lceil \frac{n_t}{k} \rceil$, where $k \in \{1.5, 2.0, 2.5, 3.0\}$. For example, when $m = \lceil \frac{n_t}{2.0} \rceil$, on average each vehicle needs to perform two trips. Similarly, we can obtain the optimal value, denoted by $\bar{v}^*$, and the corresponding minimum number of vehicles needed, denoted by $\bar{n}_v$, to perform the trips in the solution. It is worth noticing that the same instances with a limited fleet size $m = \lceil \frac{n_t}{k} \rceil$, $k \in \{1.5, 2.0, 2.5, 3.0\}$, and multiple trips disallowed, i.e., solved as the CVRPTW, are all infeasible.

We solve all the 108 instances from Sections 7.1.1 and 7.2 consisting of 27 instances for each configuration $n \in \{25, 40, 50, 70\}$, which can all be solved to optimality according to our results in Section 7.4. We compare the travel cost v^* and the minimum number of vehicles n_v needed for the CVRPTW with the travel cost $\bar{v}^*$ and the minimum number of vehicles $\bar{n}_v$ for the CMTVRPTW. We use MT-k to denote the case when $m = \lceil \frac{n_t}{k} \rceil$, where $k \in \{1.5, 2.0, 2.5, 3.0\}$. We report the average number of the 27 instances for each configuration n. Figure 4 shows the changes in travel cost as we gradually decrease the number of available vehicles m input to the CMTVRPTW.

We observe from Figure 4 that when $m = \lceil \frac{n_t}{3.0} \rceil$, we can obtain solutions with no more than 7% increase in the travel cost and more than 45% decrease in the minimum number of vehicles needed. More than 30% decrease in the minimum number of vehicles needed with less than 4% increase in the travel cost can be achieved when each vehicle approximately performs two and a half trips, i.e., $m = \lceil \frac{n_t}{2.5} \rceil$. This comparison provides industry practitioners with guidance on deciding a suitable fleet size to run the business when multiple trips are necessary. When the vehicle cost is fixed and known, the total costs can be computed to make a more direct comparison for different fleet sizes and help to identify an optimal one. In addition, the conclusion that a relatively small sacrifice in the travel cost can bring in significant savings in the number of vehicles is consistent across different problem sizes. Furthermore, for large instances, the travel cost increases less than that of smaller ones. For example, the average increase in travel cost is less than 3% for instances with 70 customers compared to the 7% when there are 40 customers. This suggests that solving the CMTVRPTW instead of the CVRPTW is even more beneficial for large instances.

7.4. Computational Results for Large Instances

In this section, we test much larger instances in terms of the number of customers, which are substantially more difficult to solve due to the exponential growth in such combinatorial problems.

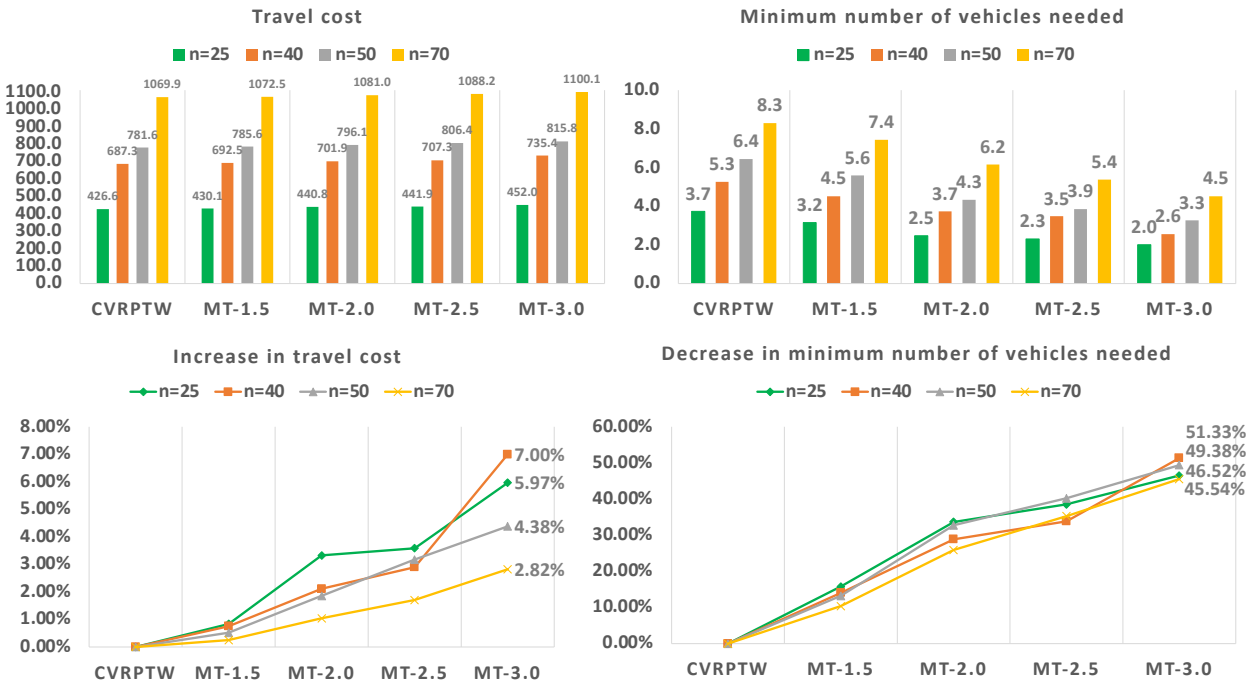

Figure 4 The trade-off between the travel cost and the minimum number of vehicles needed for the solution obtained. The top two subfigures report the actual average values of the travel cost and the minimum number of vehicles needed. The bottom two subfigures report the increase (in percentage) of the average travel cost and the decrease (in percentage) of the average minimum number of vehicles needed with respect to the CVRPTW.

Tables 2 to 6 summarize the results and more details can be found in Section EC.5 of the e-companion. In addition to the information reported in Section 7.1, we include the following items: the group name (Group), the number of customers (n), the number of instances in the group (Inst), the average optimality gap $\frac{\text{UB}-\text{LB}}{\text{UB}} \times 100\%$ (Gap%), where UB and LB are the best upper and lower bounds, the average gap between the lower bound computed in *Step 1* and UB ($\text{LB}_1\%$), the average cardinality of $\mathcal{S}_1$ yielded in *Step 1* ($|\mathcal{S}_1|$), the average gap between the initial upper bound computed in *Step 2* and UB ($\text{UB}_1\%$), the average cardinality of $\mathcal{S}_2$ yielded in *Step 3* ($|\mathcal{S}_2|$), the average gap between the lower bound computed in *Step 4* and UB ($\text{LB}_2\%$), the average cardinality of $\mathcal{S}_3$ yielded in *Step 5* ($|\mathcal{S}_3|$), the average cardinality of $\mathcal{U}_3$ yielded in *Step 6* ($|\mathcal{U}_3|$), and the average computing time of the MPSC in *Step 7* (CPU_7). The average value of Gap is computed over all instances such that a Gap value is available, i.e., gaps equal to 0 are included, and the number in the parenthesis is computed over instances with Gap values strictly positive, i.e., gaps equal to 0 are excluded. All other averages are computed over instances that can be solved within the time limit.

7.4.1. Results for the CMTVRPTW We have 81 large instances derived from the 27 type 2 Solomon instances. For each instance, we consider three cases, i.e., the first 70, 80, and all 100

customers, respectively. The numbers of vehicles are set to 6, 7, and 8, respectively. The vehicle capacity Q again equals 100 for all instances.

Table 2 Summary of the Results for the CMTVRPTW.

Group	n	Inst	Solved	Gap%	CPU	Step1		Step2	Step3	Step4	Step5	Step6	Step7
						LB_1%	$\lvert\mathcal{S}_1\rvert$	UB_1%	$\lvert\mathcal{S}_2\rvert$	LB_2%	$\lvert\mathcal{S}_3\rvert$	$\lvert\mathcal{U}_3\rvert$	CPU_7
C	70	8	8	0.0	3198.8	1.2	88,921	0.2	531,071	1.1	379,638	372,859	3125.3
C	80	8	5	0.4 (1.0)	3249.4	1.6	108,024	0.6	2,847,609	1.0	1,003,564	1,003,431	3037.0
C	100	8	5	0.4 (1.1)	6693.1	1.2	151,899	0.8	5,367,184	1.0	3,867,484	3,867,212	6148.3
R	70	11	11	0.0	538.7	1.2	48,610	0.3	207,629	1.0	119,322	114,302	452.9
R	80	11	11	0.0	998.7	1.2	63,931	0.5	987,228	1.0	516,542	503,744	777.0
R	100	11	5	0.9 (1.7)	4025.1	1.1	111,912	0.4	2,749,862	0.9	1,465,250	1,409,360	3428.4
RC	70	8	8	0.0	420.4	1.4	46,587	1.0	517,605	1.2	384,410	368,391	310.1
RC	80	8	8	0.0	333.3	0.9	55,580	1.0	564,415	0.8	408,835	395,924	57.7
RC	100	8	4	0.5 (1.0)	1982.7	1.0	91,315	0.4	1,225,467	0.8	766,495	719,641	1539.9
All		81	65	0.3 (1.3)	1943.1	1.2	76,786	0.6	1,319,589	1.0	786,539	771,915	1703.1

As shown in Table 2, the EPCEM can solve all instances with 70 customers. Instances with 70 customers are substantially harder to solve than 50-customer ones and have never been solved before. The average computing time is less than ten minutes for all instances with 70 customers except for those in group C, which can be solved within an hour on average. Only three instances with 80 customers cannot be solved within the 3-hour limit, which are all from group C. The EPCEM has difficulty in solving 100-customer instances, which is not too surprising since they are much more challenging to solve. In this case, instances from groups R and RC seem to be the most difficult ones. Although the EPCEM cannot solve some instances, the average optimality gap is 0.3% for all instances, suggesting that the solutions obtained are generally of high quality. In addition, *Step 7* is the most time-consuming step, and it on average takes up around 88% of the total time.

One of the reasons why the EPCEM fails to solve some instances is that the enumeration in *Step 3* takes too much time and memory. When the limit on the number of columns to enumerate, which is set to 20 million in our implementation, is reached, the algorithm terminates. Another reason is that even if *Step 3* is completed successfully, we may still end up with millions of superstructures. Consequently, we have an IP in *Step 7* that is beyond the reach of Gurobi.

7.4.2. Results for the CMTVRPTW-LT We use the same 81 instances from Section 7.4.1, and the loading time of each customer is also set to 20% of the service time.

As shown in Table 3, the EPCEM solves 63 of the 81 instances. Specifically, the EPCEM again solves all instances with no more than 70 customers, and only three instances from group C with 80 customers cannot be solved within the time limit. Similarly, the average optimality gap is 0.3% for all instances. In contrast to the CMTVRPTW, fewer instances with 100 customers from group C can be solved. The average computing time for all solved instances is around 33 minutes, of which *Step 7* takes up around 85%.

Table 3 Summary of the Results for the CMTVRPTW-LT.

Group	n	Inst	Solved	Gap%	CPU	Step1		Step2	Step3	Step4	Step5	Step6	Step7
						LB_1%	$\lvert\mathcal{S}_1\rvert$	UB_1%	$\lvert\mathcal{S}_2\rvert$	LB_2%	$\lvert\mathcal{S}_3\rvert$	$\lvert\mathcal{U}_3\rvert$	CPU_7
C	70	8	8	0.0	4017.7	1.3	87,457	0.2	521,002	1.2	355,409	350,013	3941.6
C	80	8	5	0.4 (1.1)	5194.7	1.5	105,756	0.5	2,133,188	1.1	803,499	803,408	4995.2
C	100	8	3	0.8 (1.2)	5244.1	1.1	164,166	0.4	3,310,073	0.9	1,830,971	1,788,414	4858.7
R	70	11	11	0.0	253.7	1.2	49,709	0.6	257,417	1.0	146,075	139,974	164.8
R	80	11	11	0.0	936.6	1.1	65,624	0.6	1,409,553	1.0	799,325	783,621	623.2
R	100	11	5	0.8 (1.4)	2237.1	1.1	120,802	0.5	4,349,987	0.9	2,284,954	2,125,918	1362.3
RC	70	8	8	0.0	938.4	1.5	45,862	1.0	538,008	1.3	403,991	382,585	693.2
RC	80	8	8	0.0	481.1	1.0	57,832	0.9	795,064	0.8	546,084	524,039	74.9
RC	100	8	4	0.4 (0.8)	3810.4	1.1	97,490	0.6	2,153,226	0.8	1,154,426	1,067,552	3176.7
All		81	63	0.3 (1.2)	1979.7	1.2	76,399	0.6	1,335,369	1.0	736,447	706,265	1673.3

7.4.3. Results for the CMTVRPTW-LD We generate 162 instances from the 81 instances in Section 7.4.2 by considering two different limits $\bar{d}$ values for each instance in the same way as in Section 7.1.3. Similarly, the vehicle capacity Q is set to 700 for instances in group C and 1,000 for groups R and RC. We enable completion bounds computation in the BLMCB, which can be turned off to accelerate the solution for small (easy) instances as in Section 7.1.3.

Table 4 shows that the EPCEM can solve 158 of the 162 instances. More precisely, it can solve all instances with up to 80 customers, and the four unsolved instances are all from group R with 100 customers. The average computing time of the 158 solved instances is less than two minutes, indicating that the EPCEM can solve large CMTVRPTW-LD instances fast in general.

Table 4 Summary of the Results for the CMTVRPTW-LD.

Group	n	$\bar{d}$	Inst	Solved	Gap%	CPU	Step1		Step2	Step3	Step4	Step5	Step6	Step7
							LB_1%	$\lvert\mathcal{S}_1\rvert$	UB_1%	$\lvert\mathcal{S}_2\rvert$	LB_2%	$\lvert\mathcal{S}_3\rvert$	$\lvert\mathcal{U}_3\rvert$	CPU_7
C	70	220	8	8	0.0	17.9	0.5	1,507	0.0	470	0.5	415	391	0.1
C	70	250	8	8	0.0	12.2	0.3	3,776	0.1	1,599	0.3	1,392	1,257	0.4
C	80	220	8	8	0.0	67.7	0.5	1,840	0.0	786	0.5	715	679	0.1
C	80	250	8	8	0.0	17.5	0.6	4,296	0.0	2,281	0.6	2,090	1,908	0.3
C	100	220	8	8	0.0	360.6	0.6	2,355	0.0	1,308	0.6	1,213	1,141	6.9
C	100	250	8	8	0.0	61.5	0.8	6,174	0.0	4,750	0.8	4,448	4,094	5.6
R	70	75	11	11	0.0	13.2	0.4	2,739	0.0	901	0.4	763	723	0.1
R	70	100	11	11	0.0	37.4	0.3	6,204	0.1	1,532	0.3	1,222	1,163	0.1
R	80	75	11	11	0.0	20.9	0.4	3,961	0.1	1,857	0.4	1,579	1,507	0.5
R	80	100	11	11	0.0	90.1	0.3	10,437	0.1	3,306	0.3	2,202	2,100	0.5
R	100	75	11	11	0.0	106.1	0.4	10,903	0.1	6,733	0.4	6,038	5,664	0.9
R	100	100	11	7	0.1 (1.1)	639.2	0.4	21,114	0.0	10,145	0.3	7,076	6,802	3.2
RC	70	75	8	8	0.0	25.6	0.7	1,711	0.1	1,163	0.7	1,064	996	0.3
RC	70	100	8	8	0.0	40.8	0.8	6,184	0.0	4,530	0.7	3,312	3,170	2.4
RC	80	75	8	8	0.0	24.0	0.4	2,005	0.1	1,056	0.4	942	884	0.6
RC	80	100	8	8	0.0	73.1	0.5	7,307	0.0	5,835	0.5	4,319	4,099	5.3
RC	100	75	8	8	0.0	116.7	0.3	4,430	0.1	1,862	0.3	1,605	1,500	68.4
RC	100	100	8	8	0.0	213.0	0.5	14,986	0.1	17,446	0.4	10,792	10,348	26.9
All			162	158	0.0 (1.1)	99.1	0.5	6,184	0.1	3,628	0.5	2,771	2,621	6.2

7.4.4. Results for the CMTVRPTW-R For the CMTVRPTW-R, we have 243 instances, derived from the 81 instances in Section 7.4.1 via the procedure in Cattaruzza et al. (2016a), where each instance is turned into three by choosing the parameter $\kappa \in \{0.25, 0.5, 0.75\}$.

As shown in Table 5, the EPCEM can solve 228 of the 243 instances. In particular, all but one instance with up to 80 customers can be solved, which belongs to the R group with 70 customers.

Table 5 Summary of the Results for the CMTVRPTW-R.

Group	n	κ	Inst	Solved	Gap%	CPU	Step1		Step2	Step3	Step4	Step5	Step6	Step7
							LB_1%	$\lvert\mathcal{S}_1\rvert$	UB_1%	$\lvert\mathcal{S}_2\rvert$	LB_2%	$\lvert\mathcal{S}_3\rvert$	$\lvert\mathcal{U}_3\rvert$	CPU_7
C	70	0.25	8	8	0.0	166.4	1.0	46,829	0.3	62,829	1.0	51,454	51,370	113.4
C	70	0.50	8	8	0.0	83.3	0.9	44,319	0.1	26,669	0.9	18,692	18,631	44.4
C	70	0.75	8	8	0.0	39.5	0.6	42,020	0.2	14,185	0.6	9,707	9,685	4.0
C	80	0.25	8	8	0.0	1238.7	1.2	62,613	0.3	161,435	0.6	50,451	49,582	81.6
C	80	0.50	8	8	0.0	975.5	1.3	58,956	0.2	130,889	0.7	37,777	37,288	44.2
C	80	0.75	8	8	0.0	656.5	1.5	56,908	0.2	348,512	0.6	29,132	28,456	213.4
C	100	0.25	8	7	0.1 (0.9)	4181.5	1.7	93,984	0.6	890,144	1.4	571,032	568,461	3773.9
C	100	0.50	8	8	0.0	2949.0	1.7	83,120	0.5	840,643	1.5	477,925	472,522	2640.6
C	100	0.75	8	6	0.6 (2.6)	2279.7	1.5	81,084	0.6	1,454,459	1.2	432,587	422,026	1568.3
R	70	0.25	11	11	0.0	248.1	0.5	33,227	0.1	16,864	0.5	8,487	8,214	5.9
R	70	0.50	11	11	0.0	169.4	0.5	31,458	0.1	13,489	0.4	6,463	6,275	4.3
R	70	0.75	11	10	0.1 (0.7)	187.1	0.5	30,560	0.2	37,478	0.5	21,438	20,758	26.6
R	80	0.25	11	11	0.0	506.1	0.4	43,305	0.1	45,542	0.3	26,782	26,148	32.3
R	80	0.50	11	11	0.0	329.3	0.5	41,896	0.2	81,716	0.4	47,782	46,816	35.3
R	80	0.75	11	11	0.0	887.3	0.5	39,057	0.2	210,479	0.4	111,772	101,254	57.4
R	100	0.25	11	9	0.3 (1.8)	1806.9	0.7	71,217	0.5	1,424,057	0.5	742,725	726,487	450.4
R	100	0.50	11	8	0.3 (1.3)	1799.6	0.7	64,720	0.3	433,000	0.5	191,619	188,165	57.5
R	100	0.75	11	8	0.4 (1.4)	1284.7	0.6	58,791	0.2	170,251	0.4	60,518	59,435	12.5
RC	70	0.25	8	8	0.0	385.1	1.1	28,365	0.5	89,401	1.0	61,492	59,297	300.6
RC	70	0.50	8	8	0.0	357.9	1.4	27,238	0.6	137,261	1.2	98,499	94,609	271.7
RC	70	0.75	8	8	0.0	115.2	0.8	25,185	0.2	26,135	0.6	14,829	14,576	14.3
RC	80	0.25	8	8	0.0	80.4	0.7	37,434	0.2	23,828	0.6	13,385	12,962	9.0
RC	80	0.50	8	8	0.0	108.6	0.8	35,783	0.3	43,986	0.7	27,413	26,792	35.4
RC	80	0.75	8	8	0.0	46.5	0.6	31,480	0.1	9,044	0.5	4,768	4,628	2.5
RC	100	0.25	8	7	0.4 (3.4)	1639.7	0.9	57,241	0.2	428,289	0.7	268,987	265,644	1298.4
RC	100	0.50	8	7	0.2 (1.7)	1122.4	0.8	54,125	0.4	466,081	0.7	288,706	285,272	705.1
RC	100	0.75	8	7	0.0 (0.2)	637.0	0.7	51,431	0.2	144,333	0.5	57,354	54,828	21.0
All			243	228	0.1 (1.6)	836.5	0.9	47,978	0.3	261,463	0.7	128,037	125,427	379.7

As for 100-customer instances, the EPCEM struggles, especially for instances in group R where 25 of the 33 can be solved. Nevertheless, the suboptimal solutions obtained are very close to optimal in view of the average gap of no more than 0.4%. Like the CMTVRPTW-LD, generating feasible structures is more challenging than proving optimality, which renders *Step 1* and *3* slow. We believe there is room to improve the BLM and the BLMCB by considering more subtle problem-specific features, which are left for future research.

7.4.5. Results for the DRP In this section, we do not use any instances from Set A since all customers have been considered in Section 7.1.5. For Set B, we use instances with the first 70, 80, and all 100 customers, which are 81 instances in total. In this case, we need to scale the demands differently to ensure feasibility. More specifically, the demands are still multiplied by 0.03 for groups C and RC, while the multiplier for group R is changed from 0.045 to 0.03. Similar to the CMTVRPTW-LD, we enable completion bounds in the BLMCB, which can be turned off for small (easy) instances as in Section 7.1.5. The results are summarized in Table 6.

All but four of the 81 instances with up to 100 customers can be solved by the EPCEM. One of the four unsolved ones is from group R with 100 customers. The other three are from group RC, one with 70, one with 80, and one with 100 customers, respectively. The average Gap values are all 0.1% (or 0.8 % for all instances whose optimality cannot be proved) for these groups, indicating that the solutions yielded are very close to optimal. The average computing time for solved instances is less

than five minutes, and the sets $\mathcal{S}_1$, $\mathcal{S}_2$, $\mathcal{S}_3$, and $|\mathcal{U}_3|$ are all of moderate sizes. We conclude that the EPCEM effectively solves the large DRP instances tested.

Table 6 Summary of the Results for the DRP.

Group	n	Inst	Solved	Gap%	CPU	Step1		Step2	Step3	Step4	Step5	Step6	Step7
						LB_1%	$\lvert\mathcal{S}_1\rvert$	UB_1%	$\lvert\mathcal{S}_2\rvert$	LB_2%	$\lvert\mathcal{S}_3\rvert$	$\lvert\mathcal{U}_3\rvert$	CPU_7
C	70	8	8	0.0	6.1	0.4	15,316	0.2	3,621	0.4	2,842	2,833	0.3
C	80	8	8	0.0	92.7	1.5	18,224	0.2	98,997	1.5	89,214	88,966	70.0
C	100	8	8	0.0	409.8	0.9	25,504	0.1	60,357	0.9	54,710	54,546	328.9
R	70	11	11	0.0	15.0	0.6	11,727	0.0	5,460	0.6	4,806	4,773	4.2
R	80	11	11	0.0	78.1	0.7	17,565	0.2	37,382	0.7	28,178	28,049	57.6
R	100	11	10	0.1 (0.8)	52.8	0.4	33,430	0.1	18,441	0.4	15,457	15,372	17.8
RC	70	8	7	0.1 (0.9)	87.7	0.9	6,415	0.1	3,967	0.9	3,845	3,820	72.8
RC	80	8	7	0.1 (0.8)	39.6	0.9	8,368	0.2	10,678	0.9	9,079	9,032	10.1
RC	100	8	7	0.1 (0.8)	2314.0	0.5	18,304	0.2	17,555	0.5	15,431	15,325	2238.1
All		81	77	0.0 (0.8)	295.0	0.7	17,668	0.1	28,375	0.7	24,545	24,451	263.6

7.4.6. Overview and Insights The EPCEM can solve 100%, 100%, 100%, 99%, and 96% of the CMTVRPTW, CMTVRPTW-LT, CMTVRPTW-LD, CMTVRPTW-R, and DRP instances with 70 customers, respectively. For 80-customer instances, the corresponding percentages are 89%, 89%, 100%, 100%, and 96%. For instances with 100 customers, the solved percentages are 52%, 44%, 93%, 100%, 83%, and 93%, respectively. For unsolved instances of each problem class, the average optimality gaps are 1.3%, 1.2%, 1.1%, 1.6%, and 0.8%, respectively.

These results suggest that the CMTVRPTW-LT is the most difficult among the five problems, followed by the CMTVRPTW. The other three problems have significantly smaller feasible regions due to the side constraints and thus are generally easier to solve. In addition, we observe that *Step 7* is rarely the most time-consuming step for the CMTVRPTW-LD. Instead, *Steps 1* and *3* are time-consuming since generating feasible structures is challenging in this case. There are much fewer feasible structures (superstructures), and thus the sizes of sets $\mathcal{S}_2$, $\mathcal{S}_3$, and $\mathcal{U}_3$ are generally much smaller than those of the CMTVRPTW or the CMTVRPTW-LT. This is the main reason why *Step 7* can be completed fast. Therefore, greater attention should be paid to achieving feasibility when we design more specialized exact methods for solving the CMTVRPTW-LD.

8. Concluding Remarks

We propose an *an exact price-cut-and-enumerate method* for the *capacitated multi-trip vehicle routing problem with time windows*. As a refinement of the structure, we introduce the superstructure that leads to a new superstructure-based formulation. In the solution process, tight lower and upper bounds are obtained by solving relaxations and restrictions of the original problem. In addition, the reduced costs are taken advantage of in multiple aspects to accelerate the solution process. Furthermore, the EPCEM can be easily modified to solve four CMTVRPTW variants effectively. An extensive numerical study has been performed to demonstrate that the EPCEM significantly outperforms the best-known exact method.

For some extremely difficult instances, *Step 3* cannot be completed successfully mainly due to two reasons: the gap is large; the labeling algorithm for enumeration is not effective enough. Therefore, three potential research directions are: (i) developing new relaxations and restrictions to obtain tighter bounds (a smaller gap); (ii) designing effective neighborhood search heuristics to improve the feasible solution obtained in *Step 2* and tighten the UB; and (iii) enhancing the current labeling algorithm by, for example, new dominance rules and tighter completion bounds. Moreover, $\mathcal{U}_3$ can have millions of elements, making the IP in *Step 7* beyond the reach of Gurobi. Although our *multi-phase sift-and-cut* method can resolve part of the difficulty, it remains challenging. More effort should be put into developing effective problem-specific cutting planes and branching strategies that can be easily incorporated into an IP solver like Gurobi or CPLEX. The travel time uncertainty in the real world can severely challenge the solution robustness when multi-trip is allowed because delays in previous trips are likely to propagate and impact subsequent trips. An interesting direction to explore is computing "robust" routing plans under travel time uncertainty by a modified EPCEM.

Going from branch-and-cut methods to branch-and-price or branch-price-and-cut methods is a giant leap toward solving difficult VPR-related problems exactly. The solution difficulty is essentially divided into two major parts: one in the master problem which is a set-partitioning/set-covering problem with side constraints; one in the pricing subproblem, which is usually a resource constrained shortest path problem. The success of the superstructure suggests that acceleration can be achieved by a better balance of the two sources of difficulty and inspires us to reconsider existing set-partitioning/set-covering formulations for various VRP-related problems.

Acknowledgments

We would like to thank Roberto Roberti, Alexandre Jacquillat, Martin Savelsbergh, the editors, and three anonymous referees for reading an earlier version of the paper and providing valuable comments and suggestions; the authors of Paradiso et al. (2020) for sharing their code and test instances.

References

Alyasiry AM, Forbes M, Bulmer M (2019) An exact algorithm for the pickup and delivery problem with time windows and last-in-first-out loading. *Transportation Science* 53(6):1695–1705.

Amazon (2021) Amazon's custom electric delivery vehicles are starting to hit the road. URL `https://www.aboutamazon.com/news/transportation/amazons-custom-electric-delivery-vehicles-are-starting-to-hit-the-road`.

Azi N, Gendreau M, Potvin JY (2007) An exact algorithm for a single-vehicle routing problem with time windows and multiple routes. *European journal of operational research* 178(3):755–766.

Azi N, Gendreau M, Potvin JY (2010) An exact algorithm for a vehicle routing problem with time windows and multiple use of vehicles. *European Journal of Operational Research* 202(3):756–763.

Azi N, Gendreau M, Potvin JY (2014) An adaptive large neighborhood search for a vehicle routing problem with multiple routes. *Computers & Operations Research* 41:167–173.

Baldacci R, Christofides N, Mingozzi A (2008) An exact algorithm for the vehicle routing problem based on the set partitioning formulation with additional cuts. *Mathematical Programming* 115(2):351–385.

Baldacci R, Mingozzi A, Roberti R (2012) New state-space relaxations for solving the traveling salesman problem with time windows. *INFORMS Journal on Computing* 24(3):356–371.

Benkebir N, Pouliquen ML, Trévien J, Bounceur A, Euler R, Pardiac E, Sevaux M (2019) On a multi-trip vehicle routing problem with time windows integrating european and french driver regulations. *Journal on Vehicle Routing Algorithms* 2(1):55–74.

Braekers K, Ramaekers K, Van Nieuwenhuyse I (2016) The vehicle routing problem: State of the art classification and review. *Computers & Industrial Engineering* 99:300–313.

Cattaruzza D, Absi N, Feillet D (2016a) The multi-trip vehicle routing problem with time windows and release dates. *Transportation Science* 50(2):676–693.

Cattaruzza D, Absi N, Feillet D (2016b) Vehicle routing problems with multiple trips. *4OR* 14(3):223–259.

Cattaruzza D, Absi N, Feillet D, Vigo D (2014) An iterated local search for the multi-commodity multi-trip vehicle routing problem with time windows. *Computers & Operations Research* 51:257–267.

Cheng C, Adulyasak Y, Rousseau LM (2020) Drone routing with energy function: Formulation and exact algorithm. *Transportation Research Part B: Methodological* 139:364–387.

Choi Y, Robertson B, Choi Y, Mavris D (2019) A multi-trip vehicle routing problem for small unmanned aircraft systems-based urban delivery. *Journal of Aircraft* 56(6):2309–2323.

Costa L, Contardo C, Desaulniers G (2019) Exact branch-price-and-cut algorithms for vehicle routing. *Transportation Science* 53(4):946–985.

Dantzig GB, Ramser JH (1959) The truck dispatching problem. *Management science* 6(1):80–91.

Derigs U, Kurowsky R, Vogel U (2011) Solving a real-world vehicle routing problem with multiple use of tractors and trailers and eu-regulations for drivers arising in air cargo road feeder services. *European Journal of Operational Research* 213(1):309–319.

Desaulniers G, Gschwind T, Irnich S (2020) Variable fixing for two-arc sequences in branch-price-and-cut algorithms on path-based models. *Transportation Science* 54(5):1170–1188.

Dorling K, Heinrichs J, Messier GG, Magierowski S (2016) Vehicle routing problems for drone delivery. *IEEE Transactions on Systems, Man, and Cybernetics: Systems* 47(1):70–85.

Feillet D, Dejax P, Gendreau M, Gueguen C (2004) An exact algorithm for the elementary shortest path problem with resource constraints: Application to some vehicle routing problems. *Networks: An International Journal* 44(3):216–229.

Figliozzi MA (2020) Carbon emissions reductions in last mile and grocery deliveries utilizing air and ground autonomous vehicles. *Transportation Research Part D: Transport and Environment* 85:102443.

Fleischmann B (1990) The vehicle routing problem with multiple use of vehicles. *Department of Economics, Universität Hamburg* .

François V, Arda Y, Crama Y (2019) Adaptive large neighborhood search for multitrip vehicle routing with time windows. *Transportation Science* 53(6):1706–1730.

Golden BL, Raghavan S, Wasil EA (2008) *The vehicle routing problem: latest advances and new challenges*, volume 43 (Springer Science & Business Media).

Gurobi Optimization, LLC (2021) Gurobi Optimizer Reference Manual. URL `https://www.gurobi.com`.

He P, Li J (2019) The two-echelon multi-trip vehicle routing problem with dynamic satellites for crop harvesting and transportation. *Applied Soft Computing* 77:387–398.

Hernandez F, Feillet D, Giroudeau R, Naud O (2014) A new exact algorithm to solve the multi-trip vehicle routing problem with time windows and limited duration. *4or* 12(3):235–259.

Hernandez F, Feillet D, Giroudeau R, Naud O (2016) Branch-and-price algorithms for the solution of the multi-trip vehicle routing problem with time windows. *European Journal of Operational Research* 249(2):551–559.

Homberger J, Gehring H (2005) A two-phase hybrid metaheuristic for the vehicle routing problem with time windows. *European journal of operational research* 162(1):220–238.

Irnich S, Desaulniers G (2005) Shortest path problems with resource constraints. *Column generation*, 33–65 (Springer).

Irnich S, Desaulniers G, Desrosiers J, Hadjar A (2010) Path-reduced costs for eliminating arcs in routing and scheduling. *INFORMS Journal on Computing* 22(2):297–313.

Janic M (2007) Modelling the full costs of an intermodal and road freight transport network. *Transportation Research Part D: Transport and Environment* 12(1):33–44.

Jepsen M, Petersen B, Spoorendonk S, Pisinger D (2008) Subset-row inequalities applied to the vehicle-routing problem with time windows. *Operations Research* 56(2):497–511.

Kunovjanek M, Wankmüller C (2021) Containing the covid-19 pandemic with drones-feasibility of a drone enabled back-up transport system. *Transport Policy* 106:141–152.

Labadie N, Mansini R, Melechovskỳ J, Calvo RW (2012) The team orienteering problem with time windows: An lp-based granular variable neighborhood search. *European Journal of Operational Research* 220(1):15–27.

Lim A, Zhang Z, Qin H (2017) Pickup and delivery service with manpower planning in hong kong public hospitals. *Transportation Science* 51(2):688–705.

Liu S, Wu H, Xiang S, Li X (2017) Mobile robot scheduling with multiple trips and time windows. *International Conference on Advanced Data Mining and Applications*, 608–620 (Springer).

Lyons L, Lozano A, Granados F, Guzmán A (2017) Impacts of time restriction on heavy truck corridors: The case study of mexico city. *Transportation Research Part A: Policy and Practice* 102:119–129.

Macedo R, Alves C, Valério de Carvalho J, Clautiaux F, Hanafi S (2011) Solving the vehicle routing problem with time windows and multiple routes exactly using a pseudo-polynomial model. *European Journal of Operational Research* 214(3):536–545.

Pan B, Zhang Z, Lim A (2021) Multi-trip time-dependent vehicle routing problem with time windows. *European Journal of Operational Research* 291(1):218–231.

Paradiso R, Roberti R, Laganá D, Dullaert W (2020) An exact solution framework for multitrip vehicle-routing problems with time windows. *Operations Research* 68(1):180–198.

Pecin D, Contardo C, Desaulniers G, Uchoa E (2017a) New enhancements for the exact solution of the vehicle routing problem with time windows. *INFORMS Journal on Computing* 29(3):489–502.

Pecin D, Pessoa A, Poggi M, Uchoa E (2017b) Improved branch-cut-and-price for capacitated vehicle routing. *Mathematical Programming Computation* 9(1):61–100.

Pelletier S, Jabali O, Laporte G (2016) 50th anniversary invited articleâĂŤgoods distribution with electric vehicles: review and research perspectives. *Transportation science* 50(1):3–22.

Pessoa A, Sadykov R, Uchoa E, Vanderbeck F (2020) A generic exact solver for vehicle routing and related problems. *Mathematical Programming* 183(1):483–523.

Righini G, Salani M (2006) Symmetry helps: Bounded bi-directional dynamic programming for the elementary shortest path problem with resource constraints. *Discrete Optimization* 3(3):255–273.

Righini G, Salani M (2008) New dynamic programming algorithms for the resource constrained elementary shortest path problem. *Networks: An International Journal* 51(3):155–170.

Salhi S (1987) *The integration of routing into the location-allocation and vehicle composition problems.* Ph.D. thesis, University of Lancaster.

Schrijver A, et al. (2003) *Combinatorial optimization: polyhedra and efficiency*, volume 24 (Springer).

Solomon MM (1987) Algorithms for the vehicle routing and scheduling problems with time window constraints. *Operations research* 35(2):254–265.

Sun Y, Wang D, Lang M, Zhou X (2019) Solving the time-dependent multi-trip vehicle routing problem with time windows and an improved travel speed model by a hybrid solution algorithm. *Cluster Computing* 22(6):15459–15470.

Tang J, Yu Y, Li J (2015) An exact algorithm for the multi-trip vehicle routing and scheduling problem of pickup and delivery of customers to the airport. *Transportation Research Part E: Logistics and Transportation Review* 73:114–132.

Tilk C, Irnich S (2017) Dynamic programming for the minimum tour duration problem. *Transportation Science* 51(2):549–565.

Toth P, Vigo D (2014) *Vehicle routing: problems, methods, and applications* (SIAM).

Vansteenwegen P, Souffriau W, Berghe GV, Van Oudheusden D (2009) Iterated local search for the team orienteering problem with time windows. *Computers & Operations Research* 36(12):3281–3290.

Vidal T, Laporte G, Matl P (2020) A concise guide to existing and emerging vehicle routing problem variants. *European Journal of Operational Research* 286(2):401–416.

Wang Z, Liang W, Hu X (2014) A metaheuristic based on a pool of routes for the vehicle routing problem with multiple trips and time windows. *Journal of the Operational Research Society* 65(1):37–48.

Online Supplement

EC.1. Proofs

EC.1.1. Proof of Theorem 1

Proof We first show that $\bar{z}^{\mathcal{U}} \le \bar{z}^{\mathcal{S}}$. Let $\hat{x}$ be an optimal solution to the root LP of the structure-based formulation $\mathrm{F}^{\mathcal{S}}$. Set $\hat{y}_u := \sum_{s\in\Psi^{-1}(u)} \hat{x}_s$ for $u \in \mathcal{U}$. By the definition of superstructure, we have $\alpha'_{i\Psi(s)} = \alpha_{is}$. Because $\{\Psi^{-1}(u) : u \in \mathcal{U}\}$ defines a partition of $\mathcal{S}$, we have $\sum_{u\in\mathcal{U}} \alpha'_{iu}\hat{y}_u = \sum_{u\in\mathcal{U}} \alpha'_{iu}\left(\sum_{s\in\Psi^{-1}(u)} \hat{x}_s\right) = \sum_{u\in\mathcal{U}}\sum_{s\in\Psi^{-1}(u)} \alpha_{is}\hat{x}_s = \sum_{s\in\mathcal{S}} \alpha_{is}\hat{x}_s = 1$. Thus, constraints (2) are satisfied by $\hat{y}_u$. For constraints (3), we need to prove that $\sum_{u\in\overline{\mathcal{U}}} \hat{y}_u \le \zeta_m(\overline{\mathcal{U}})$ for all $\overline{\mathcal{U}} \subseteq \mathcal{U}$. Note that $\sum_{s\in\Psi^{-1}(u)} \hat{x}_s \le 1$ for any $u \in \mathcal{U}$, i.e., at most one of the structures corresponding to the same superstructure can be selected. Due to the feasibility of $\hat{x}$ and Property P3, we have $\sum_{u\in\overline{\mathcal{U}}} \hat{y}_u = \sum_{u\in\overline{\mathcal{U}}}\sum_{s\in\Psi^{-1}(u)} \hat{x}_s = \sum_{s\in\Psi^{-1}(\overline{\mathcal{U}})} \hat{x}_s \le \eta_m(\Psi^{-1}(\overline{\mathcal{U}})) \le \zeta_m(\overline{\mathcal{U}})$. So constraints (3) are also satisfied. Lastly, $0 \le \hat{y}_u = \sum_{s\in\Psi^{-1}(u)} \hat{x}_s \le 1$ for $u \in \mathcal{U}$ and thus $\hat{y}$ is a feasible solution to $\mathrm{F}^{\mathcal{U}}$. Since the cost of any structure equals its corresponding superstructure, i.e., $c_{\Psi(s)} = c_s$, we conclude that $\bar{z}^{\mathcal{U}} \le \bar{z}^{\mathcal{S}}$.

To prove the reverse direction, let $\hat{y}$ be an optimal solution to the root LP of the superstructure-based formulation $\mathrm{F}^{\mathcal{U}}$. Due to the feasibility of $\hat{y}$, we have $\hat{y} \in P_{\zeta_m}$. By Lemma 1, there exits $\hat{x} \in P_{\eta_m} \cap \{x \in \mathbb{R}^{\mathcal{S}} : \sum_{s\in\Psi^{-1}(u)} x_s = \hat{y}_u\}$. By similar arguments as in the previous case, $\hat{x}$ satisfies the set-partitioning constraints. Thus $\hat{x}$ is a feasible solution to the structure-based formulation and it has the same cost as $\hat{y}$. Therefore, $\bar{z}^{\mathcal{S}} \le \bar{z}^{\mathcal{U}}$, which completes the proof. ■

EC.1.2. Proof of Lemma 1

Proof By Farkas' Lemma,

$$P_{\eta_m} \cap \left\{ x \in \mathbb{R}^{\mathcal{S}} : \sum_{s\in\Psi^{-1}(u)} x_s = \hat{y}_u, \forall u \in \mathcal{U} \right\} \neq \emptyset$$

$$\Longleftrightarrow \left\{ (z,w) \in \mathbb{R}^{\mathcal{U}} \times \mathbb{R}^{2^{\mathcal{S}}}_{+} : \begin{array}{c} z_{\Psi(s)} \le \sum_{\overline{\mathcal{S}}\subseteq\mathcal{S}} |\overline{\mathcal{S}} \cap \{s\}| w_{\overline{\mathcal{S}}}, \forall s \in \mathcal{S} \\ \sum_{u\in\mathcal{U}} \hat{y}_u z_u > \sum_{\overline{\mathcal{S}}\subseteq\mathcal{S}} \eta_m(\overline{\mathcal{S}}) w_{\overline{\mathcal{S}}} \end{array} \right\} = \emptyset.$$

It suffices to prove that $\sum_{u\in\mathcal{U}} \hat{y}_u z_u \le \sum_{\overline{\mathcal{S}}\subseteq\mathcal{S}} \eta_m(\overline{\mathcal{S}}) w_{\overline{\mathcal{S}}}$ for all $(z,w) \in \mathbb{R}^{\mathcal{U}} \times \mathbb{R}^{2^{\mathcal{S}}}_{+}$ such that $z_{\Psi(s)} \le \sum_{\overline{\mathcal{S}}\subseteq\mathcal{S}} |\overline{\mathcal{S}} \cap \{s\}| w_{\overline{\mathcal{S}}}, \forall s \in \mathcal{S}$. For any given z, we order $u \in \mathcal{U} = \{u_1, \cdots, u_p\}$ such that $z_{u_1} \ge \cdots \ge z_{u_p}$, where $p := |\mathcal{U}|$. Let $\mathcal{U}^i := \{u_1, u_2, \cdots, u_i\}$ for $i = 1, \cdots, p$ and $\mathcal{U}^0 = \emptyset$. Since $\hat{y}$ is in the polymatroid P_{ζ_m} defined by the submodular function ζ_m, by Theorem 44.3 in Schrijver et al. (2003), we have $\sum_{u\in\mathcal{U}} \hat{y}_u z_u \le \sum_{i=1}^{p} y^*_i z_{u_i}$, where $y^*_i := \zeta_m(\mathcal{U}^i) - \zeta_m(\mathcal{U}^{i-1})$ for $i = 1, \cdots, p$. Obviously, $0 \le y^*_i \le 1$.

Then, y_i^* is either 0 or 1 for $i=1,\cdots,p$ because ζ_m takes integer values. Let $\mathcal{U}^* := \{u_i \in \mathcal{U} : y_i^* = 1\}$. We have $|\mathcal{U}^*| = \sum_{u_i \in \mathcal{U}^*} y_i^* = \sum_{i=1}^{p} y_i^* = \zeta_m(\mathcal{U}^p) - \zeta_m(\emptyset) = \zeta_m(\mathcal{U})$.

For convenience, for each $s \in \mathcal{S}$, let $w(s) := \sum_{\overline{\mathcal{S}} \subseteq \mathcal{S}} |\overline{\mathcal{S}} \cap \{s\}| w_{\overline{\mathcal{S}}}$. For each $u \in \mathcal{U}^*$, we pick one $\hat{s}(u) \in \operatorname{argmin}_{s \in \Psi^{-1}(u)} w(s)$ and define $\widehat{\mathcal{S}} := \{\hat{s}(u) : u \in \mathcal{U}^*\}$. Then $|\widehat{\mathcal{S}}| = |\mathcal{U}^*|$. We have $\sum_{i=1}^{p} y_i^* z_{u_i} = \sum_{u \in \mathcal{U}^*} z_u \le \sum_{u \in \mathcal{U}^*} \sum_{\overline{\mathcal{S}} \subseteq \mathcal{S}} |\overline{\mathcal{S}} \cap \{\hat{s}(u)\}| w_{\overline{\mathcal{S}}} = \sum_{\overline{\mathcal{S}} \subseteq \mathcal{S}} |\overline{\mathcal{S}} \cap \widehat{\mathcal{S}}| w_{\overline{\mathcal{S}}}$. Note that there exists $\mathcal{S}^* \subseteq \Psi^{-1}(\mathcal{U}^*)$ such that $|\mathcal{S}^*| = \eta_m(\mathcal{S}^*) = \zeta_m(\mathcal{U}^*) = |\mathcal{U}^*| = |\widehat{\mathcal{S}}|$. By Properties P1 to P4, it is easy to verify that $\eta_m(\widetilde{\mathcal{S}}) = |\widetilde{\mathcal{S}}|$ for any $\widetilde{\mathcal{S}} \subseteq \mathcal{S}^*$. Then $\eta_m(\overline{\mathcal{S}}) \ge \eta_m(\overline{\mathcal{S}} \cap \mathcal{S}^*) = |\overline{\mathcal{S}} \cap \mathcal{S}^*|$. Because $w_{\overline{\mathcal{S}}} \ge 0$ for all $\overline{\mathcal{S}} \subseteq \mathcal{S}$, we have $\sum_{\overline{\mathcal{S}} \subseteq \mathcal{S}} |\overline{\mathcal{S}} \cap \mathcal{S}^*| w_{\overline{\mathcal{S}}} \le \sum_{\overline{\mathcal{S}} \subseteq \mathcal{S}} \eta_m(\overline{\mathcal{S}}) w_{\overline{\mathcal{S}}}$. It suffices to prove that $\sum_{\overline{\mathcal{S}} \subseteq \mathcal{S}} |\overline{\mathcal{S}} \cap \widehat{\mathcal{S}}| w_{\overline{\mathcal{S}}} \le \sum_{\overline{\mathcal{S}} \subseteq \mathcal{S}} |\overline{\mathcal{S}} \cap \mathcal{S}^*| w_{\overline{\mathcal{S}}}$.

If $\widehat{\mathcal{S}} = \mathcal{S}^*$, then we are done. Suppose not, then $\exists \hat{s} \in \widehat{\mathcal{S}} \setminus \mathcal{S}^*$ and $\exists s^* \in \mathcal{S}^* \setminus \widehat{\mathcal{S}}$ such that $\Psi(\hat{s}) = \Psi(s^*)$. Such $\hat{s}$ and s^* exist because $|\mathcal{S}^* \cap \Psi^{-1}(u)| = |\widehat{\mathcal{S}} \cap \Psi^{-1}(u)| = |\hat{s}(u)| = 1$ for each $u \in \mathcal{U}^*$. To see this, if there exists $u \in \mathcal{U}^*$ such that $\mathcal{S}^* \cap \Psi^{-1}(u) = \emptyset$, then there exists $u' \in \mathcal{U}^*$ such that $|\mathcal{S}^* \cap \Psi^{-1}(u')| \ge 2$ because $\sum_{u \in \mathcal{U}^*} |\mathcal{S}^* \cap \Psi^{-1}(u)| = |\mathcal{S}^* \cap \Psi^{-1}(\mathcal{U}^*)| = |\mathcal{S}^*| = |\mathcal{U}^*|$. In view of Properties P1 and P2, $\eta_m(\mathcal{S}^* \cap \Psi^{-1}(u')) \le \eta_m(\Psi^{-1}(u')) = 1$. Note that $\mathcal{S}^* \cap \Psi^{-1}(u') \subseteq \mathcal{S}^*$, thus $\eta_m(\mathcal{S}^* \cap \Psi^{-1}(u')) = |\mathcal{S}^* \cap \Psi^{-1}(u')|$. This leads to a contradiction because $1 \ge \eta_m(\mathcal{S}^* \cap \Psi^{-1}(u')) = |\mathcal{S}^* \cap \Psi^{-1}(u')| \ge 2$. Thus $\mathcal{S}^* \cap \Psi^{-1}(u) \ne \emptyset$ for all $u \in \mathcal{U}^*$. Furthermore, $1 = \eta_m(\Psi^{-1}(u)) \ge \eta_m(\mathcal{S}^* \cap \Psi^{-1}(u)) = |\mathcal{S}^* \cap \Psi^{-1}(u)| \ge 1 \Rightarrow |\mathcal{S}^* \cap \Psi^{-1}(u)| = 1$ for $u \in \mathcal{U}^*$. Let $\widehat{\mathcal{S}}' = \widehat{\mathcal{S}} \setminus \{\hat{s}\} \cup \{s^*\}$. Then we have $\sum_{\overline{\mathcal{S}} \subseteq \mathcal{S}} |\overline{\mathcal{S}} \cap \widehat{\mathcal{S}}| w_{\overline{\mathcal{S}}} = \sum_{\overline{\mathcal{S}} \subseteq \mathcal{S}} |\overline{\mathcal{S}} \cap \widehat{\mathcal{S}}'| w_{\overline{\mathcal{S}}} + \sum_{\overline{\mathcal{S}} \subseteq \mathcal{S}} |\overline{\mathcal{S}} \cap \{\hat{s}\}| w_{\overline{\mathcal{S}}} - \sum_{\overline{\mathcal{S}} \subseteq \mathcal{S}} |\overline{\mathcal{S}} \cap \{s^*\}| w_{\overline{\mathcal{S}}} = \sum_{\overline{\mathcal{S}} \subseteq \mathcal{S}} |\overline{\mathcal{S}} \cap \widehat{\mathcal{S}}'| w_{\overline{\mathcal{S}}} + w(\hat{s}) - w(s^*)$. Since $\Psi(\hat{s}) = \Psi(s^*)$ and $\hat{s} \in \widehat{\mathcal{S}}$, we have $w(\hat{s}) \le w(s^*)$ by the definition of $\widehat{\mathcal{S}}$. Thus, $\sum_{\overline{\mathcal{S}} \subseteq \mathcal{S}} |\overline{\mathcal{S}} \cap \widehat{\mathcal{S}}| w_{\overline{\mathcal{S}}} \le \sum_{\overline{\mathcal{S}} \subseteq \mathcal{S}} |\overline{\mathcal{S}} \cap \widehat{\mathcal{S}}'| w_{\overline{\mathcal{S}}}$. This argument can be performed inductively and thus we have $\sum_{\overline{\mathcal{S}} \subseteq \mathcal{S}} |\overline{\mathcal{S}} \cap \widehat{\mathcal{S}}| w_{\overline{\mathcal{S}}} \le \sum_{\overline{\mathcal{S}} \subseteq \mathcal{S}} |\overline{\mathcal{S}} \cap \mathcal{S}^*| w_{\overline{\mathcal{S}}}$, which completes the proof. ■

EC.1.3. Proof of Proposition 1

Proof It suffices to show that if (i) to (vi) hold then $\forall j \in V \setminus N^{\mathfrak{b}_2}$ such that $L^{\mathfrak{b}_2}$ can be extended to a feasible $L^{\mathfrak{b}_2'}$, we have that $L^{\mathfrak{b}_1}$ can also be extended to a feasible $L^{\mathfrak{b}_1'}$ by visiting j and (i) to (vi) still hold for $L^{\mathfrak{b}_1'}$ and $L^{\mathfrak{b}_2'}$. Firstly, (ii), (iii), (iv), and (vi) imply that $\gamma^{\mathfrak{b}_1} \le \gamma^{\mathfrak{b}_2}$, which can be proved as follows. Recall the definition in (6) that

$$\gamma^{\mathfrak{b}} = \beta^{\mathfrak{b}} - \sum_{t \in \mathcal{H}} \mathbb{1}_{[\ell^{\mathfrak{b}}, e^{\mathfrak{b}} + d^{\mathfrak{b}})}(t)\, \pi_t^{\mathcal{H}} - \sum_{(i,j,k) \in \mathcal{I}} \mathbb{1}_{C^{\mathfrak{b}}}((i,j,k))\, \pi_{(i,j,k)}^{\mathcal{I}}.$$

In view of (iii) $\ell^{\mathfrak{b}_1} \ge \ell^{\mathfrak{b}_2}$ and (iv) $e^{\mathfrak{b}_1} + d^{\mathfrak{b}_1} \le e^{\mathfrak{b}_2} + d^{\mathfrak{b}_2}$, we have $[\ell^{\mathfrak{b}_1}, e^{\mathfrak{b}_1} + d^{\mathfrak{b}_1}) \subseteq [\ell^{\mathfrak{b}_2}, e^{\mathfrak{b}_2} + d^{\mathfrak{b}_2})$, and thus, $\forall t \in \mathcal{H}$, $0 \le \mathbb{1}_{[\ell^{\mathfrak{b}_1}, e^{\mathfrak{b}_1} + d^{\mathfrak{b}_1})}(t) \le \mathbb{1}_{[\ell^{\mathfrak{b}_2}, e^{\mathfrak{b}_2} + d^{\mathfrak{b}_2})}(t)$. Furthermore, due to $N^{\mathfrak{b}_1} \subseteq N^{\mathfrak{b}_2}$, we have

$$C^{\mathfrak{b}_1} = \{(i,j,k) \in C : |N^{\mathfrak{b}_1} \cap \{i,j,k\}| \ge 2\} \subseteq \{(i,j,k) \in C : |N^{\mathfrak{b}_2} \cap \{i,j,k\}| \ge 2\} = C^{\mathfrak{b}_2}.$$

Thus, $\forall(i,j,k)\in\mathcal{I}$, we have $0\le \mathbb{1}_{C^{\mathcal{b}_1}}((i,j,k))\le \mathbb{1}_{C^{\mathcal{b}_2}}((i,j,k))$. Lastly, since $\pi_t^{\mathcal{H}}\le 0$ and $\pi_{ijk}^{\mathcal{I}}\le 0$, $\forall t\in\mathcal{H}$ and $\forall(i,j,k)\in\mathcal{I}$, we have

$$\begin{aligned}&-\sum_{t\in\mathcal{H}}\mathbb{1}_{[\ell^{\mathcal{b}_1},e^{\mathcal{b}_1}+d^{\mathcal{b}_1})}(t)\,\pi_t^{\mathcal{H}}-\sum_{(i,j,k)\in\mathcal{I}}\mathbb{1}_{C^{\mathcal{b}_1}}((i,j,k))\,\pi_{(i,j,k)}^{\mathcal{I}}\\ \le&-\sum_{t\in\mathcal{H}}\mathbb{1}_{[\ell^{\mathcal{b}_2},e^{\mathcal{b}_2}+d^{\mathcal{b}_2})}(t)\,\pi_t^{\mathcal{H}}-\sum_{(i,j,k)\in\mathcal{I}}\mathbb{1}_{C^{\mathcal{b}_2}}((i,j,k))\,\pi_{(i,j,k)}^{\mathcal{I}},\end{aligned}$$

which combined with the condition that (vi) $\beta^{\mathcal{b}_1}\le\beta^{\mathcal{b}_2}$ leads to $\gamma^{\mathcal{b}_1}\le\gamma^{\mathcal{b}_2}$.

We then prove the feasibility of $L^{\mathcal{b}_1'}$ by showing the conditions in (7) hold for $L^{\mathcal{b}_1'}$. In view of (8) and (ii), we have $q^{\mathcal{b}_1'}=q^{\mathcal{b}_1}+q_j\le q^{\mathcal{b}_2}+q_j=q^{\mathcal{b}_2'}\le Q$. In addition, $\ell^{\mathcal{b}_1'}=\min\{\ell^{\mathcal{b}_1}-t'_{ji^{\mathcal{b}_1}},b_j\}\ge\min\{\ell^{\mathcal{b}_2}-t'_{ji^{\mathcal{b}_2}},b_j\}=\ell^{\mathcal{b}_2'}\ge a_j$ due to (i), (iii), and the feasibility of $L^{\mathcal{b}_2'}$. Owing to (9), (iv), and (v), we have $e^{\mathcal{b}_1'}+d^{\mathcal{b}_1'}\le e^{\mathcal{b}_2'}+d^{\mathcal{b}_2'}\le b_0$, which confirms that $L^{\mathcal{b}_1'}$ is feasible and (iv) holds for $L^{\mathcal{b}_1'}$ and $L^{\mathcal{b}_2'}$.

Note that (i) and (ii) hold trivially for $L^{\mathcal{b}_1'}$, and $L^{\mathcal{b}_2'}$ and we have proved (iii) and (iv). It remains to show (v) and (vi). $d^{\mathcal{b}_1'}=d^{\mathcal{b}_1}+\max\{t'_{ji^{\mathcal{b}_1}},e^{\mathcal{b}_1}-b_j\}\le d^{\mathcal{b}_2}+\max\{t'_{ji^{\mathcal{b}_2}},e^{\mathcal{b}_2}-b_j\}=d^{\mathcal{b}_2'}$ due to (iv) and (v) for $L^{\mathcal{b}_1}$ and $L^{\mathcal{b}_2}$. In addition, $\beta^{\mathcal{b}_1'}=\beta^{\mathcal{b}_1}+\bar{c}_{ji^{\mathcal{b}_1}}\le\beta^{\mathcal{b}_2}+\bar{c}_{ji^{\mathcal{b}_2}}=\beta^{\mathcal{b}_2'}$, which completes the proof. ■

EC.1.4. Proof of Proposition 2

Proof Any given structure $s=(i_0,i_1,\cdots,i_k,i_0)$ with $i_0=0$ can be broken into a forward path $f:=\{i_0,i_1,\cdots,i_{k_1}\}$ and a backward path $\mathcal{b}:=\{i_0,i_k,i_{k-1},\cdots,i_{k_1}\}$. Let $i^f=i^{\mathcal{b}}=i_{k_1}$, since $i^{\mathcal{b}}$ appears both in the forward and backward paths, then $q^f+q^{\mathcal{b}}=\sum_{i\in N_s}q_i+q_{i^{\mathcal{b}}}\le Q+q_{i^{\mathcal{b}}}\Rightarrow q^f\le Q+q_{i^{\mathcal{b}}}-q^{\mathcal{b}}\Rightarrow\beta^f\ge\bar{\omega}(i^{\mathcal{b}},Q+q_{i^{\mathcal{b}}}-q^{\mathcal{b}})\Rightarrow\beta_s:=\sum_{g=0}^{k-1}\bar{c}_{i_gi_{g+1}}+\bar{c}_{i_ki_0}=\beta^f+\beta^{\mathcal{b}}\ge\bar{\omega}(i^{\mathcal{b}},Q+q_{i^{\mathcal{b}}}-q^{\mathcal{b}})+\beta^{\mathcal{b}}$.

In view of (8) and (9), we conclude that $\ell^{\mathcal{b}}$ is non-increasing and $e^{\mathcal{b}}+d^{\mathcal{b}}$ is non-decreasing when $\mathcal{b}$ is extended, which means $\ell^{\mathcal{b}}\ge\ell_s$ and $e^{\mathcal{b}}+d^{\mathcal{b}}\le e_s+d_s$. Due to the fact that $\forall t\in\mathcal{H}$, $\pi_t^{\mathcal{H}}\le 0$, we have $\sum_{t\in\mathcal{H}}\mathbb{1}_{[\ell_s,e_s+d_s)}(t)\,\pi_t^{\mathcal{H}}\le\sum_{t\in\mathcal{H}}\mathbb{1}_{[\ell^{\mathcal{b}},e^{\mathcal{b}}+d^{\mathcal{b}})}(t)\,\pi_t^{\mathcal{H}}$. Moreover, since $N^{\mathcal{b}}\subseteq N_s$ and $\pi_{(i,j,k)}^{\mathcal{I}}\le 0$, $\forall(i,j,k)\in\mathcal{I}$, we have $\sum_{(i,j,k)\in\mathcal{I}}\mathbb{1}_{C_s}((i,j,k))\,\pi_{(i,j,k)}^{\mathcal{I}}\le\sum_{(i,j,k)\in\mathcal{I}}\mathbb{1}_{C^{\mathcal{b}}}((i,j,k))\,\pi_{(i,j,k)}^{\mathcal{I}}$. Thus,

$$\begin{aligned}\gamma_s&=\beta_s-\sum_{t\in\mathcal{H}}\mathbb{1}_{[\ell_s,e_s+d_s)}(t)\,\pi_t^{\mathcal{H}}-\sum_{(i,j,k)\in\mathcal{I}}\mathbb{1}_{C_s}((i,j,k))\,\pi_{(i,j,k)}^{\mathcal{I}}\\&\ge\bar{\omega}(i^{\mathcal{b}},Q+q_{i^{\mathcal{b}}}-q^{\mathcal{b}})+\beta^{\mathcal{b}}-\sum_{t\in\mathcal{H}}\mathbb{1}_{[\ell^{\mathcal{b}},e^{\mathcal{b}}+d^{\mathcal{b}})}(t)\,\pi_t^{\mathcal{H}}-\sum_{(i,j,k)\in\mathcal{I}}\mathbb{1}_{C^{\mathcal{b}}}((i,j,k))\,\pi_{(i,j,k)}^{\mathcal{I}}\\&=\bar{\omega}(i^{\mathcal{b}},Q+q_{i^{\mathcal{b}}}-q^{\mathcal{b}})+\gamma^{\mathcal{b}}\ge 0,\end{aligned}$$

which completes the proof. ■

EC.1.5. Proof of Proposition 3

Proof By the same argument as in Section EC.1.3, we have that (i) to (vi) hold when $L^{\mathcal{b}_1}$ and $L^{\mathcal{b}_2}$ perform the same extension. Then, it suffices to consider the case when $L^{\mathcal{b}_1}$ and $L^{\mathcal{b}_2}$ finish all future extensions, i.e., extend back to the depot 0. When $i^{\mathcal{b}_1}=i^{\mathcal{b}_2}=0$, $\mathcal{b}_1$ and $\mathcal{b}_2$ actually correspond to two structures. With a slight abuse of notation, let $\mathcal{b}_1$ and $\mathcal{b}_2$ denote the corresponding structures.

It suffices to show that in any optimal solution of $\mathrm{F}^{\mathcal{S}}$ such that $\mathcal{b}_2$ is used, we can obtain a new optimal solution by replacing $\mathcal{b}_2$ with $\mathcal{b}_1$. Since $c^{\mathcal{b}_1} \le c^{\mathcal{b}_2}$, it suffices to show that this replacement will not affect the solution feasibility. That is, if $\mathcal{b}_2$ is started at time $t \le \ell^{\mathcal{b}_2}$, $\mathcal{b}_1$ can be started at time $\bar{t} \ge t$ such that it finishes no later than $\mathcal{b}_2$.

We can start $\mathcal{b}_1$ at $\bar{t} = \max\{e^{\mathcal{b}_1}, t\} \ge t$. Due to (iii) and $t \le \ell^{\mathcal{b}_2}$, we have $\bar{t} \le \ell^{\mathcal{b}_1}$. Then, $\mathcal{b}_1$ will be completed at $\bar{t} + d^{\mathcal{b}_1} = \max\{e^{\mathcal{b}_1}, t\} + d^{\mathcal{b}_1}$ and $\mathcal{b}_2$ finishes at $\max\{e^{\mathcal{b}_2}, t\} + d^{\mathcal{b}_2}$. When $e^{\mathcal{b}_1} > \ell^{\mathcal{b}_2}$, we have $e^{\mathcal{b}_1} > \ell^{\mathcal{b}_2} \ge t \Rightarrow \max\{e^{\mathcal{b}_1}, t\} + d^{\mathcal{b}_1} = e^{\mathcal{b}_1} + d^{\mathcal{b}_1} \le e^{\mathcal{b}_2} + d^{\mathcal{b}_2} \le \max\{e^{\mathcal{b}_2}, t\} + d^{\mathcal{b}_2}$ due to (iv). When $e^{\mathcal{b}_1} \le \ell^{\mathcal{b}_2}$, due to (iv) and (v), we have that $\max\{e^{\mathcal{b}_1}, t\} + d^{\mathcal{b}_1} \le \max\{e^{\mathcal{b}_2}, t\} + d^{\mathcal{b}_2}$. ■

EC.1.6. Proof of Proposition 4

Proof Consider the following standard form IP, denoted by FP.

$$\begin{array}{llll} \text{(FP)} \quad z^* = \min & c^T x & & \text{(}\overline{\text{FP}}\text{)} \quad \bar{z} = \min & c^T x \\ \text{s.t.} & Ax = b, & \xrightarrow{LP\ \ relaxation} & \text{s.t.} & Ax = b, \\ & x \in \mathbb{Z}_+^n. & & & x \ge \mathbf{0}. \end{array}$$

Suppose FP has a valid upper bound $\hat{z}$. Let $\bar{z}$ be the optimal value of its LP relaxation $\overline{\text{FP}}$, π_* be the corresponding optimal dual solution, and $\gamma := c - A^T\pi_*$ be the vector of reduced costs. It suffices to prove $z > \hat{z}$ for the following auxiliary LP, denoted by $\widehat{\text{FP}}$.

$$\begin{array}{llll} \text{(}\widehat{\text{FP}}\text{)} \quad z = \min & c^T x & & \text{(}\widehat{\text{DFP}}\text{)} \quad \max & b^T\pi + ku \\ \text{s.t.} & Ax = b, & \xrightarrow{Dual} & \text{s.t.} & A^T\pi + fu \le c, \\ & f^T x \ge k, & & & u \ge 0, \\ & x \ge \mathbf{0}, & & & \end{array}$$

where $f_i := \mathbb{1}_{\{\gamma:\gamma > \frac{\hat{z}-\bar{z}}{k}\}}(\gamma_i)$. Let $u_* = \min_{1\le i\le n}\{\gamma_i :\ \gamma_i > \frac{\hat{z}-\bar{z}}{k}\}$, then by definition, (π_*, u_*) is a feasible solution to its dual $(\widehat{\text{DFP}})$, which has an objective value $b^T\pi_* + ku_* = \bar{z} + ku_* > \bar{z} + k\frac{\hat{z}-\bar{z}}{k} = \hat{z}$. Thus, $z \ge b^T\pi_* + ku_* > \hat{z}$, which completes the proof. ■

EC.2. Some Implementation Details

EC.2.1. Completion Bounds

Each time value is first multiplied by 10^τ to be integral, where τ is the number of decimal places that define the instance precision. The notation with a "$\hat{}$" sign is used to denote the scaled value. For example, $\hat{a}_i$ denotes the scaled starting time of customer i's time window a_i. The set of all states is defined as $\Omega := \{\,(i,q,t) : \forall i \in N,\ \forall q \in \{q_{\min}, \cdots, Q\},\ \forall t \in \{\hat{a}_{\min}, \cdots, \hat{b}_0\}\,\}$, where $q_{\min} = \min_{i\in N}\{q_i\}$, and $\hat{a}_{\min} = \min_{i\in N}\{\hat{a}_i\}$.

We initialize the states $\omega(j, q_j, t) = \bar{c}_{0j},\ \forall t \in \{\hat{a}'_j, \cdots, \hat{b}_j\}$, where $\hat{a}'_j = \max\{\hat{a}_0 + \hat{t}'_{0j}, \hat{a}_j\}$, and all other states in Ω are initialized to $+\infty$. Then, the following Bellman-type recursion is applied for all $(i, q, t) \in \Omega$.

$$\omega(i, q, t) = \min_{\substack{j \in N, j \neq i \\ t - \hat{t}'_{ji} \geq \hat{a}_j}} \left\{ \omega\left(j,\, q - q_i,\, \min\{t - \hat{t}'_{ji}, \hat{b}_j\}\right) + \bar{c}_{ji} \right\}. \tag{EC.1}$$

More precisely, the above step is conducted by three nested "for" loops, where q goes from $q_{\min}$ to Q in the most outer loop, i iterates through each customer $i \in N$ in the second loop, and t goes from $\hat{a}_i$ to $\hat{b}_i$ in the most inner loop. Then, $\bar{\omega}(i, q) := \min_{(i,q,t)\in\Omega} \{\min_{q' \leq q} \omega(i, q', t)\}$ is a lower bound on the partial reduced cost β^f of any feasible forward path $f := \{0, i_1, \cdots, i_{k_f} = i\}$ that starts from the depot and serves a set of customers $N^f = \{i_1, \cdots, i_{k_f}\}$ exactly once in the required time windows with $q^f = \sum_{i \in N^f} q_i \leq Q$.

When $\hat{b}_0$ is large, the recursion in equation (EC.1) will be computationally intensive. One acceleration technique is to scale down all time values. For example, dividing all numbers by 100 and rounding down will yield a state space Ω that is only 1% of its original size. Since infeasible forward paths (in the sense of non-scaled values) can be used to compute equation (EC.1), the lower bound obtained may be looser but must still be valid.

EC.2.2. The Row Generation

Let $x^* = (x^*_s)_{s \in \overline{\mathcal{S}}_1}$ be an optimal solution to the current RMP, where $\overline{\mathcal{S}}_1$ is the set of structures generated so far. For RSFCs, we start with an array $\xi = (\xi_t)_{t \in \{0, \cdots, \hat{b}_0\}}$ of length $\hat{b}_0 + 1$ where each element ξ_t is initialized to 0. For each $s \in \overline{\mathcal{S}}_1$ such that $x^*_s \neq 0$, the array is updated by $\xi_t \leftarrow \xi_t + x^*_s$, $\forall t \in \{\hat{e}_s, \cdots, \hat{\ell}_s + \hat{d}_s - 1\}$. Any $\xi_t > m$ corresponds to a violated RSFC. For SRIs, we start with an array $\delta = (\delta_{ijk})_{(i,j,k)\in\mathcal{C}}$ of length $\binom{n}{3}$ with all δ_{ijk} initialized to 0. For each $s \in \overline{\mathcal{S}}_1$ such that $x^*_s \neq 0$, δ is updated by $\delta_{ijk} \leftarrow \delta_{ijk} + x^*_s$, $\forall (i, j, k) \in \mathcal{C}_s$. A violated SRI is identified when $\delta_{ijk} > 1$.

EC.3. Adapting the EPCEM to Solving Four Variants

The EPCEM can be modified to solve CMTVRPTW variants subject to application-specific constraints. The additional constraints will affect how we define feasible structures and superstructures. But once all qualified superstructures are enumerated, the problem can be solved similarly. We only need to modify the BLM and the BLMCB in *Steps 1* and *3* slightly.

EC.3.1. Modifications for the CMTVRPTW-LT

Let $\mathrm{lt}^{\mathscr{b}} := \sum_{i \in N^{\mathscr{b}}} \mathrm{lt}_i$ be the loading time of path $\mathscr{b}$, and a label $L^{\mathscr{b}}$ is considered feasible if (7) and (EC.2) hold, which requires there to be enough time to go back to the depot.

$$a_0 + t'_{0i^{\mathscr{b}}} + \mathrm{lt}^{\mathscr{b}} \leq \ell^{\mathscr{b}}, \quad \text{when} \ \ i^{\mathscr{b}} \neq 0. \tag{EC.2}$$

Since the loading time happens only once at the depot, it does not affect the intermediate extension in our labeling algorithms. For the BLM, it suffices to make the following changes when we extend the label back to the depot, and all other equations in (8) that are not shown in (EC.3) remain unchanged.

$$\text{When } j=0, \qquad \begin{cases} e^{\acute{\ell}'} = \begin{cases} b_j, & \text{if } e^{\acute{\ell}} > b_j + t'_{ji^{\acute{\ell}}} + \mathrm{lt}^{\acute{\ell}}, \\ e^{\acute{\ell}} - t'_{ji^{\acute{\ell}}} - \mathrm{lt}^{\acute{\ell}}, & \text{if } a_j + t'_{ji^{\acute{\ell}}} + \mathrm{lt}^{\acute{\ell}} \le e^{\acute{\ell}} \le b_j + t'_{ji^{\acute{\ell}}} + \mathrm{lt}^{\acute{\ell}}, \\ a_j, & \text{otherwise,} \end{cases} \\ \ell^{\acute{\ell}'} = \min\{\ell^{\acute{\ell}} - t'_{ji^{\acute{\ell}}} - \mathrm{lt}^{\acute{\ell}}, b_j\}, \quad d^{\acute{\ell}'} = d^{\acute{\ell}} + \max\{t'_{ji^{\acute{\ell}}} + \mathrm{lt}^{\acute{\ell}}, e^{\acute{\ell}} - b_j\}. \end{cases} \tag{EC.3}$$

The dominance rule in Proposition 1 can be proved valid by the same argument and the additional fact that $\mathrm{lt}^{\acute{\ell}_1} \le \mathrm{lt}^{\acute{\ell}_2}$ when $N^{\acute{\ell}_1} \subseteq N^{\acute{\ell}_2}$. For the BLMCB, the above changes should also be made in the backward extension. In addition, the initialization of the completion bounds should be changed accordingly. We set $\omega(j, q_j, t) = \bar{c}_{0j}$, $\forall t \in \{\hat{a}'_j, \hat{a}'_j + 1, \cdots, \hat{b}_j\}$, where $\hat{a}'_j = \max\{\hat{a}_0 + \hat{t}'_{0j} + \hat{\mathrm{lt}}_j, \hat{a}_j\}$. All other states in Ω are initialized to $+\infty$.

EC.3.2. Modifications for the CMTVRPTW-LD

Besides the modifications described in EC.3.1, we need to adjust the definition of feasibility. Let $i_1^{\acute{\ell}}$ be the first customer visited in the backward path $\acute{\ell}$, then a label is feasible if (7), (EC.2), and $d^{\acute{\ell}} - t'_{i_1^{\acute{\ell}},0} - \mathrm{lt}^{\acute{\ell}} \le \bar{d}$ are satisfied. The dominance rule in Proposition 1 is modified to that $L^{\acute{\ell}_1}$ dominates $L^{\acute{\ell}_2}$ if (i) to (vi) and $t'_{i_1^{\acute{\ell}_1},0} \le t'_{i_1^{\acute{\ell}_2},0}$ hold.

EC.3.3. Modifications for the CMTVRPTW-R

For the CMTVRPTW-R, we assume that $a_i \ge \mathrm{rd}_i$. Otherwise, we can simply replace a_i with rd_i. Obviously, $b_i \ge \mathrm{rd}_i$, $\forall i \in N$, and $b_0 \ge \max_{i \in N} \mathrm{rd}_i$ need to be satisfied to ensure feasibility. A label in the BLM is considered feasible if (7) and $\ell^{\acute{\ell}} \ge \mathrm{rd}^{\acute{\ell}}$ hold, where $\mathrm{rd}^{\acute{\ell}} := \max_{i \in N^{\acute{\ell}}} \mathrm{rd}_i$. When extending the label back to the depot, we need to make the following change to equation (8).

$$\text{When } j=0, \qquad e^{\acute{\ell}'} = \begin{cases} b_j, & \text{if } e^{\acute{\ell}} > b_j + t'_{ji^{\acute{\ell}}}, \\ \max\{\mathrm{rd}^{\acute{\ell}}, e^{\acute{\ell}} - t'_{ji^{\acute{\ell}}}\}, & \text{if } a_j + t'_{ji^{\acute{\ell}}} \le e^{\acute{\ell}} \le b_j + t'_{ji^{\acute{\ell}}}, \\ \max\{\mathrm{rd}^{\acute{\ell}}, a_j\}, & \text{otherwise.} \end{cases} \tag{EC.4}$$

For the BLMCB, we initialize the state value $\omega(j, q_j, t) = \bar{c}_{0j}$, $\forall t \in \{\hat{a}'_j, \hat{a}'_j + 1, \cdots, \hat{b}_j\}$, where $\hat{a}'_j = \max\{\hat{a}_0 + \hat{t}'_{0j}, \hat{\mathrm{rd}}_j + \hat{t}'_{0j}, \hat{a}_j\}$, and all other states are initialized to $+\infty$. Equation (EC.1) is replaced by

$$\omega(i, q, t) = \min_{\substack{j \in N, j \ne i \\ t - \hat{t}'_{ji} \ge \max\{\hat{a}_j, \hat{\mathrm{rd}}_j\}}} \left\{ \omega(j,\, q - q_i,\, \min\{t - \hat{t}'_{ji}, \hat{b}_j\}) + \bar{c}_{ji} \right\}. \tag{EC.5}$$

EC.3.4. Modifications for the DRP

Let $\overline{\text{en}}$ be the battery capacity, en_{ijq} and ce_{ijq} be the energy consumption and energy cost, respectively, when the drone travels from customer i to j with load q, and $\text{en}^{\mathscr{b}}$ be the total energy consumption of path $\mathscr{b}$. A feasible label needs to further satisfy the battery constraint $\text{en}^{\mathscr{b}} \leq \overline{\text{en}}$.

For the extension in the BLM, we first redefine the label $L^{\mathscr{b}}$ by adding the element $\text{en}^{\mathscr{b}}$, which is initialized to 0. Thus, each label $L^{\mathscr{b}} := (N^{\mathscr{b}}, q^{\mathscr{b}}, e^{\mathscr{b}}, \ell^{\mathscr{b}}, d^{\mathscr{b}}, i^{\mathscr{b}}, \text{en}^{\mathscr{b}}, \beta^{\mathscr{b}}, \gamma^{\mathscr{b}})$ will be a 9-tuple. Then (8) is modified as below.

$$\begin{cases} \text{en}^{\mathscr{b}'} = \text{en}^{\mathscr{b}} + \text{en}_{ji^{\mathscr{b}}q^{\mathscr{b}}}, \\ \beta^{\mathscr{b}'} = \beta^{\mathscr{b}} + \bar{c}_{ji^{\mathscr{b}}} + \text{ce}_{ji^{\mathscr{b}}q^{\mathscr{b}}}. \end{cases} \tag{EC.6}$$

All other equations in (8) that are not shown in (EC.6) remain unchanged. For the dominance rule in Proposition 1, the condition that $\text{en}^{\mathscr{b}_1} \leq \text{en}^{\mathscr{b}_2}$ needs to be added. The resulting rule can be easily proved valid by the same argument. For the BLMCB, we adopt the same changes described above for the backward extension part. Besides, we need to change the way of computing the completion bounds. We initialize the state value $\omega(j, q_j, t) = \bar{c}_{0j} + \text{ce}_{0jq_j}$, $\forall t \in \{\hat{a}'_j, \hat{a}'_j + 1, \cdots, \hat{b}_j\}$, where $\hat{a}'_j = \max\{\hat{a}_0 + \hat{t}'_{0j}, \hat{a}_j\}$, and all other states in Ω are initialized to $+\infty$. Equation (EC.1) is replaced by $\omega(i, q, t) = \min_{\substack{j \in N, j \neq i \\ t - \hat{t}'_{ji} \geq \hat{a}_j}} \left\{ \omega(j,\, q - q_i,\, \min\{t - \hat{t}'_{ji}, \hat{b}_j\}) + \bar{c}_{ji} + \text{ce}_{jiq_i} \right\}$.

EC.4. Detailed Results for Small Instances on Machine 1

Tables EC.4.1 to EC.5.5 present detailed results for each individual instance, where the following information is included: the instance name (Name), the number of customers (n), the limit on the trip duration for the CMTVRPTW-LD ($\bar{d}$), the best upper bound at termination (UB), the optimality gap $\frac{\text{UB}-\text{LB}}{\text{UB}} \times 100\%$ (Gap%), the computing time of each instance in seconds (CPU), the gap between the lower bound computed in *Step 1* and UB ($\text{LB}_1\%$), the cardinality of $\mathcal{S}_1$ yielded in *Step 1* ($|\mathcal{S}_1|$), the gap between the initial upper bound computed in *Step 2* and UB ($\text{UB}_1\%$), the cardinality of $\mathcal{S}_2$ yielded in *Step 3* ($|\mathcal{S}_2|$), the gap between the lower bound computed in *Step 4* and UB ($\text{LB}_2\%$), the cardinality of $\mathcal{S}_3$ yielded in *Step 5* ($|\mathcal{S}_3|$), the cardinality of $\mathcal{U}_3$ yielded in *Step 6* ($|\mathcal{U}_3|$), and the computing time of the MPSC in *Step 7* (CPU_7). If for an instance, the EPCEM terminates at *Step 1* when the limit in the BLM or the BLMCB is reached, all values are reported as "—" in the tables. When it terminates at *Step 3* due to the enumeration limit, the values corresponding to *Steps 3* to *7* are reported as "—".

EC.4.1. Detailed Results for the CMTVRPTW on Machine 1

Table EC.1: Detailed Results for the CMTVRPTW on Machine 1.

Name	n	UB	Gap%	CPU	Step1		Step2	Step3	Step4	Step5	Step6	Step7
					$\text{LB}_1\%$	$\lvert\mathcal{S}_1\rvert$	$\text{UB}_1\%$	$\lvert\mathcal{S}_2\rvert$	$\text{LB}_2\%$	$\lvert\mathcal{S}_3\rvert$	$\lvert\mathcal{U}_3\rvert$	CPU_7

Continued on next page

Table EC.1 – *Continued from previous page*

Name	n	UB	Gap%	T_{tol}	Step1		Step2	Step3	Step4	Step5	Step6	Step7
					LB_1%	$\lvert\mathcal{S}_1\rvert$	UB_1%	$\lvert\mathcal{S}_2\rvert$	LB_2%	$\lvert\mathcal{S}_3\rvert$	$\lvert\mathcal{U}_3\rvert$	CPU_7
C201	25	378.6	0.00	2.6	2.12	4,741	0.58	2,563	2.12	1,675	1,675	0.7
C202	25	363.0	0.00	3.1	0.00	6,951	0.00	0	0.00	0	0	0.0
C203	25	358.8	0.00	2.8	0.00	6,975	0.00	0	0.00	0	0	0.0
C204	25	358.8	0.00	4.9	0.32	7,237	0.00	130	0.32	95	94	0.0
C205	25	368.3	0.00	2.7	1.00	5,647	0.00	389	1.00	249	249	0.1
C206	25	367.2	0.00	5.4	2.13	6,484	0.30	3,273	2.13	2,570	2,563	1.0
C207	25	358.8	0.00	3.8	1.15	4,455	0.08	1,051	1.15	600	571	0.0
C208	25	359.1	0.00	4.9	0.81	5,398	0.00	582	0.81	305	305	0.1
R201	25	546.8	0.00	2.4	0.80	4,515	0.00	318	0.80	109	109	0.0
R202	25	482.8	0.00	6.1	2.35	6,617	0.00	1,579	2.35	1,072	1,062	0.3
R203	25	442.6	0.00	14.3	1.25	8,746	0.16	742	1.25	465	464	0.2
R204	25	404.9	0.00	32.0	2.08	9,050	0.77	8,970	2.08	6,082	5,660	3.4
R205	25	448.4	0.00	5.4	0.36	8,407	0.00	96	0.36	64	63	0.0
R206	25	413.9	0.00	5.2	0.17	7,705	0.00	83	0.17	47	45	0.0
R207	25	399.8	0.00	4.9	1.38	7,958	0.00	478	1.38	124	118	0.0
R208	25	394.3	0.00	4.7	1.88	10,258	0.00	933	1.88	650	602	0.1
R209	25	418.3	0.00	8.6	1.51	8,124	0.00	507	1.51	146	145	0.0
R210	25	448.3	0.00	8.2	0.62	6,757	0.33	354	0.62	245	244	0.0
R211	25	399.9	0.00	7.8	1.45	9,380	0.05	942	1.45	493	483	0.4
RC201	25	660.0	0.00	1.1	2.45	3,345	0.00	370	2.45	249	249	0.0
RC202	25	576.1	0.00	854.9	6.79	4,478	0.00	4,484	6.79	2,384	2,180	847.9
RC203	25	528.8	0.00	61.1	1.85	7,176	0.00	1,363	1.85	1,117	932	28.0
RC204	25	516.5	0.00	14.7	1.09	7,712	0.00	1,082	1.09	623	471	0.5
RC205	25	603.0	0.00	2.2	1.01	5,078	0.38	635	1.01	318	304	0.1
RC206	25	575.1	0.00	18.3	2.12	4,813	1.15	2,307	2.12	1,333	1,310	0.5
RC207	25	526.4	0.00	2.2	1.18	6,449	0.00	290	1.18	182	169	0.1
RC208	25	506.4	0.00	5.5	0.14	9,414	0.00	141	0.14	64	48	0.0
C201	40	625.6	0.00	236.6	1.92	30,444	0.27	29,380	1.92	23,647	23,647	212.6
C202	40	616.1	0.00	504.5	1.73	29,729	0.60	63,262	1.73	47,818	47,798	463.4
C203	40	611.9	0.00	102.6	1.35	22,718	0.46	40,703	1.34	34,720	34,111	71.8
C204	40	609.9	0.00	220.0	1.34	29,864	0.84	93,843	1.33	77,549	71,940	150.9
C205	40	621.0	0.00	253.2	2.22	33,124	0.13	27,639	2.22	23,766	23,763	222.1
C206	40	612.4	0.00	85.0	1.66	32,463	0.78	48,124	1.66	40,830	40,810	46.7
C207	40	609.9	0.00	222.3	1.48	24,158	1.08	71,772	1.48	62,857	62,586	151.9
C208	40	609.9	0.00	31.7	1.38	29,109	0.77	33,959	1.38	27,708	27,680	14.8
R201	40	731.7	0.00	3.1	0.00	13,247	0.00	0	0.00	0	0	0.0
R202	40	638.7	0.00	8.2	0.00	20,080	0.00	0	0.00	0	0	0.0
R203	40	604.7	0.00	14.5	0.96	17,617	0.00	1,732	0.89	822	803	0.5
R204	40	572.6	0.00	13.1	0.19	19,186	0.00	267	0.13	128	111	0.0
R205	40	632.9	0.00	8.3	0.67	18,262	0.08	642	0.65	379	378	0.2
R206	40	598.8	0.00	9.9	0.71	21,087	0.00	833	0.71	656	643	0.2
R207	40	577.9	0.00	15.7	0.51	19,697	0.48	2,135	0.44	1,258	1,201	0.3
R208	40	569.4	0.00	25.3	0.02	20,009	0.00	156	0.00	0	0	0.0
R209	40	587.0	0.00	5.0	0.00	17,621	0.00	0	0.00	0	0	0.0
R210	40	591.5	0.00	5.2	0.00	21,399	0.00	0	0.00	0	0	0.0
R211	40	576.1	0.00	18.7	0.87	18,219	0.17	2,403	0.78	1,253	1,223	1.3
RC201	40	1014.7	0.00	9.9	1.32	13,023	0.00	929	1.32	660	658	0.1
RC202	40	907.3	0.00	7.8	0.33	19,307	0.00	372	0.18	101	95	0.0
RC203	40	887.7	0.00	137.0	1.52	19,868	0.00	5,356	0.70	1,002	897	5.0
RC204	40	865.4	0.00	29.8	0.16	28,057	0.08	548	0.00	191	148	0.0
RC205	40	940.6	0.00	14.0	0.76	20,593	0.58	1,706	0.34	594	579	0.2
RC206	40	937.9	0.00	10.4	1.79	17,002	0.10	4,888	1.10	1,234	1,215	1.1
RC207	40	881.8	0.00	10.0	0.70	21,597	0.00	903	0.00	0	0	0.0
RC208	40	864.4	0.00	18.1	0.45	25,568	0.00	997	0.00	0	0	0.0
C201	50	704.4	0.00	40.5	0.95	38,041	1.14	58,109	0.88	40,194	40,194	13.4
C202	50	692.1	0.00	47.2	1.20	44,176	0.00	11,010	1.17	6,898	6,892	13.3
C203	50	686.5	0.00	36.8	0.86	37,440	0.22	18,311	0.79	10,992	10,770	9.0
C204	50	685.1	0.00	97.0	0.86	58,207	0.07	21,170	0.85	12,760	11,862	24.5
C205	50	698.5	0.00	31.1	1.06	46,225	0.09	11,499	1.01	5,922	5,919	7.5
C206	50	688.6	0.00	26.4	0.88	43,034	0.25	9,627	0.88	6,835	6,827	5.1
C207	50	687.4	0.00	132.8	1.13	36,952	0.19	34,964	1.09	21,699	21,593	110.1
C208	50	687.4	0.00	230.4	1.18	38,686	0.79	90,050	1.18	66,316	66,282	191.7
R201	50	909.8	0.00	28.8	0.92	26,091	0.00	2,016	0.88	1,098	1,098	0.7
R202	50	815.2	0.00	38.4	1.48	31,586	0.07	10,467	1.47	7,448	7,416	9.7

Continued on next page

Table EC.1 – *Continued from previous page*

Name	n	UB	Gap%	T_{tol}	Step1		Step2	Step3	Step4	Step5	Step6	Step7
					LB_1%	$\|\mathcal{S}_1\|$	UB_1%	$\|\mathcal{S}_2\|$	LB_2%	$\|\mathcal{S}_3\|$	$\|\mathcal{U}_3\|$	CPU_7
R203	50	742.4	0.00	119.9	1.85	39,108	0.00	23,863	1.61	12,213	11,911	84.0
R204	50	702.3	0.00	67.0	1.25	31,624	0.41	48,032	0.96	20,177	17,243	18.6
R205	50	805.9	0.00	65.6	1.39	30,531	0.17	13,375	1.30	7,924	7,905	11.9
R206	50	755.9	0.00	428.0	1.90	34,435	0.69	117,127	1.75	72,510	71,556	350.1
R207	50	715.7	0.00	70.9	1.26	35,640	0.77	51,321	1.13	28,719	27,465	11.5
R208	50	699.6	0.00	113.4	1.02	29,885	1.27	166,615	0.94	101,247	84,235	16.8
R209	50	745.0	0.00	88.1	1.89	26,808	0.30	34,796	1.56	14,554	14,371	51.9
R210	50	775.5	0.00	4363.1	2.47	32,839	0.52	208,339	2.23	132,619	131,192	4080.9
R211	50	711.5	0.00	3912.8	2.23	25,531	1.41	759,251	1.94	487,178	476,085	3517.0
RC201	50	1086.2	0.00	4.3	0.00	21,746	0.00	0	0.00	0	0	0.0
RC202	50	981.2	0.00	4.8	0.00	23,944	0.00	0	0.00	0	0	0.0
RC203	50	941.2	0.00	59.2	0.87	28,828	0.00	2,395	0.58	678	593	15.7
RC204	50	915.9	0.00	41.3	0.00	35,888	0.00	0	0.00	0	0	0.0
RC205	50	1055.2	0.00	26.8	2.58	24,216	0.12	13,649	2.58	6,930	6,804	5.1
RC206	50	1027.4	0.00	146.4	3.42	25,737	0.00	45,688	2.66	16,730	16,603	117.7
RC207	50	941.7	0.00	44.0	0.59	29,042	0.00	1,107	0.59	666	644	5.1
RC208	50	915.0	0.00	136.3	0.36	33,913	0.16	1,545	0.29	706	588	0.5

EC.4.2. Detailed Results for the CMTVRPTW-LT on Machine 1

Table EC.2: Detailed Results for the CMTVRPTW-LT on Machine 1.

Name	n	UB	Gap%	CPU	Step1		Step2	Step3	Step4	Step5	Step6	Step7
					LB_1%	$\|\mathcal{S}_1\|$	UB_1%	$\|\mathcal{S}_2\|$	LB_2%	$\|\mathcal{S}_3\|$	$\|\mathcal{U}_3\|$	CPU_7
C201	25	380.8	0.00	2.1	2.65	3,427	0.00	1,781	2.65	1,225	1,225	0.8
C202	25	368.6	0.00	10.0	0.75	6,401	0.00	535	0.75	361	361	0.1
C203	25	361.7	0.00	2.6	0.00	6,059	0.00	0	0.00	0	0	0.0
C204	25	358.8	0.00	4.5	0.23	7,236	0.00	94	0.23	58	57	0.0
C205	25	377.2	0.00	3.9	3.14	5,633	0.27	3,146	3.14	1,394	1,392	1.4
C206	25	367.2	0.00	9.2	1.86	5,619	2.31	11,985	1.86	8,606	8,597	2.5
C207	25	359.1	0.00	4.4	1.12	3,746	0.00	859	1.12	584	557	0.1
C208	25	360.9	0.00	5.9	1.03	5,715	0.00	648	1.03	537	536	0.1
R201	25	554.6	0.00	5.8	0.74	4,780	0.00	248	0.74	159	159	0.1
R202	25	485.0	0.00	11.2	1.25	6,664	0.00	690	1.25	510	506	0.3
R203	25	444.2	0.00	18.3	0.41	8,784	0.23	275	0.41	221	219	0.1
R204	25	407.5	0.00	31.8	2.19	8,002	0.12	3,934	2.18	2,527	2,354	0.9
R205	25	448.4	0.00	6.2	0.09	8,409	0.00	66	0.09	49	48	0.0
R206	25	413.9	0.00	4.9	0.00	7,507	0.00	0	0.00	0	0	0.0
R207	25	400.1	0.00	4.8	1.45	8,456	0.00	557	1.45	103	97	0.0
R208	25	394.3	0.00	5.4	1.88	9,566	0.00	1,278	1.88	561	526	0.1
R209	25	418.3	0.00	4.7	0.53	7,959	0.00	98	0.53	66	64	0.0
R210	25	448.3	0.00	13.0	0.22	6,927	0.33	254	0.22	160	160	0.0
R211	25	400.1	0.00	4.0	1.30	9,484	0.00	419	1.30	325	318	0.0
RC201	25	660.0	0.00	1.0	1.98	3,311	0.00	306	1.98	220	219	0.0
RC202	25	596.8	0.00	3607.8	10.02	5,271	0.28	22,933	10.02	8,548	8,097	3054.3
RC203	25	530.1	0.00	37.0	1.63	7,698	0.00	1,058	1.63	635	517	26.4
RC204	25	518.0	0.00	10.7	1.14	7,849	0.00	1,002	1.14	563	408	1.5
RC205	25	605.3	0.00	2.2	0.73	5,031	0.00	230	0.73	154	149	0.0
RC206	25	575.1	0.00	2.1	0.95	4,877	0.00	346	0.94	228	219	0.1
RC207	25	528.2	0.00	2.8	1.17	6,399	0.00	296	1.17	207	192	0.1
RC208	25	506.4	0.00	5.0	0.14	9,270	0.00	134	0.14	68	50	0.0
C201	40	626.6	0.00	166.3	1.60	22,028	0.65	33,834	1.60	27,831	27,831	72.2
C202	40	617.9	0.00	84.0	1.37	31,230	0.37	14,685	1.37	12,639	12,632	64.6
C203	40	611.9	0.00	36.2	1.11	22,501	0.56	25,659	1.10	19,526	19,223	13.5
C204	40	609.9	0.00	220.1	1.34	29,864	0.84	93,843	1.33	77,549	71,940	150.4
C205	40	621.0	0.00	398.7	2.16	33,078	0.21	36,629	2.16	30,921	30,918	367.3
C206	40	613.0	0.00	89.3	1.71	30,425	0.64	42,657	1.71	33,553	33,540	50.5
C207	40	609.9	0.00	144.3	1.48	25,721	0.00	14,475	1.48	12,347	12,244	118.2
C208	40	610.1	0.00	66.3	1.41	31,155	0.57	25,497	1.41	23,885	23,865	24.8
R201	40	732.1	0.00	2.6	0.00	12,604	0.00	0	0.00	0	0	0.0
R202	40	639.8	0.00	8.3	0.00	21,747	0.00	0	0.00	0	0	0.0

Continued on next page

Table EC.2 – *Continued from previous page*

Name	n	UB	Gap%	T_{tol}	Step1		Step2	Step3	Step4	Step5	Step6	Step7
					LB_1%	$\lvert\mathcal{S}_1\rvert$	UB_1%	$\lvert\mathcal{S}_2\rvert$	LB_2%	$\lvert\mathcal{S}_3\rvert$	$\lvert\mathcal{U}_3\rvert$	CPU_7
R203	40	604.7	0.00	8.5	0.64	19,827	0.00	624	0.64	411	404	0.0
R204	40	572.6	0.00	27.9	0.15	19,065	0.00	261	0.15	206	177	0.0
R205	40	632.9	0.00	9.3	0.26	19,579	0.00	176	0.24	95	95	0.0
R206	40	598.8	0.00	12.4	0.71	21,647	0.00	794	0.71	475	460	0.1
R207	40	577.9	0.00	11.5	0.48	18,838	0.42	1,681	0.39	803	768	0.2
R208	40	569.4	0.00	24.3	0.00	18,464	0.12	231	0.00	164	143	0.0
R209	40	587.0	0.00	5.4	0.00	17,620	0.00	0	0.00	0	0	0.0
R210	40	603.4	0.00	12.5	0.23	21,712	0.00	170	0.17	69	69	0.0
R211	40	576.1	0.00	19.6	0.80	18,094	0.35	2,987	0.75	1,607	1,573	1.5
RC201	40	1018.7	0.00	9.5	1.58	12,324	0.00	1,390	1.58	843	839	0.2
RC202	40	908.1	0.00	16.1	0.26	19,894	0.00	312	0.26	186	174	0.0
RC203	40	887.7	0.00	61.8	0.92	21,638	0.00	2,366	0.70	1,218	1,114	5.8
RC204	40	865.4	0.00	28.0	0.35	28,327	0.08	851	0.00	184	142	0.0
RC205	40	942.1	0.00	8.7	0.39	19,854	0.00	322	0.00	0	0	0.0
RC206	40	939.6	0.00	13.0	1.49	18,204	0.00	2,932	1.11	1,097	1,075	1.0
RC207	40	881.8	0.00	10.0	0.78	21,083	0.31	1,931	0.00	236	223	0.0
RC208	40	864.4	0.00	28.7	0.49	25,966	0.00	1,093	0.00	0	0	0.0
C201	50	714.2	0.00	152.9	1.65	35,064	0.76	72,373	1.65	57,490	57,490	114.8
C202	50	700.1	0.00	266.9	1.59	41,954	0.36	69,025	1.59	50,663	50,629	236.7
C203	50	688.0	0.00	85.3	0.91	40,252	0.29	26,576	0.87	16,520	16,107	49.3
C204	50	685.1	0.00	101.4	0.86	58,207	0.07	21,170	0.85	12,760	11,862	24.4
C205	50	699.1	0.00	40.0	0.89	46,791	0.21	12,607	0.82	5,859	5,856	9.4
C206	50	694.6	0.00	172.8	1.44	43,475	0.62	72,850	1.40	45,693	45,675	108.8
C207	50	688.6	0.00	297.3	1.31	39,385	0.01	42,969	1.26	23,218	23,113	274.2
C208	50	688.6	0.00	132.6	1.31	45,439	0.00	21,243	1.30	15,676	15,659	113.3
R201	50	909.8	0.00	65.8	0.64	26,244	1.56	18,237	0.64	9,417	9,414	7.9
R202	50	816.0	0.00	53.1	1.36	32,107	0.40	18,405	1.32	8,698	8,650	7.9
R203	50	742.4	0.00	99.2	1.49	34,308	0.30	28,802	1.32	14,769	14,444	31.2
R204	50	702.3	0.00	70.4	1.17	30,004	0.41	41,500	0.96	19,668	16,796	22.7
R205	50	807.3	0.00	29.1	1.23	29,146	0.00	5,793	1.18	3,151	3,143	3.8
R206	50	758.2	0.00	485.4	2.01	33,611	0.66	117,973	1.81	72,028	71,058	397.3
R207	50	715.7	0.00	162.0	1.16	30,045	0.92	64,760	0.99	35,546	33,995	13.8
R208	50	699.6	0.00	93.7	1.06	30,378	0.33	26,461	0.94	12,536	10,345	15.3
R209	50	745.0	0.00	98.4	1.66	26,798	0.30	27,374	1.47	14,407	14,224	52.5
R210	50	777.2	0.00	2988.3	2.25	29,962	1.20	385,481	1.94	245,751	243,119	2679.1
R211	50	716.8	0.73	10800.4	2.78	25,571	1.88	3,003,061	2.38	1,803,385	1,768,963	9279.0
RC201	50	1096.6	0.00	4.8	0.47	23,482	0.00	310	0.47	192	192	0.0
RC202	50	1001.6	0.00	112.3	0.98	23,290	0.00	1,159	0.98	845	801	101.3
RC203	50	941.2	0.00	68.8	0.46	25,797	0.00	1,237	0.46	796	650	0.2
RC204	50	915.9	0.00	166.9	0.00	37,799	0.00	0	0.00	0	0	0.0
RC205	50	1058.7	0.00	38.0	1.31	24,044	0.00	2,840	0.70	649	636	0.4
RC206	50	1027.4	0.00	190.5	3.11	26,251	0.58	38,747	2.51	21,446	21,262	159.2
RC207	50	941.7	0.00	11.0	0.44	25,326	0.00	654	0.44	410	396	0.1
RC208	50	916.8	0.00	266.2	0.33	33,890	0.00	824	0.33	549	471	0.4

EC.4.3. Detailed Results for the CMTVRPTW-LD on Machine 1

Table EC.3: Detailed Results for the CMTVRPTW-LD on Machine 1.

Name	n	$\bar{d}$	UB	Gap%	CPU	Step1		Step2	Step3	Step4	Step5	Step6	Step7
						LB_1%	$\lvert\mathcal{S}_1\rvert$	UB_1%	$\lvert\mathcal{S}_2\rvert$	LB_2%	$\lvert\mathcal{S}_3\rvert$	$\lvert\mathcal{U}_3\rvert$	CPU_7
C201	25	220	657.8	0.00	0.1	1.54	105	0.00	54	1.54	45	45	0.0
C201	25	250	539.8	0.00	0.0	0.00	144	0.00	0	0.00	0	0	0.0
C202	25	220	652.1	0.00	0.1	1.56	300	0.00	117	1.56	110	95	0.0
C202	25	250	532.5	0.00	0.1	0.75	683	0.47	127	0.75	99	96	0.0
C203	25	220	645.2	0.00	0.1	1.85	452	0.00	203	1.85	172	138	0.0
C203	25	250	531.8	0.00	0.1	0.75	1,133	0.47	245	0.75	198	191	0.0
C204	25	220	601.3	0.00	0.2	1.08	523	0.00	138	1.08	117	101	0.0
C204	25	250	524.6	0.00	0.2	1.39	1,440	0.00	430	1.39	335	301	0.0
C205	25	220	635.2	0.00	0.1	2.85	186	0.00	94	2.85	72	72	0.0
C205	25	250	528.9	0.00	0.0	0.00	341	0.00	0	0.00	0	0	0.0

Continued on next page

Table EC.3 – *Continued from previous page*

Name	n	$\bar{d}$	UB	Gap%	T_{tol}	Step1		Step2	Step3	Step4	Step5	Step6	Step7
						LB_1%	$\lvert\mathcal{S}_1\rvert$	UB_1%	$\lvert\mathcal{S}_2\rvert$	LB_2%	$\lvert\mathcal{S}_3\rvert$	$\lvert\mathcal{U}_3\rvert$	CPU_7
C206	25	220	635.2	0.00	0.1	2.85	212	0.38	137	2.85	116	113	0.0
C206	25	250	526.9	0.00	0.1	0.44	396	0.00	63	0.44	40	37	0.0
C207	25	220	602.1	0.00	0.0	0.00	270	0.00	0	0.00	0	0	0.0
C207	25	250	524.6	0.00	0.0	0.00	661	0.00	0	0.00	0	0	0.0
C208	25	220	610.3	0.00	0.0	0.00	255	0.00	0	0.00	0	0	0.0
C208	25	250	524.6	0.00	0.0	0.00	501	0.00	0	0.00	0	0	0.0
R201	25	75	761.4	0.00	0.0	0.00	133	0.00	0	0.00	0	0	0.0
R201	25	100	697.2	0.00	0.0	0.58	266	0.00	41	0.58	33	32	0.0
R202	25	75	644.7	0.00	0.0	0.00	257	0.00	0	0.00	0	0	0.0
R202	25	100	616.6	0.00	0.1	0.00	698	0.41	50	0.00	36	27	0.0
R203	25	75	620.9	0.00	0.0	0.00	362	0.00	0	0.00	0	0	0.0
R203	25	100	576.6	0.00	0.1	0.00	933	1.08	171	0.00	78	59	0.0
R204	25	75	576.6	0.00	0.0	0.00	426	0.00	0	0.00	0	0	0.0
R204	25	100	482.1	0.00	0.1	0.00	1,116	0.00	0	0.00	0	0	0.0
R205	25	75	632.9	0.00	0.0	0.00	238	0.00	0	0.00	0	0	0.0
R205	25	100	557.9	0.00	0.0	0.13	630	0.00	37	0.13	20	18	0.0
R206	25	75	595.7	0.00	0.0	0.00	357	0.00	0	0.00	0	0	0.0
R206	25	100	522.5	0.00	0.0	0.00	886	0.00	0	0.00	0	0	0.0
R207	25	75	584.7	0.00	0.0	0.00	364	0.00	0	0.00	0	0	0.0
R207	25	100	510.9	0.00	0.2	1.37	908	0.22	298	1.37	192	160	0.0
R208	25	75	576.6	0.00	0.0	0.00	433	0.00	0	0.00	0	0	0.0
R208	25	100	482.1	0.00	0.1	0.00	1,165	0.00	0	0.00	0	0	0.0
R209	25	75	601.2	0.00	0.0	0.00	358	0.00	0	0.00	0	0	0.0
R209	25	100	516.5	0.00	0.1	0.48	750	0.00	69	0.48	44	39	0.0
R210	25	75	634.9	0.00	0.0	0.58	348	0.00	56	0.58	33	27	0.0
R210	25	100	546.2	0.00	0.0	0.00	759	0.00	0	0.00	0	0	0.0
R211	25	75	574.8	0.00	0.1	0.55	449	0.30	104	0.55	85	77	0.0
R211	25	100	473.4	0.00	0.2	0.00	1,062	0.00	0	0.00	0	0	0.0
RC201	25	75	986.5	0.00	1.8	0.68	112	0.00	42	0.68	35	33	0.0
RC201	25	100	824.9	0.00	0.2	4.30	238	0.00	113	4.30	68	65	0.0
RC202	25	75	880.4	0.00	0.1	3.70	278	0.00	225	3.70	211	144	0.0
RC202	25	100	678.8	0.00	0.0	0.00	729	0.00	0	0.00	0	0	0.0
RC203	25	75	748.1	0.00	0.1	4.36	382	0.00	365	4.36	310	215	0.0
RC203	25	100	592.7	0.00	0.2	0.00	1,115	0.00	0	0.00	0	0	0.0
RC204	25	75	743.7	0.00	0.3	9.14	545	0.00	513	9.14	513	367	0.0
RC204	25	100	586.2	0.00	1.1	0.80	1,912	0.00	725	0.80	536	339	0.0
RC205	25	75	839.2	0.00	0.3	0.56	253	0.00	89	0.56	71	52	0.0
RC205	25	100	701.3	0.00	0.1	0.02	690	0.00	44	0.02	25	23	0.0
RC206	25	75	759.7	0.00	0.0	0.08	238	0.00	45	0.08	35	34	0.0
RC206	25	100	602.9	0.00	0.0	0.00	615	0.00	0	0.00	0	0	0.0
RC207	25	75	737.8	0.00	4.7	4.84	504	0.11	329	4.84	328	275	0.1
RC207	25	100	513.9	0.00	0.4	0.39	1,138	0.00	73	0.39	54	49	0.0
RC208	25	75	727.2	0.00	0.7	12.89	576	0.06	501	12.89	501	443	0.0
RC208	25	100	501.4	0.00	8.4	1.69	2,585	0.80	1,228	0.00	243	206	0.0
C201	40	220	1121.8	0.00	0.1	0.00	199	0.00	0	0.00	0	0	0.0
C201	40	250	922.2	0.00	0.0	0.00	301	0.00	0	0.00	0	0	0.0
C202	40	220	1108.2	0.00	0.1	0.00	606	0.00	66	0.00	51	46	0.0
C202	40	250	918.3	0.00	0.1	0.00	1,297	0.00	0	0.00	0	0	0.0
C203	40	220	1086.8	0.00	0.4	0.27	858	0.00	124	0.27	89	72	0.0
C203	40	250	913.5	0.00	1.5	1.36	2,263	0.02	1,328	1.36	1,194	1,040	0.9
C204	40	220	1037.5	0.00	0.2	0.00	1,152	0.00	0	0.00	0	0	0.0
C204	40	250	906.7	0.00	2.5	1.17	3,520	0.00	1,269	1.17	1,121	1,016	0.8
C205	40	220	1082.1	0.00	0.1	0.44	376	0.00	92	0.44	76	75	0.0
C205	40	250	919.5	0.00	0.2	0.45	768	0.00	166	0.45	128	125	0.0
C206	40	220	1079.6	0.00	0.2	0.32	486	0.00	99	0.32	82	77	0.0
C206	40	250	915.2	0.00	0.1	0.17	1,024	0.00	125	0.17	94	87	0.0
C207	40	220	1052.0	0.00	0.2	0.15	653	0.00	89	0.15	72	65	0.0
C207	40	250	908.7	0.00	0.7	0.62	1,631	0.00	485	0.62	417	374	0.1
C208	40	220	1068.5	0.00	0.1	0.00	563	0.00	0	0.00	0	0	0.0
C208	40	250	913.9	0.00	0.3	0.27	1,352	0.00	173	0.27	137	123	0.0
R201	40	75	1159.3	0.00	0.0	0.00	321	0.00	0	0.00	0	0	0.0
R201	40	100	1013.8	0.00	0.1	0.13	786	0.00	69	0.13	50	50	0.0
R202	40	75	991.5	0.00	0.0	0.00	778	0.00	0	0.00	0	0	0.0
R202	40	100	898.7	0.00	0.2	0.00	1,942	0.00	0	0.00	0	0	0.0

Continued on next page

Table EC.3 – *Continued from previous page*

Name	n	$\bar{d}$	UB	Gap%	T_{tol}	Step1		Step2	Step3	Step4	Step5	Step6	Step7
						LB_1%	$\lvert\mathcal{S}_1\rvert$	UB_1%	$\lvert\mathcal{S}_2\rvert$	LB_2%	$\lvert\mathcal{S}_3\rvert$	$\lvert\mathcal{U}_3\rvert$	CPU_7
R203	40	75	953.6	0.00	0.2	1.00	1,055	0.00	440	1.00	335	295	0.0
R203	40	100	803.8	0.00	0.5	0.00	2,451	0.00	0	0.00	0	0	0.0
R204	40	75	856.3	0.00	0.3	0.97	1,367	0.00	393	0.97	246	227	0.0
R204	40	100	704.1	0.00	6.1	0.99	3,416	0.00	821	0.99	652	582	0.3
R205	40	75	971.8	0.00	0.1	0.12	639	0.00	68	0.12	45	42	0.0
R205	40	100	836.7	0.00	0.2	0.00	1,468	0.00	0	0.00	0	0	0.0
R206	40	75	911.3	0.00	0.2	0.37	1,031	0.12	133	0.37	102	90	0.0
R206	40	100	806.0	0.00	1.4	0.70	2,178	0.00	390	0.70	268	254	0.1
R207	40	75	884.2	0.00	0.2	0.11	1,063	0.00	66	0.11	47	44	0.0
R207	40	100	759.7	0.00	1.7	0.47	2,619	0.00	249	0.47	178	170	0.0
R208	40	75	856.3	0.00	0.6	0.97	1,214	0.65	865	0.97	688	602	0.1
R208	40	100	703.2	0.00	4.9	0.89	3,398	0.00	769	0.89	536	466	0.2
R209	40	75	933.7	0.00	0.3	0.28	917	0.00	105	0.28	92	87	0.0
R209	40	100	762.5	0.00	0.4	0.00	2,208	0.00	0	0.00	0	0	0.0
R210	40	75	942.7	0.00	0.2	1.03	894	0.00	297	1.03	237	220	0.0
R210	40	100	799.1	0.00	0.9	0.14	2,236	0.00	101	0.14	72	67	0.0
R211	40	75	840.6	0.00	0.3	0.69	1,241	0.00	202	0.69	164	157	0.0
R211	40	100	671.2	0.00	1.1	0.00	3,289	0.00	0	0.00	0	0	0.0
RC201	40	75	1786.4	0.00	0.1	0.00	153	0.00	0	0.00	0	0	0.0
RC201	40	100	1369.8	0.00	0.0	0.00	369	0.00	0	0.00	0	0	0.0
RC202	40	75	1593.0	0.00	0.3	2.05	354	0.00	270	2.05	236	163	0.0
RC202	40	100	1237.1	0.00	0.3	0.00	1,032	0.00	0	0.00	0	0	0.0
RC203	40	75	1449.8	0.00	0.4	2.25	498	0.00	421	2.25	360	252	0.0
RC203	40	100	1084.6	0.00	1.0	0.00	1,804	0.00	0	0.00	0	0	0.0
RC204	40	75	1360.9	0.00	0.6	4.99	814	0.00	633	4.99	633	464	0.0
RC204	40	100	984.6	0.00	4.8	1.58	3,143	0.00	1,685	1.58	1,593	1,049	0.1
RC205	40	75	1549.4	0.00	0.1	0.00	361	0.00	0	0.00	0	0	0.0
RC205	40	100	1298.3	0.00	0.2	0.06	948	0.00	84	0.06	58	52	0.0
RC206	40	75	1551.6	0.00	0.2	2.53	321	0.00	170	2.53	162	156	0.0
RC206	40	100	1125.8	0.00	0.2	0.20	878	0.00	124	0.20	80	76	0.0
RC207	40	75	1444.4	0.00	0.2	5.21	621	0.00	472	5.21	470	389	0.0
RC207	40	100	976.1	0.00	1.1	1.68	1,893	0.08	873	1.68	771	686	0.0
RC208	40	75	1342.5	0.00	1.2	6.84	822	0.24	625	6.84	625	550	0.0
RC208	40	100	899.8	0.00	14.3	6.03	4,253	0.00	3,621	1.65	2,050	1,797	0.2
C201	50	220	1322.1	0.00	0.2	0.00	291	0.00	0	0.00	0	0	0.0
C201	50	250	1098.6	0.00	0.1	0.00	445	0.00	0	0.00	0	0	0.0
C202	50	220	1308.4	0.00	0.6	0.00	896	0.00	79	0.00	65	61	0.0
C202	50	250	1076.3	0.00	0.2	0.00	1,840	0.00	0	0.00	0	0	0.0
C203	50	220	1245.5	0.00	0.9	0.23	1,382	0.00	157	0.23	131	110	0.0
C203	50	250	1071.3	0.00	1.6	0.93	3,479	0.26	2,010	0.93	1,770	1,535	0.2
C204	50	220	1193.3	0.00	1.8	0.66	1,779	0.00	350	0.66	289	270	0.0
C204	50	250	1060.4	0.00	3.4	1.08	5,411	0.12	2,155	1.08	1,977	1,791	0.4
C205	50	220	1263.4	0.00	0.4	1.13	546	0.17	244	1.13	189	187	0.0
C205	50	250	1095.9	0.00	0.4	0.86	1,016	0.00	364	0.86	315	310	0.0
C206	50	220	1260.2	0.00	2.4	1.26	743	0.46	420	1.26	352	336	0.2
C206	50	250	1089.3	0.00	0.4	0.69	1,342	0.21	594	0.69	517	493	0.1
C207	50	220	1214.0	0.00	0.9	0.13	969	0.34	254	0.13	223	206	0.1
C207	50	250	1074.3	0.00	0.5	0.23	2,547	0.00	249	0.23	215	186	0.0
C208	50	220	1244.9	0.00	1.9	0.67	779	0.00	228	0.67	190	184	0.0
C208	50	250	1074.3	0.00	0.5	0.23	1,964	0.00	210	0.23	166	149	0.0
R201	50	75	1399.0	0.00	0.1	0.00	460	0.00	0	0.00	0	0	0.0
R201	50	100	1223.2	0.00	0.1	0.00	1,025	0.00	0	0.00	0	0	0.0
R202	50	75	1227.6	0.00	0.3	0.61	955	0.18	391	0.61	233	218	0.0
R202	50	100	1102.8	0.00	0.9	0.02	2,643	0.01	79	0.02	58	57	0.0
R203	50	75	1101.9	0.00	0.5	0.20	1,471	0.16	164	0.20	96	88	0.0
R203	50	100	974.1	0.00	4.0	0.62	3,705	0.00	801	0.62	654	608	0.4
R204	50	75	1029.3	0.00	1.4	0.84	1,947	0.04	593	0.84	438	396	0.2
R204	50	100	821.6	0.00	5.1	0.00	4,344	0.00	0	0.00	0	0	0.0
R205	50	75	1228.0	0.00	0.1	0.00	816	0.00	0	0.00	0	0	0.0
R205	50	100	1041.5	0.00	0.7	0.03	2,125	0.00	84	0.03	66	65	0.0
R206	50	75	1152.1	0.00	0.2	0.00	1,411	0.00	0	0.00	0	0	0.0
R206	50	100	966.3	0.00	0.7	0.00	3,247	0.00	0	0.00	0	0	0.0
R207	50	75	1092.2	0.00	0.7	0.45	1,557	0.34	519	0.45	377	347	0.1
R207	50	100	904.0	0.00	3.2	0.00	4,305	0.00	0	0.00	0	0	0.0

Continued on next page

Table EC.3 – *Continued from previous page*

Name	n	$\bar{d}$	UB	Gap%	T_{tol}	Step1		Step2	Step3	Step4	Step5	Step6	Step7
						LB_1%	$\lvert\mathcal{S}_1\rvert$	UB_1%	$\lvert\mathcal{S}_2\rvert$	LB_2%	$\lvert\mathcal{S}_3\rvert$	$\lvert\mathcal{U}_3\rvert$	CPU_7
R208	50	75	1029.3	0.00	1.2	0.84	1,912	0.04	605	0.84	448	408	0.1
R208	50	100	821.6	0.00	5.4	0.00	4,313	0.00	0	0.00	0	0	0.0
R209	50	75	1133.3	0.00	0.3	0.07	1,182	0.00	100	0.07	80	76	0.0
R209	50	100	918.1	0.00	1.3	0.00	2,802	0.00	0	0.00	0	0	0.0
R210	50	75	1159.4	0.00	0.5	0.34	1,393	0.00	163	0.34	141	133	0.0
R210	50	100	976.3	0.00	1.2	0.00	3,371	0.00	0	0.00	0	0	0.0
R211	50	75	1031.1	0.00	3.9	1.48	1,939	0.00	1,583	1.48	1,418	1,356	0.9
R211	50	100	831.2	0.00	190.5	1.90	4,732	0.47	8,295	1.90	6,994	6,742	59.0
RC201	50	75	1873.9	0.00	0.1	0.00	230	0.00	0	0.00	0	0	0.0
RC201	50	100	1461.5	0.00	0.1	0.00	569	0.06	80	0.00	46	45	0.0
RC202	50	75	1761.7	0.00	0.3	1.55	530	0.00	365	1.55	280	224	0.0
RC202	50	100	1360.2	0.00	0.4	0.00	1,456	0.00	0	0.00	0	0	0.0
RC203	50	75	1593.5	0.00	1.1	2.17	889	0.00	674	2.17	520	368	0.0
RC203	50	100	1242.6	0.00	7.3	3.06	2,016	0.06	3,034	3.06	2,857	2,089	1.3
RC204	50	75	1455.9	0.00	3.9	2.15	1,216	0.00	1,114	2.15	1,018	763	0.2
RC204	50	100	1069.2	0.00	53.9	3.94	4,103	0.00	7,876	3.79	7,774	5,315	1.5
RC205	50	75	1777.9	0.00	0.4	2.89	494	0.00	380	2.89	289	237	0.0
RC205	50	100	1470.0	0.00	0.6	0.33	1,483	0.00	191	0.33	118	111	0.0
RC206	50	75	1712.1	0.00	0.4	2.95	490	0.00	343	2.95	315	299	0.0
RC206	50	100	1258.4	0.00	1.1	0.22	1,681	0.00	240	0.22	155	152	0.0
RC207	50	75	1620.7	0.00	29.2	5.89	928	0.00	975	5.89	975	829	0.2
RC207	50	100	1049.4	0.00	6.7	2.47	3,679	0.00	2,889	2.47	2,342	2,182	0.0
RC208	50	75	1438.5	0.00	82.8	3.52	1,356	0.70	1,333	3.52	1,328	1,178	1.1
RC208	50	100	991.0	0.00	153.8	4.97	5,009	0.84	10,286	4.01	9,881	8,796	5.7

EC.4.4. Detailed Results for the CMTVRPTW-R on Machine 1

Table EC.4: Detailed Results for the CMTVRPTW-R on Machine 1.

Name	n	UB	Gap%	CPU	Step1		Step2	Step3	Step4	Step5	Step6	Step7
					LB_1%	$\lvert\mathcal{S}_1\rvert$	UB_1%	$\lvert\mathcal{S}_2\rvert$	LB_2%	$\lvert\mathcal{S}_3\rvert$	$\lvert\mathcal{U}_3\rvert$	CPU_7
C201R0.25	25	380.8	0.00	1.7	2.68	1,868	0.00	1,281	2.68	1,038	1,038	0.7
C201R0.5	25	380.8	0.00	2.4	2.68	2,168	0.00	1,230	2.68	1,023	1,023	0.5
C201R0.75	25	380.8	0.00	1.7	2.68	1,567	0.00	1,156	2.68	1,026	1,026	0.7
C202R0.25	25	412.6	0.00	5.1	1.05	3,753	0.00	362	1.05	314	314	0.1
C202R0.5	25	412.6	0.00	4.1	1.05	3,670	0.00	441	1.05	326	326	0.2
C202R0.75	25	412.6	0.00	4.4	1.02	4,273	0.00	366	1.02	282	282	0.1
C203R0.25	25	431.3	0.00	26.9	2.08	5,895	0.00	4,295	2.08	3,506	3,447	4.0
C203R0.5	25	431.3	0.00	44.7	2.08	5,864	1.67	20,743	2.08	17,130	16,704	12.2
C203R0.75	25	435.5	0.00	80.0	2.81	4,834	0.64	20,872	2.81	16,508	16,129	52.2
C204R0.25	25	407.8	0.00	48.4	1.89	6,374	0.22	2,115	1.89	1,323	1,287	0.9
C204R0.5	25	407.8	0.00	8.7	1.89	6,006	0.00	1,616	1.89	1,036	1,014	0.7
C204R0.75	25	407.8	0.00	8.7	1.48	6,479	0.22	2,412	1.48	1,531	1,489	0.5
C205R0.25	25	378.2	0.00	3.9	2.61	2,774	0.00	1,680	2.61	1,334	1,332	1.1
C205R0.5	25	378.2	0.00	3.1	2.61	2,967	1.35	2,800	2.61	2,314	2,311	1.2
C205R0.75	25	378.2	0.00	3.6	2.61	2,510	1.35	3,123	2.61	2,318	2,315	1.6
C206R0.25	25	378.2	0.00	8.4	3.80	3,154	0.00	2,849	3.80	2,386	2,377	4.2
C206R0.5	25	378.2	0.00	6.7	3.80	3,144	0.00	2,990	3.80	2,402	2,393	3.3
C206R0.75	25	378.2	0.00	7.3	3.80	3,499	0.00	3,203	3.80	2,398	2,389	3.7
C207R0.25	25	377.4	0.00	19.2	3.76	2,690	0.00	5,839	3.76	5,568	5,370	13.9
C207R0.5	25	377.4	0.00	19.7	3.76	2,535	0.00	5,707	3.76	5,576	5,378	14.0
C207R0.75	25	377.4	0.00	16.7	3.76	2,721	0.13	6,181	3.76	5,785	5,580	12.7
C208R0.25	25	377.1	0.00	12.4	3.68	3,799	0.08	4,128	3.68	3,084	3,066	6.3
C208R0.5	25	377.4	0.00	11.5	3.75	3,626	0.00	3,618	3.75	3,072	3,055	7.1
C208R0.75	25	377.4	0.00	11.2	3.75	3,393	0.00	4,076	3.75	3,099	3,082	7.0
R201R0.25	25	549.4	0.00	0.2	0.00	1,998	0.00	0	0.00	0	0	0.0
R201R0.5	25	555.8	0.00	0.4	0.44	1,744	0.00	109	0.44	56	56	0.0
R201R0.75	25	570.0	0.00	0.4	0.18	1,790	0.00	99	0.18	26	26	0.0
R202R0.25	25	524.2	0.00	0.4	0.00	3,066	0.00	0	0.00	0	0	0.0
R202R0.5	25	524.2	0.00	0.2	0.00	3,340	0.00	0	0.00	0	0	0.0
R202R0.75	25	533.3	0.00	0.3	0.00	2,834	0.00	0	0.00	0	0	0.0

Continued on next page

Table EC.4 – *Continued from previous page*

Name	n	UB	Gap%	T_{tol}	Step1		Step2	Step3	Step4	Step5	Step6	Step7
					LB_1%	$\lvert\mathcal{S}_1\rvert$	UB_1%	$\lvert\mathcal{S}_2\rvert$	LB_2%	$\lvert\mathcal{S}_3\rvert$	$\lvert\mathcal{U}_3\rvert$	CPU_7
R203R0.25	25	518.4	0.00	0.8	0.00	3,707	0.00	0	0.00	0	0	0.0
R203R0.5	25	518.4	0.00	0.7	0.00	3,489	0.00	0	0.00	0	0	0.0
R203R0.75	25	518.5	0.00	0.4	0.00	4,141	0.00	0	0.00	0	0	0.0
R204R0.25	25	526.3	0.00	1.7	0.00	6,176	0.00	0	0.00	0	0	0.0
R204R0.5	25	526.3	0.00	1.7	0.00	6,176	0.00	0	0.00	0	0	0.0
R204R0.75	25	526.3	0.00	1.0	0.00	6,439	0.00	0	0.00	0	0	0.0
R205R0.25	25	453.9	0.00	0.3	0.00	4,338	0.00	0	0.00	0	0	0.0
R205R0.5	25	461.7	0.00	0.1	0.00	2,833	0.00	0	0.00	0	0	0.0
R205R0.75	25	471.6	0.00	0.1	0.00	2,747	0.00	0	0.00	0	0	0.0
R206R0.25	25	442.3	0.00	0.4	0.00	4,332	0.00	0	0.00	0	0	0.0
R206R0.5	25	459.0	0.00	2.0	0.33	3,965	0.00	71	0.33	34	33	0.0
R206R0.75	25	475.0	0.00	1.4	0.68	3,371	0.00	79	0.68	38	36	0.0
R207R0.25	25	477.0	0.00	3.1	0.00	6,333	0.00	0	0.00	0	0	0.0
R207R0.5	25	477.0	0.00	4.6	0.00	5,675	0.00	0	0.00	0	0	0.0
R207R0.75	25	477.1	0.00	2.8	0.00	6,401	0.00	0	0.00	0	0	0.0
R208R0.25	25	474.3	0.00	2.4	0.00	6,880	0.00	0	0.00	0	0	0.0
R208R0.5	25	474.3	0.00	2.4	0.00	6,880	0.00	0	0.00	0	0	0.0
R208R0.75	25	488.0	0.00	1.8	0.00	6,801	0.00	0	0.00	0	0	0.0
R209R0.25	25	452.6	0.00	0.7	0.00	4,699	0.00	0	0.00	0	0	0.0
R209R0.5	25	452.6	0.00	0.9	0.00	4,202	0.00	0	0.00	0	0	0.0
R209R0.75	25	467.6	0.00	0.2	0.00	2,904	0.00	0	0.00	0	0	0.0
R210R0.25	25	469.8	0.00	1.3	1.31	4,156	0.00	203	1.31	69	69	0.0
R210R0.5	25	472.3	0.00	1.8	0.42	3,897	0.00	75	0.42	42	41	0.0
R210R0.75	25	542.0	0.00	5.5	0.29	4,437	0.00	134	0.29	85	80	0.0
R211R0.25	25	400.1	0.00	4.2	0.00	6,429	0.00	0	0.00	0	0	0.0
R211R0.5	25	400.1	0.00	2.7	0.00	5,327	0.00	0	0.00	0	0	0.0
R211R0.75	25	406.0	0.00	0.9	0.00	5,272	0.00	0	0.00	0	0	0.0
RC201R0.25	25	660.0	0.00	0.6	1.84	1,844	0.00	222	1.84	143	143	0.0
RC201R0.5	25	660.0	0.00	1.2	0.93	1,559	4.58	1,304	0.93	702	697	0.0
RC201R0.75	25	660.0	0.00	0.3	0.78	1,307	0.00	89	0.78	43	43	0.0
RC202R0.25	25	611.4	0.00	323.1	4.60	2,729	3.63	5,022	4.60	2,688	2,538	26.7
RC202R0.5	25	611.4	0.00	158.5	4.60	2,281	0.00	1,137	4.60	573	525	3.5
RC202R0.75	25	643.9	0.00	0.8	1.34	2,150	0.00	209	1.34	82	75	0.0
RC203R0.25	25	594.0	0.00	5.9	0.93	6,747	0.08	1,126	0.93	293	270	0.0
RC203R0.5	25	594.0	0.00	8.1	0.93	6,660	0.00	842	0.93	244	223	0.0
RC203R0.75	25	639.6	0.00	1.9	0.00	4,487	0.63	101	0.00	46	39	0.0
RC204R0.25	25	595.7	0.00	5.0	0.34	5,767	0.00	184	0.34	89	75	0.0
RC204R0.5	25	595.7	0.00	5.1	0.34	5,767	0.00	184	0.34	89	75	0.0
RC204R0.75	25	672.0	0.00	10.4	0.24	4,779	0.00	293	0.24	212	169	0.0
RC205R0.25	25	603.0	0.00	1.3	0.89	3,055	0.00	211	0.89	171	163	0.0
RC205R0.5	25	603.0	0.00	1.2	0.89	2,900	0.55	403	0.89	288	280	0.0
RC205R0.75	25	642.4	0.00	0.3	0.00	1,933	0.00	0	0.00	0	0	0.0
RC206R0.25	25	575.2	0.00	1.4	0.56	3,081	0.00	171	0.56	117	113	0.0
RC206R0.5	25	575.2	0.00	1.1	0.10	2,826	0.00	78	0.10	46	43	0.0
RC206R0.75	25	588.7	0.00	0.1	0.00	2,278	0.00	0	0.00	0	0	0.0
RC207R0.25	25	538.8	0.00	0.2	0.00	2,997	0.00	0	0.00	0	0	0.0
RC207R0.5	25	538.8	0.00	0.2	0.00	3,832	0.00	0	0.00	0	0	0.0
RC207R0.75	25	575.5	0.00	0.7	0.24	2,439	0.00	80	0.24	42	42	0.0
RC208R0.25	25	510.8	0.00	7.2	0.74	5,325	0.10	210	0.74	139	133	0.1
RC208R0.5	25	513.8	0.00	38.9	1.32	5,496	0.00	264	1.32	167	162	0.2
RC208R0.75	25	525.2	0.00	10.8	0.57	4,290	0.00	227	0.57	117	114	0.0
C201R0.25	40	628.6	0.00	8.1	1.50	9,836	0.35	9,652	1.50	7,041	7,041	3.7
C201R0.5	40	636.2	0.00	6.7	0.91	6,268	0.31	4,042	0.91	3,449	3,449	1.8
C201R0.75	40	651.5	0.00	2.7	0.40	6,265	0.08	593	0.40	466	466	0.2
C202R0.25	40	682.6	0.00	11.6	0.60	8,897	0.00	587	0.60	491	491	0.1
C202R0.5	40	684.3	0.00	12.2	0.44	9,864	0.00	439	0.44	337	337	0.1
C202R0.75	40	689.2	0.00	9.9	1.05	7,941	0.01	1,612	1.05	1,430	1,430	0.5
C203R0.25	40	690.6	0.00	35.7	0.75	13,177	0.84	7,220	0.65	3,255	3,222	0.9
C203R0.5	40	690.6	0.00	20.8	0.39	14,312	0.00	401	0.36	277	277	0.0
C203R0.75	40	690.6	0.00	31.5	0.19	14,343	0.00	231	0.18	135	135	0.0
C204R0.25	40	695.9	0.00	60.0	1.27	25,738	0.00	9,837	1.27	7,663	7,595	8.8
C204R0.5	40	695.9	0.00	69.8	1.27	26,082	0.00	12,103	1.27	8,654	8,555	8.3
C204R0.75	40	698.5	0.00	185.1	1.64	25,289	0.07	29,821	1.64	18,288	18,007	128.5
C205R0.25	40	621.0	0.00	11.9	0.98	15,175	1.34	15,720	0.98	11,391	11,387	1.3

Continued on next page

Table EC.4 – *Continued from previous page*

Name	n	UB	Gap%	T_{tol}	Step1		Step2	Step3	Step4	Step5	Step6	Step7
					LB_1%	$\lvert\mathcal{S}_1\rvert$	UB_1%	$\lvert\mathcal{S}_2\rvert$	LB_2%	$\lvert\mathcal{S}_3\rvert$	$\lvert\mathcal{U}_3\rvert$	CPU_7
C205R0.5	40	634.0	0.00	9.9	0.98	11,482	0.02	2,877	0.98	2,105	2,104	1.3
C205R0.75	40	643.1	0.00	6.3	0.40	9,459	0.26	1,835	0.38	1,015	1,014	0.5
C206R0.25	40	613.0	0.00	24.0	0.93	18,693	2.27	26,589	0.93	23,551	23,522	2.8
C206R0.5	40	622.0	0.00	8.4	1.48	14,860	0.29	5,984	1.48	4,145	4,137	1.6
C206R0.75	40	641.7	0.00	19.9	1.44	13,030	0.72	12,496	1.44	8,472	8,455	8.5
C207R0.25	40	611.7	0.00	15.3	0.88	13,705	0.95	12,646	0.88	10,614	10,471	3.5
C207R0.5	40	615.8	0.00	19.5	1.33	14,079	0.39	8,149	1.33	6,919	6,766	7.1
C207R0.75	40	621.6	0.00	28.0	1.07	13,308	0.18	3,314	1.07	1,831	1,775	0.8
C208R0.25	40	613.0	0.00	49.3	1.12	19,070	2.14	36,313	1.12	33,043	32,998	4.7
C208R0.5	40	619.0	0.00	18.8	1.61	17,936	0.23	5,997	1.61	4,797	4,777	3.8
C208R0.75	40	632.4	0.00	13.3	1.18	11,510	0.00	3,149	1.18	2,421	2,409	1.4
R201R0.25	40	766.4	0.00	1.6	0.00	6,533	0.00	0	0.00	0	0	0.0
R201R0.5	40	767.4	0.00	0.6	0.00	6,521	0.00	0	0.00	0	0	0.0
R201R0.75	40	779.6	0.00	0.3	0.00	6,352	0.00	0	0.00	0	0	0.0
R202R0.25	40	722.9	0.00	1.4	0.00	8,556	0.00	0	0.00	0	0	0.0
R202R0.5	40	735.2	0.00	5.0	0.00	8,613	0.00	0	0.00	0	0	0.0
R202R0.75	40	735.2	0.00	7.4	0.00	8,547	0.00	0	0.00	0	0	0.0
R203R0.25	40	745.0	0.00	5.0	0.00	10,854	0.00	0	0.00	0	0	0.0
R203R0.5	40	745.0	0.00	6.0	0.00	9,084	0.00	0	0.00	0	0	0.0
R203R0.75	40	746.7	0.00	6.2	0.00	9,720	0.00	0	0.00	0	0	0.0
R204R0.25	40	719.0	0.00	555.0	0.37	14,769	0.38	1,832	0.37	1,166	1,040	0.4
R204R0.5	40	719.0	0.00	553.0	0.37	14,769	0.38	1,832	0.37	1,166	1,040	0.4
R204R0.75	40	727.8	0.00	210.4	0.07	15,618	0.00	197	0.07	120	107	0.0
R205R0.25	40	658.2	0.00	1.8	0.00	10,298	0.00	0	0.00	0	0	0.0
R205R0.5	40	668.0	0.00	4.5	0.00	10,124	0.00	0	0.00	0	0	0.0
R205R0.75	40	686.3	0.00	1.2	0.00	7,981	0.00	0	0.00	0	0	0.0
R206R0.25	40	664.0	0.00	3.4	0.09	9,453	0.00	60	0.09	33	33	0.0
R206R0.5	40	681.1	0.00	2.9	0.00	10,526	0.00	0	0.00	0	0	0.0
R206R0.75	40	698.8	0.00	5.5	0.00	8,913	0.00	0	0.00	0	0	0.0
R207R0.25	40	666.7	0.00	3.6	0.00	12,213	0.00	0	0.00	0	0	0.0
R207R0.5	40	676.6	0.00	7.5	0.00	11,313	0.00	0	0.00	0	0	0.0
R207R0.75	40	699.5	0.00	236.2	0.93	11,773	0.00	2,298	0.91	1,067	1,022	1.3
R208R0.25	40	674.1	0.00	269.4	0.45	15,473	0.00	838	0.45	596	523	0.2
R208R0.5	40	674.1	0.00	633.6	0.48	16,316	0.00	993	0.45	386	338	0.1
R208R0.75	40	683.2	0.00	776.0	0.94	15,396	0.00	3,401	0.90	1,541	1,328	1.6
R209R0.25	40	636.1	0.00	7.0	0.17	10,929	0.00	83	0.17	45	44	0.0
R209R0.5	40	636.1	0.00	6.6	0.17	11,433	0.31	190	0.17	97	95	0.0
R209R0.75	40	685.9	0.00	6.7	0.00	9,037	0.00	0	0.00	0	0	0.0
R210R0.25	40	667.7	0.00	8.3	0.41	10,009	0.00	228	0.41	114	113	0.0
R210R0.5	40	667.7	0.00	2.1	0.00	9,351	0.00	0	0.00	0	0	0.0
R210R0.75	40	735.9	0.00	59.4	0.82	10,246	0.00	1,169	0.82	625	621	0.7
R211R0.25	40	588.7	0.00	11.6	0.00	13,870	0.00	0	0.00	0	0	0.0
R211R0.5	40	588.7	0.00	8.5	0.00	13,109	0.00	0	0.00	0	0	0.0
R211R0.75	40	608.3	0.00	36.9	0.90	10,957	0.23	2,033	0.85	1,105	1,086	1.5
RC201R0.25	40	1038.1	0.00	2.8	1.32	4,960	0.00	664	1.32	439	437	0.1
RC201R0.5	40	1038.1	0.00	0.6	0.00	4,540	0.00	0	0.00	0	0	0.0
RC201R0.75	40	1048.6	0.00	0.3	0.00	4,282	0.00	0	0.00	0	0	0.0
RC202R0.25	40	972.2	0.00	0.4	0.00	6,214	0.00	0	0.00	0	0	0.0
RC202R0.5	40	972.2	0.00	0.8	0.00	6,407	0.00	0	0.00	0	0	0.0
RC202R0.75	40	1092.9	0.00	3.3	0.29	4,919	0.00	241	0.29	182	140	0.0
RC203R0.25	40	1041.9	0.00	33.7	0.70	14,498	0.02	1,178	0.70	916	839	0.1
RC203R0.5	40	1041.9	0.00	38.9	0.70	15,702	0.00	1,121	0.70	937	849	0.1
RC203R0.75	40	1145.7	0.00	50.7	1.41	13,901	0.00	3,831	1.41	2,909	2,618	1.9
RC204R0.25	40	1012.9	0.00	103.8	1.65	23,985	0.00	8,469	1.35	4,310	4,052	8.7
RC204R0.5	40	1012.9	0.00	104.0	1.65	23,985	0.00	8,469	1.35	4,310	4,052	8.7
RC204R0.75	40	1035.9	0.00	25.3	0.00	23,276	0.00	0	0.00	0	0	0.0
RC205R0.25	40	972.2	0.00	3.7	0.32	6,366	0.00	172	0.32	129	124	0.0
RC205R0.5	40	973.6	0.00	2.1	0.25	7,187	0.00	115	0.25	80	79	0.0
RC205R0.75	40	1071.7	0.00	2.3	0.86	5,907	0.00	319	0.86	264	254	0.0
RC206R0.25	40	984.7	0.00	11.4	0.64	7,638	0.45	1,170	0.64	922	903	0.1
RC206R0.5	40	984.7	0.00	6.8	0.00	8,231	0.00	0	0.00	0	0	0.0
RC206R0.75	40	1007.9	0.00	1.0	0.00	4,885	0.00	0	0.00	0	0	0.0
RC207R0.25	40	908.6	0.00	6.0	0.04	10,832	0.00	94	0.04	60	57	0.0
RC207R0.5	40	908.6	0.00	4.5	0.04	8,704	0.00	84	0.04	50	47	0.0

Continued on next page

Table EC.4 – *Continued from previous page*

Name	n	UB	Gap%	T_{tol}	Step1		Step2	Step3	Step4	Step5	Step6	Step7
					LB_1%	$\lvert\mathcal{S}_1\rvert$	UB_1%	$\lvert\mathcal{S}_2\rvert$	LB_2%	$\lvert\mathcal{S}_3\rvert$	$\lvert\mathcal{U}_3\rvert$	CPU_7
RC207R0.75	40	1006.4	0.00	17.4	0.43	7,482	0.00	351	0.43	274	266	0.0
RC208R0.25	40	868.5	0.00	38.0	0.57	16,944	0.00	688	0.06	131	121	0.0
RC208R0.5	40	872.1	0.00	92.9	0.91	18,098	0.18	1,802	0.47	611	598	1.9
RC208R0.75	40	885.5	0.00	29.8	0.97	14,929	0.00	1,087	0.17	141	140	0.0
C201R0.25	50	711.9	0.00	6.7	0.56	12,207	0.00	1,268	0.56	939	939	0.9
C201R0.5	50	716.2	0.00	6.5	0.55	10,277	0.24	2,494	0.54	1,696	1,696	1.5
C201R0.75	50	747.3	0.00	4.1	0.21	10,948	0.00	306	0.21	183	183	0.0
C202R0.25	50	780.5	0.00	31.6	1.49	16,456	0.00	9,761	1.47	6,673	6,660	3.3
C202R0.5	50	781.1	0.00	9.5	0.75	16,401	0.06	1,430	0.75	911	911	0.1
C202R0.75	50	790.3	0.00	18.1	0.54	17,610	0.77	5,104	0.35	2,939	2,939	0.2
C203R0.25	50	784.2	0.00	66.3	0.37	24,717	0.82	15,294	0.33	8,835	8,700	3.3
C203R0.5	50	788.4	0.00	26.7	0.00	23,756	0.00	0	0.00	0	0	0.0
C203R0.75	50	788.4	0.00	47.2	0.00	25,365	0.00	0	0.00	0	0	0.0
C204R0.25	50	770.2	0.00	176.3	0.52	51,447	0.00	4,485	0.49	2,468	2,451	1.6
C204R0.5	50	770.2	0.00	190.4	0.50	49,774	0.00	4,650	0.49	2,553	2,526	1.7
C204R0.75	50	770.2	0.00	194.1	0.50	47,914	0.00	4,717	0.49	2,430	2,419	1.7
C205R0.25	50	705.6	0.00	9.9	0.16	19,631	0.00	253	0.16	166	166	0.0
C205R0.5	50	709.5	0.00	12.2	0.11	17,870	0.24	644	0.11	456	456	0.0
C205R0.75	50	738.1	0.00	21.9	0.14	14,335	0.04	327	0.07	131	131	0.0
C206R0.25	50	703.3	0.00	20.3	1.05	20,959	1.05	15,960	1.05	13,165	13,140	2.2
C206R0.5	50	705.1	0.00	24.4	0.83	21,057	0.00	2,905	0.82	2,034	2,026	1.2
C206R0.75	50	734.0	0.00	29.0	0.57	20,572	0.67	5,853	0.51	4,067	4,052	2.4
C207R0.25	50	700.8	0.00	14.4	0.77	24,064	0.46	6,834	0.77	5,328	5,222	1.1
C207R0.5	50	703.6	0.00	18.0	0.82	21,883	0.06	3,015	0.82	2,315	2,238	1.8
C207R0.75	50	703.7	0.00	17.0	0.24	21,568	0.33	1,466	0.24	1,034	991	0.1
C208R0.25	50	702.8	0.00	22.5	1.05	25,156	0.38	9,088	1.05	6,831	6,792	3.4
C208R0.5	50	703.7	0.00	18.4	0.74	21,393	0.80	8,776	0.73	6,116	6,086	5.7
C208R0.75	50	703.7	0.00	14.4	0.27	22,564	0.33	1,154	0.27	704	695	0.0
R201R0.25	50	920.5	0.00	4.3	0.34	10,339	0.00	299	0.34	212	212	0.0
R201R0.5	50	929.8	0.00	3.5	0.00	12,189	0.00	0	0.00	0	0	0.0
R201R0.75	50	963.3	0.00	4.7	0.63	9,189	0.29	952	0.63	380	380	0.1
R202R0.25	50	870.7	0.00	13.8	0.05	12,952	0.00	127	0.05	105	105	0.0
R202R0.5	50	899.0	0.00	27.3	0.10	11,985	0.00	143	0.10	86	86	0.0
R202R0.75	50	903.2	0.00	39.0	0.11	12,493	0.01	153	0.11	82	82	0.0
R203R0.25	50	886.8	0.00	64.6	0.27	13,753	0.26	1,083	0.22	723	660	0.3
R203R0.5	50	897.7	0.00	16.8	0.00	14,279	0.00	0	0.00	0	0	0.0
R203R0.75	50	930.1	0.00	1573.5	0.17	15,275	0.00	325	0.16	222	204	0.0
R204R0.25	50	836.4	0.00	693.5	0.74	23,142	0.20	4,591	0.74	2,824	2,542	1.0
R204R0.5	50	836.4	0.00	694.1	0.74	23,142	0.20	4,591	0.74	2,824	2,542	1.0
R204R0.75	50	845.3	0.00	1123.9	0.25	22,942	0.20	1,261	0.23	688	635	0.2
R205R0.25	50	821.2	0.00	7.5	0.07	13,736	0.00	124	0.07	81	80	0.0
R205R0.5	50	842.5	0.00	9.6	0.18	15,053	0.00	195	0.18	134	133	0.0
R205R0.75	50	855.7	0.00	10.6	0.09	12,324	0.00	133	0.09	82	79	0.0
R206R0.25	50	820.7	0.00	38.1	0.50	14,827	0.00	710	0.46	413	398	0.2
R206R0.5	50	831.4	0.00	52.2	0.36	13,412	0.00	469	0.25	184	177	0.0
R206R0.75	50	833.5	0.00	65.8	0.39	13,285	0.43	1,995	0.39	1,288	1,259	0.4
R207R0.25	50	819.0	0.00	44.6	0.00	15,656	0.00	0	0.00	0	0	0.0
R207R0.5	50	839.1	0.00	167.3	0.68	15,744	0.15	2,640	0.60	1,377	1,255	1.6
R207R0.75	50	855.4	0.00	385.4	0.33	16,039	0.00	617	0.31	365	352	0.0
R208R0.25	50	784.1	0.00	76.5	0.00	27,517	0.00	0	0.00	0	0	0.0
R208R0.5	50	784.1	0.00	76.5	0.00	25,053	0.00	0	0.00	0	0	0.0
R208R0.75	50	789.6	0.00	203.4	0.00	25,683	0.00	0	0.00	0	0	0.0
R209R0.25	50	758.7	0.00	42.8	0.51	20,356	0.00	1,303	0.41	324	320	0.1
R209R0.5	50	758.7	0.00	26.3	0.24	17,444	0.00	309	0.23	170	167	0.0
R209R0.75	50	801.2	0.00	6.5	0.00	15,440	0.00	0	0.00	0	0	0.0
R210R0.25	50	810.2	0.00	27.1	0.19	17,652	0.77	2,153	0.19	1,728	1,717	0.1
R210R0.5	50	823.5	0.00	43.4	0.78	16,654	0.00	1,651	0.77	946	937	0.5
R210R0.75	50	879.7	0.00	103.5	0.17	13,491	0.05	300	0.17	145	145	0.0
R211R0.25	50	724.8	0.00	185.6	1.33	21,720	0.00	9,399	1.03	3,564	3,449	6.2
R211R0.5	50	724.8	0.00	224.7	1.29	21,425	0.00	8,851	0.98	3,306	3,223	4.5
R211R0.75	50	748.1	0.00	557.3	1.63	19,763	0.45	40,845	1.43	23,686	23,309	63.7
RC201R0.25	50	1096.6	0.00	7.2	0.00	10,927	0.00	0	0.00	0	0	0.0
RC201R0.5	50	1111.3	0.00	2.5	0.00	8,259	0.00	0	0.00	0	0	0.0
RC201R0.75	50	1151.1	0.00	2.7	0.33	8,379	0.00	254	0.33	188	187	0.0

Continued on next page

Table EC.4 – *Continued from previous page*

Name	n	UB	Gap%	T_{tol}	Step1		Step2	Step3	Step4	Step5	Step6	Step7
					LB_1%	$\|\mathcal{S}_1\|$	UB_1%	$\|\mathcal{S}_2\|$	LB_2%	$\|\mathcal{S}_3\|$	$\|\mathcal{U}_3\|$	CPU_7
RC202R0.25	50	1140.9	0.00	30.4	1.58	10,938	0.08	2,895	1.58	2,071	1,965	1.0
RC202R0.5	50	1142.7	0.00	28.7	1.27	9,491	0.00	1,834	1.27	1,080	1,012	0.2
RC202R0.75	50	1201.7	0.00	8.7	0.87	6,739	0.12	1,054	0.87	305	279	0.0
RC203R0.25	50	1172.4	0.00	70.5	0.65	22,378	0.85	11,563	0.34	4,100	3,737	0.5
RC203R0.5	50	1204.4	0.00	161.7	2.18	18,420	0.38	44,425	1.41	20,709	19,440	23.1
RC203R0.75	50	1274.2	0.00	107.4	1.38	18,752	0.00	8,041	1.22	5,535	5,034	3.6
RC204R0.25	50	1113.1	0.00	151.1	3.10	28,289	0.82	284,765	1.10	52,100	47,739	21.9
RC204R0.5	50	1113.1	0.00	151.1	3.10	28,289	0.82	284,765	1.10	52,100	47,739	22.2
RC204R0.75	50	1158.7	0.00	245.5	2.90	28,484	0.65	164,539	0.05	3,605	3,297	1.1
RC205R0.25	50	1059.4	0.00	20.5	2.44	12,065	0.99	6,203	2.44	2,728	2,647	0.6
RC205R0.5	50	1126.3	0.00	9.6	0.00	11,817	0.00	0	0.00	0	0	0.0
RC205R0.75	50	1212.2	0.00	3.9	0.00	8,279	0.00	0	0.00	0	0	0.0
RC206R0.25	50	1036.3	0.00	10.3	0.92	15,642	0.38	3,485	0.92	2,377	2,342	0.7
RC206R0.5	50	1036.3	0.00	10.3	0.86	14,807	0.38	2,809	0.86	1,926	1,896	0.5
RC206R0.75	50	1096.2	0.00	11.7	1.73	11,623	0.35	2,801	1.73	1,788	1,746	0.4
RC207R0.25	50	965.1	0.00	10.0	0.04	16,143	0.00	103	0.04	51	50	0.0
RC207R0.5	50	965.1	0.00	5.4	0.04	17,792	0.00	95	0.04	46	45	0.0
RC207R0.75	50	1117.9	0.00	66.2	0.62	16,312	0.00	1,238	0.24	282	274	0.0
RC208R0.25	50	925.1	0.00	286.9	0.74	26,836	0.72	4,957	0.71	3,233	3,071	55.5
RC208R0.5	50	927.2	0.00	1013.1	0.94	23,403	0.15	3,216	0.94	2,030	1,956	285.0
RC208R0.75	50	941.8	0.00	276.4	0.03	23,157	0.42	579	0.03	372	372	0.0

EC.4.5. Detailed Results for the DRP on Machine 1

Table EC.5: Detailed Results for the DRP on Machine 1.

Name	n	UB	Gap%	CPU	Step1		Step2	Step3	Step4	Step5	Step6	Step7
					LB_1%	$\|\mathcal{S}_1\|$	UB_1%	$\|\mathcal{S}_2\|$	LB_2%	$\|\mathcal{S}_3\|$	$\|\mathcal{U}_3\|$	CPU_7
Set_A1_Cust_10_1	10	3132.0	0.00	0.1	4.00	95	0.00	42	4.00	39	39	0.0
Set_A1_Cust_10_2	10	4738.9	0.00	0.0	0.00	68	0.00	0	0.00	0	0	0.0
Set_A1_Cust_10_3	10	4556.3	0.00	0.0	2.85	125	0.00	46	2.85	44	44	0.0
Set_A1_Cust_10_4	10	4391.5	0.00	0.0	8.19	119	0.00	102	8.19	62	62	0.0
Set_A1_Cust_10_5	10	4524.2	0.00	0.0	0.19	88	0.00	22	0.19	17	17	0.0
Set_A1_Cust_15_1	15	7072.0	0.00	0.0	0.70	221	0.14	49	0.70	46	46	0.0
Set_A1_Cust_15_2	15	4397.8	0.00	0.1	0.29	560	0.00	43	0.29	31	31	0.0
Set_A1_Cust_15_3	15	5968.2	0.00	0.5	5.99	370	0.00	418	5.99	401	401	0.3
Set_A1_Cust_15_4	15	5491.0	0.00	0.0	0.81	234	0.68	58	0.81	53	53	0.0
Set_A1_Cust_15_5	15	7383.4	0.00	0.1	3.09	336	0.00	126	3.09	115	115	0.0
Set_A1_Cust_20_1	20	8284.9	0.00	0.0	0.00	352	0.00	0	0.00	0	0	0.0
Set_A1_Cust_20_2	20	9548.0	0.00	0.1	0.81	355	0.00	87	0.81	76	76	0.0
Set_A1_Cust_20_3	20	8816.1	0.00	0.2	1.71	354	0.00	188	1.71	166	166	0.1
Set_A1_Cust_20_4	20	6693.8	0.00	0.0	0.00	434	0.00	0	0.00	0	0	0.0
Set_A1_Cust_20_5	20	7782.1	0.00	0.8	2.73	352	0.00	255	2.73	192	192	0.3
Set_A1_Cust_25_1	25	10680.0	0.00	0.6	2.31	796	0.00	539	2.31	496	496	0.2
Set_A1_Cust_25_2	25	8636.2	0.00	0.2	1.10	1,092	0.00	210	1.10	158	158	0.0
Set_A1_Cust_25_3	25	10094.5	0.00	1.4	2.21	785	0.10	492	2.21	483	483	0.9
Set_A1_Cust_25_4	25	10146.6	0.00	0.0	0.00	470	0.00	0	0.00	0	0	0.0
Set_A1_Cust_25_5	25	11166.0	0.00	0.1	1.40	484	0.00	256	1.40	227	227	0.0
Set_A1_Cust_30_1	30	9831.6	0.00	0.1	0.00	1,219	0.00	0	0.00	0	0	0.0
Set_A1_Cust_30_2	30	12665.0	0.00	0.1	0.19	963	0.00	67	0.19	57	57	0.0
Set_A1_Cust_30_3	30	12359.4	0.00	1.8	2.08	926	0.00	870	2.08	718	718	1.1
Set_A1_Cust_30_4	30	12512.8	0.00	0.9	0.97	1,021	0.11	385	0.97	290	290	0.6
Set_A1_Cust_30_5	30	12086.1	0.00	0.3	0.81	1,099	0.00	262	0.81	194	194	0.0
Set_A1_Cust_35_1	35	12434.0	0.00	9.6	1.61	2,709	0.12	3,497	1.61	2,997	2,996	7.2
Set_A1_Cust_35_2	35	13020.8	0.00	1.5	0.84	1,660	0.60	1,267	0.84	1,121	1,121	0.4
Set_A1_Cust_35_3	35	13230.4	0.00	0.2	0.00	1,282	0.00	0	0.00	0	0	0.0
Set_A1_Cust_35_4	35	13863.5	0.00	0.1	0.00	1,329	0.00	0	0.00	0	0	0.0
Set_A1_Cust_35_5	35	13281.6	0.00	0.4	0.51	1,013	0.00	159	0.51	136	136	0.1
Set_A1_Cust_40_1	40	15540.1	0.00	0.9	0.49	1,761	0.01	325	0.49	297	296	0.1
Set_A1_Cust_40_2	40	16881.3	0.00	3.1	0.35	1,028	0.07	176	0.35	168	168	0.5
Set_A1_Cust_40_3	40	14178.4	0.00	0.3	0.22	2,230	0.04	157	0.22	152	152	0.0

Continued on next page

Table EC.5 – *Continued from previous page*

Name	n	UB	Gap%	T_{tol}	Step1		Step2	Step3	Step4	Step5	Step6	Step7
					LB_1%	$\lvert\mathcal{S}_1\rvert$	UB_1%	$\lvert\mathcal{S}_2\rvert$	LB_2%	$\lvert\mathcal{S}_3\rvert$	$\lvert\mathcal{U}_3\rvert$	CPU_7
Set_A1_Cust_40_4	40	16286.8	0.00	0.4	0.21	1,360	0.00	114	0.21	94	94	0.0
Set_A1_Cust_40_5	40	15620.2	0.00	4.2	0.48	1,013	0.24	289	0.48	250	249	1.2
Set_A1_Cust_45_1	45	14569.0	0.00	5.6	0.38	3,336	0.05	558	0.38	527	527	0.3
Set_A1_Cust_45_2	45	19727.5	0.00	6.0	0.91	1,759	0.11	903	0.91	812	811	3.1
Set_A1_Cust_45_3	45	18825.4	0.00	0.4	0.21	2,132	0.00	158	0.21	152	152	0.0
Set_A1_Cust_45_4	45	16298.5	0.00	8.5	0.68	1,575	0.00	711	0.68	670	670	0.6
Set_A1_Cust_45_5	45	18728.7	0.00	0.9	0.44	2,361	0.01	242	0.44	199	199	0.1
Set_A2_Cust_10_1	10	4999.0	0.00	0.0	3.98	79	0.00	27	3.98	19	19	0.0
Set_A2_Cust_10_2	10	5825.5	0.00	0.0	0.00	34	0.00	0	0.00	0	0	0.0
Set_A2_Cust_10_3	10	5269.9	0.00	0.0	0.00	65	0.00	0	0.00	0	0	0.0
Set_A2_Cust_10_4	10	6157.2	0.00	0.0	4.85	49	0.00	33	4.85	29	29	0.0
Set_A2_Cust_10_5	10	5534.0	0.00	0.0	0.78	48	0.00	14	0.78	13	13	0.0
Set_A2_Cust_15_1	15	6869.6	0.00	0.0	0.19	140	0.00	19	0.19	13	13	0.0
Set_A2_Cust_15_2	15	8535.0	0.00	0.1	1.43	115	0.00	39	1.43	39	39	0.0
Set_A2_Cust_15_3	15	6612.0	0.00	0.0	0.00	88	0.00	0	0.00	0	0	0.0
Set_A2_Cust_15_4	15	8777.9	0.00	0.2	7.69	119	0.00	76	7.69	59	59	0.1
Set_A2_Cust_15_5	15	8672.1	0.00	0.0	0.00	99	0.00	0	0.00	0	0	0.0
Set_A2_Cust_20_1	20	11422.7	0.00	0.8	3.35	136	0.00	100	3.35	88	88	0.2
Set_A2_Cust_20_2	20	9730.0	0.00	0.4	3.50	263	0.00	151	3.50	111	111	0.1
Set_A2_Cust_20_3	20	10093.7	0.00	0.0	0.00	141	0.00	0	0.00	0	0	0.0
Set_A2_Cust_20_4	20	9492.4	0.00	0.0	0.00	152	0.00	0	0.00	0	0	0.0
Set_A2_Cust_20_5	20	8299.5	0.00	0.2	1.73	319	0.77	191	1.73	164	164	0.0
Set_A2_Cust_25_1	25	11436.3	0.00	0.0	0.01	298	0.00	32	0.01	24	24	0.0
Set_A2_Cust_25_2	25	12426.4	0.00	0.0	0.00	343	0.00	0	0.00	0	0	0.0
Set_A2_Cust_25_3	25	10973.4	0.00	1.3	3.71	266	0.68	230	3.71	145	145	0.7
Set_A2_Cust_25_4	25	12275.4	0.00	0.0	0.69	231	0.00	49	0.69	38	38	0.0
Set_A2_Cust_25_5	25	11788.0	0.00	0.0	0.15	259	0.00	40	0.15	30	30	0.0
Set_A2_Cust_30_1	30	14997.4	0.00	0.1	0.45	373	0.00	80	0.45	74	74	0.0
Set_A2_Cust_30_2	30	12794.3	0.00	0.2	0.96	552	0.00	181	0.96	102	102	0.0
Set_A2_Cust_30_3	30	12234.4	0.00	0.2	0.81	524	0.00	238	0.81	225	225	0.1
Set_A2_Cust_30_4	30	11587.3	0.00	0.1	0.19	608	0.00	52	0.19	44	44	0.0
Set_A2_Cust_30_5	30	13261.5	0.00	0.5	1.23	688	0.27	317	1.23	263	262	0.2
Set_A2_Cust_35_1	35	14282.9	0.00	0.2	0.42	781	0.00	184	0.42	170	170	0.0
Set_A2_Cust_35_2	35	17443.4	0.00	1.0	0.27	359	0.35	83	0.27	69	69	0.2
Set_A2_Cust_35_3	35	14691.3	0.00	0.3	0.92	901	0.00	213	0.92	157	157	0.1
Set_A2_Cust_35_4	35	17689.3	0.00	0.2	1.20	508	0.00	339	1.20	284	284	0.0
Set_A2_Cust_35_5	35	16812.4	0.00	0.1	0.45	727	0.00	143	0.45	112	112	0.0
Set_A2_Cust_40_1	40	17002.9	0.00	0.3	0.23	672	0.00	113	0.23	93	93	0.0
Set_A2_Cust_40_2	40	17949.0	0.00	0.7	1.07	846	0.19	414	1.07	389	388	0.1
Set_A2_Cust_40_3	40	18078.8	0.00	0.4	0.16	736	0.00	81	0.16	57	57	0.0
Set_A2_Cust_40_4	40	18559.6	0.00	6.1	0.59	718	0.00	185	0.59	147	147	1.6
Set_A2_Cust_40_5	40	13798.5	0.00	1.0	0.51	1,156	0.00	133	0.51	110	110	0.4
Set_A2_Cust_45_1	45	18654.7	0.00	0.1	0.07	749	0.00	72	0.07	63	63	0.0
Set_A2_Cust_45_2	45	19590.6	0.00	1.2	0.21	1,322	0.00	115	0.21	102	102	0.6
Set_A2_Cust_45_3	45	20207.2	0.00	2.9	0.73	771	0.18	393	0.73	348	348	0.5
Set_A2_Cust_45_4	45	17306.9	0.00	2.1	0.52	1,424	0.02	274	0.52	242	242	0.3
Set_A2_Cust_45_5	45	24311.7	0.00	1.2	0.72	392	0.00	222	0.72	204	204	0.0
Set_A2_Cust_50_1	50	24698.5	0.00	15.3	0.79	1,353	0.02	798	0.79	717	717	12.4
Set_A2_Cust_50_2	50	21939.4	0.00	5.8	0.94	885	0.00	490	0.94	449	449	0.9
Set_A2_Cust_50_3	50	19700.0	0.00	0.2	0.19	1,396	0.00	124	0.19	99	99	0.0
Set_A2_Cust_50_4	50	19841.8	0.00	2.9	0.12	1,188	0.00	94	0.12	52	52	0.3
Set_A2_Cust_50_5	50	23721.5	0.00	0.8	0.59	836	0.00	239	0.59	207	207	0.0
C201	25	644.7	0.00	0.1	0.90	935	0.00	110	0.90	92	92	0.0
C202	25	644.1	0.00	0.2	2.14	1,333	0.00	549	2.14	385	382	0.0
C203	25	643.9	0.00	0.5	2.16	1,309	0.25	1,009	2.16	623	619	0.3
C204	25	643.9	0.00	0.4	2.17	1,852	0.00	787	2.17	582	577	0.2
C205	25	644.4	0.00	0.1	2.12	1,188	0.00	357	2.12	291	291	0.0
C206	25	643.8	0.00	0.2	2.10	1,080	0.00	403	2.10	325	324	0.0
C207	25	643.6	0.00	0.3	2.14	1,114	0.31	700	2.14	508	505	0.1
C208	25	643.6	0.00	0.3	2.09	1,239	0.00	450	2.09	337	337	0.1
R201	25	752.8	0.00	0.0	0.22	672	0.00	50	0.22	33	33	0.0
R202	25	730.4	0.00	0.0	0.00	895	0.00	0	0.00	0	0	0.0
R203	25	721.6	0.00	0.0	0.00	1,096	0.00	0	0.00	0	0	0.0
R204	25	721.4	0.00	0.0	0.00	1,252	0.00	0	0.00	0	0	0.0

Continued on next page

Table EC.5 – *Continued from previous page*

Name	n	UB	Gap%	T_{tol}	Step1		Step2	Step3	Step4	Step5	Step6	Step7
					LB_1%	$\|\mathcal{S}_1\|$	UB_1%	$\|\mathcal{S}_2\|$	LB_2%	$\|\mathcal{S}_3\|$	$\|\mathcal{U}_3\|$	CPU_7
R205	25	731.8	0.00	0.0	0.00	845	0.00	0	0.00	0	0	0.0
R206	25	725.5	0.00	0.0	0.00	901	0.00	0	0.00	0	0	0.0
R207	25	721.6	0.00	0.0	0.00	1,076	0.00	0	0.00	0	0	0.0
R208	25	721.4	0.00	0.0	0.00	1,240	0.00	0	0.00	0	0	0.0
R209	25	721.7	0.00	0.0	0.00	907	0.00	0	0.00	0	0	0.0
R210	25	725.5	0.00	0.0	0.00	905	0.00	0	0.00	0	0	0.0
R211	25	721.4	0.00	0.0	0.00	1,231	0.00	0	0.00	0	0	0.0
RC201	25	1022.3	0.00	0.1	2.05	425	0.00	143	2.05	142	142	0.0
RC202	25	1007.1	0.00	0.2	2.16	528	0.26	208	2.16	208	203	0.0
RC203	25	1000.0	0.00	0.1	1.96	623	0.32	254	1.96	253	243	0.0
RC204	25	1000.0	0.00	0.1	1.97	628	0.31	247	1.97	246	237	0.0
RC205	25	1013.4	0.00	0.1	2.74	488	0.07	216	2.74	214	209	0.0
RC206	25	1013.8	0.00	0.1	2.43	501	0.00	195	2.43	195	195	0.0
RC207	25	1005.5	0.00	0.1	2.37	594	0.00	223	2.37	222	218	0.0
RC208	25	999.8	0.00	0.1	1.96	660	0.00	249	1.96	249	248	0.0
C201	40	1103.5	0.00	0.3	0.52	3,098	0.17	299	0.52	265	265	0.0
C202	40	1102.3	0.00	0.5	0.80	3,344	0.00	443	0.80	347	344	0.0
C203	40	1101.7	0.00	1.1	0.87	3,363	0.20	1,257	0.87	910	901	0.2
C204	40	1101.2	0.00	1.3	0.89	5,006	0.06	895	0.89	717	713	0.3
C205	40	1101.5	0.00	0.5	0.70	3,004	0.20	464	0.70	369	369	0.1
C206	40	1101.2	0.00	0.9	0.77	3,356	0.00	426	0.77	323	323	0.1
C207	40	1101.1	0.00	0.5	0.89	2,808	0.11	753	0.89	617	615	0.2
C208	40	1101.1	0.00	1.0	0.77	3,244	0.21	592	0.77	519	519	0.1
R201	40	1200.1	0.00	0.2	0.31	1,171	0.00	110	0.31	100	100	0.0
R202	40	1145.3	0.00	0.1	0.00	1,462	0.00	0	0.00	0	0	0.0
R203	40	1142.4	0.00	0.1	0.00	1,670	0.00	0	0.00	0	0	0.0
R204	40	1140.6	0.00	0.2	0.00	1,851	0.00	0	0.00	0	0	0.0
R205	40	1159.7	0.00	0.1	0.00	1,453	0.00	0	0.00	0	0	0.0
R206	40	1141.8	0.00	0.1	0.00	1,769	0.00	0	0.00	0	0	0.0
R207	40	1141.8	0.00	0.2	0.00	1,732	0.00	0	0.00	0	0	0.0
R208	40	1140.6	0.00	0.2	0.00	1,981	0.00	0	0.00	0	0	0.0
R209	40	1149.1	0.00	0.1	0.00	1,847	0.00	0	0.00	0	0	0.0
R210	40	1142.4	0.00	0.1	0.00	1,858	0.00	0	0.00	0	0	0.0
R211	40	1140.6	0.00	0.1	0.00	1,942	0.00	0	0.00	0	0	0.0
RC201	40	1692.1	0.00	17.5	1.72	722	0.00	277	1.72	259	259	6.2
RC202	40	1642.4	0.00	0.9	1.32	862	0.16	391	1.32	377	371	0.1
RC203	40	1635.3	0.00	0.2	1.20	1,152	0.20	455	1.20	450	437	0.0
RC204	40	1635.3	0.00	0.3	1.20	1,342	0.01	344	1.20	340	330	0.1
RC205	40	1650.6	0.00	0.2	1.57	864	0.00	387	1.57	376	370	0.1
RC206	40	1658.9	0.00	0.2	1.57	865	0.00	358	1.57	342	341	0.0
RC207	40	1639.0	0.00	0.2	1.37	1,096	0.00	404	1.37	401	394	0.0
RC208	40	1635.1	0.00	0.2	1.20	1,349	0.01	456	1.20	456	449	0.0

EC.5. Detailed Results for Large Instances on Machine 2

EC.5.1. Detailed Results for the CMTVRPTW on Machine 2

Table EC.6: Detailed Results for the CMTVRPTW on Machine 2.

Name	n	UB	Gap%	CPU	Step1		Step2	Step3	Step4	Step5	Step6	Step7
					LB_1%	$\|\mathcal{S}_1\|$	UB_1%	$\|\mathcal{S}_2\|$	LB_2%	$\|\mathcal{S}_3\|$	$\|\mathcal{U}_3\|$	CPU_7
C201	70	1052.2	0.00	33.0	0.76	78,205	0.00	35,775	0.69	17,190	17,190	16.4
C202	70	1047.7	0.00	3163.8	1.29	82,338	0.26	446,599	1.22	323,687	323,652	3107.1
C203	70	1040.4	0.00	4918.9	1.28	81,018	0.28	696,979	1.13	453,190	448,894	4833.4
C204	70	1036.8	0.00	5421.5	1.27	108,787	0.41	1,342,568	1.16	927,726	878,179	5208.1
C205	70	1047.9	0.00	4051.9	1.42	85,449	0.01	433,254	1.37	316,736	316,731	4007.4
C206	70	1042.0	0.00	2193.3	1.23	95,816	0.00	231,703	1.19	178,723	178,704	2146.9
C207	70	1040.3	0.00	3730.5	1.25	91,863	0.28	596,896	1.19	466,281	466,007	3659.1
C208	70	1040.3	0.00	2077.3	1.25	87,889	0.24	464,796	1.17	353,570	353,517	2023.7
R201	70	1118.4	0.00	23.2	0.86	48,598	0.12	9,152	0.76	3,531	3,529	1.5
R202	70	1041.1	0.00	328.8	1.57	43,281	0.17	150,454	1.43	93,310	92,815	289.1

Continued on next page

Table EC.6 – *Continued from previous page*

Name	n	UB	Gap%	T_{tol}	Step1		Step2	Step3	Step4	Step5	Step6	Step7
					LB_1%	$\lvert\mathcal{S}_1\rvert$	UB_1%	$\lvert\mathcal{S}_2\rvert$	LB_2%	$\lvert\mathcal{S}_3\rvert$	$\lvert\mathcal{U}_3\rvert$	CPU_7
R203	70	958.0	0.00	248.8	0.81	43,225	0.74	162,448	0.69	97,375	94,955	23.4
R204	70	921.8	0.00	152.1	1.01	53,647	0.38	209,438	0.87	117,934	103,995	78.6
R205	70	1033.4	0.00	3027.7	1.70	55,318	0.23	253,182	1.48	154,445	154,039	2923.1
R206	70	985.9	0.00	1287.3	1.59	46,052	0.51	633,336	1.40	382,139	377,973	1167.6
R207	70	942.0	0.00	70.1	0.97	46,398	0.00	33,463	0.90	19,168	18,342	36.2
R208	70	917.5	0.00	219.4	1.09	55,097	0.40	317,239	1.00	173,924	144,556	154.0
R209	70	955.3	0.00	138.1	1.17	45,632	0.54	154,158	1.04	85,150	84,124	75.1
R210	70	980.4	0.00	365.7	1.24	49,804	0.57	327,783	1.02	168,587	166,718	211.5
R211	70	914.8	0.00	64.0	0.88	47,654	0.09	33,268	0.75	16,984	16,273	21.8
RC201	70	1364.5	0.00	39.3	1.41	35,050	1.17	73,500	1.13	47,078	47,055	8.3
RC202	70	1284.6	0.00	27.0	1.22	31,092	0.43	29,670	1.20	24,563	24,330	12.3
RC203	70	1230.5	0.00	39.5	0.85	53,186	0.51	35,366	0.65	21,570	20,186	7.8
RC204	70	1206.6	0.00	259.2	1.33	62,776	0.56	148,646	1.16	112,531	93,272	206.5
RC205	70	1335.3	0.00	97.6	1.46	42,537	0.81	89,944	1.10	54,703	54,450	32.4
RC206	70	1285.5	0.00	167.9	1.69	47,884	0.69	114,240	1.50	83,588	83,191	108.8
RC207	70	1236.5	0.00	1180.1	1.72	44,312	2.21	1,610,655	1.36	1,158,141	1,141,217	849.7
RC208	70	1208.2	0.00	1552.6	1.66	55,862	1.88	2,038,815	1.46	1,573,105	1,483,430	1254.8
C201	80	1182.5	0.00	623.4	2.32	85,315	0.25	3,459,096	0.93	197,977	197,977	548.2
C202	80	1178.4	0.78	10800.6	2.02	112,333	0.22	3,206,566	1.40	851,120	850,952	10592.9
C203	80	1172.1	1.00	10801.8	2.06	91,755	0.62	11,202,068	1.44	3,134,639	3,095,400	9949.1
C204	80	1163.1	1.24	10802.4	1.60	152,090	0.57	7,850,318	1.36	4,537,312	4,309,874	1506.1
C205	80	1170.6	0.00	719.4	1.11	114,227	0.57	996,264	0.90	588,153	588,142	585.1
C206	80	1168.9	0.00	2401.5	1.37	112,009	0.84	3,830,232	0.99	1,609,632	1,609,565	2105.4
C207	80	1167.2	0.00	8257.8	1.57	110,411	0.61	3,554,934	1.16	1,444,514	1,444,074	7944.3
C208	80	1167.2	0.00	4245.0	1.42	118,158	0.55	2,397,521	1.18	1,177,543	1,177,399	4001.8
R201	80	1201.5	0.00	227.9	1.37	53,977	0.61	300,632	1.19	185,751	185,716	160.0
R202	80	1121.2	0.00	1188.8	1.47	55,278	0.62	1,291,460	1.16	563,002	561,498	954.9
R203	80	1034.6	0.00	459.3	1.13	64,472	0.21	218,739	1.00	117,805	115,813	365.5
R204	80	1002.1	0.00	1032.3	1.11	74,189	0.61	1,489,980	0.94	841,404	755,407	808.8
R205	80	1103.6	0.00	1769.9	1.49	62,160	0.70	1,275,591	1.24	675,157	673,797	1494.6
R206	80	1055.4	0.00	2489.5	1.48	60,732	0.97	4,035,038	1.11	1,980,899	1,965,997	1728.5
R207	80	1011.3	0.00	174.3	0.49	65,916	1.09	694,281	0.35	366,548	357,958	12.1
R208	80	993.5	0.00	233.5	0.73	73,820	0.32	188,139	0.63	98,569	82,514	40.1
R209	80	1034.9	0.00	720.9	1.31	64,045	0.43	529,079	1.09	315,575	312,320	577.2
R210	80	1052.8	0.00	1653.7	1.32	61,823	0.44	647,884	1.21	436,001	432,851	1479.0
R211	80	999.0	0.00	1036.0	1.14	66,828	0.00	188,681	1.04	101,253	97,312	925.9
RC201	80	1545.8	0.00	22.9	0.86	42,858	0.19	12,182	0.79	7,648	7,640	3.0
RC202	80	1458.3	0.00	148.4	1.31	55,477	0.64	141,698	1.21	103,785	103,106	100.5
RC203	80	1392.3	0.00	129.6	0.36	56,996	1.59	301,718	0.23	204,231	194,381	3.0
RC204	80	1366.5	0.00	42.6	0.41	61,661	0.39	36,283	0.27	16,823	13,499	2.5
RC205	80	1516.8	0.00	173.4	1.30	50,852	0.46	101,301	1.06	59,597	59,410	99.2
RC206	80	1455.6	0.00	664.2	1.36	55,556	1.85	1,424,343	1.25	1,071,857	1,069,140	97.5
RC207	80	1402.9	0.00	686.2	1.22	53,897	0.57	195,273	1.01	110,689	108,289	132.0
RC208	80	1364.1	0.00	799.1	0.53	67,342	2.17	2,302,525	0.39	1,696,048	1,611,925	23.9
C201	100	1473.3	0.00	8028.8	1.28	129,064	1.16	6,420,412	0.97	4,203,970	4,203,969	7185.6
C202	100	1464.2	0.29	10800.5	1.38	135,726	0.61	5,329,806	1.09	3,184,708	3,181,525	10376.6
C203	100	1456.3	0.61	10801.9	1.42	140,184	0.36	5,534,953	1.13	2,710,100	2,673,659	10347.8
C204	100	1462.9	2.30	1543.3	2.30	198,479	0.00	—	—	—	—	—
C205	100	1460.2	0.00	6751.6	1.28	161,459	0.79	4,660,567	1.10	3,658,860	3,658,841	6246.8
C206	100	1455.1	0.00	7773.8	1.21	165,213	0.53	3,472,458	1.07	2,606,372	2,606,273	7397.3
C207	100	1454.5	0.00	6904.3	1.06	151,000	0.40	2,240,089	0.87	1,354,217	1,353,827	6644.0
C208	100	1451.9	0.00	4007.2	1.15	152,760	1.16	10,042,392	0.98	7,514,000	7,513,149	3267.9
R201	100	1399.6	0.00	3557.6	1.44	109,684	0.32	1,140,600	1.24	589,274	589,124	3297.7
R202	100	1304.7	0.79	10801.9	1.55	100,724	0.41	7,968,435	1.16	2,921,716	2,905,345	9367.8
R203	100	1204.8	0.46	10800.5	1.15	110,469	0.60	8,440,737	0.95	4,729,553	4,626,712	9360.0
R204	100	1162.2	0.00	3928.4	0.93	131,784	0.42	4,395,386	0.78	2,660,568	2,419,768	3047.9
R205	100	1267.3	0.00	8347.3	1.38	110,249	0.34	2,350,901	1.15	1,067,631	1,065,094	7881.5
R206	100	1233.2	2.37	1963.7	2.37	97,673	0.00	—	—	—	—	—
R207	100	1193.1	1.96	1825.1	1.96	120,608	0.00	—	—	—	—	—
R208	100	1171.0	2.08	1846.5	2.08	136,807	0.00	—	—	—	—	—
R209	100	1205.4	0.00	803.2	0.86	110,023	0.36	740,587	0.68	351,456	348,275	335.5
R210	100	1211.8	0.00	3488.8	1.02	97,820	0.64	5,121,835	0.80	2,657,322	2,624,540	2579.3
R211	100	1173.4	2.35	1982.2	2.35	129,853	0.00	—	—	—	—	—
RC201	100	1806.8	0.00	56.2	0.76	76,342	0.21	43,398	0.60	20,485	20,473	17.2

Continued on next page

Table EC.6 – *Continued from previous page*

Name	n	UB	Gap%	T_{tol}	Step1		Step2	Step3	Step4	Step5	Step6	Step7
					LB_1%	$\lvert\mathcal{S}_1\rvert$	UB_1%	$\lvert\mathcal{S}_2\rvert$	LB_2%	$\lvert\mathcal{S}_3\rvert$	$\lvert\mathcal{U}_3\rvert$	CPU_7
RC202	100	1680.2	0.00	1686.5	1.27	80,899	0.67	1,612,994	1.15	1,114,503	1,108,061	1382.3
RC203	100	1601.0	0.00	1035.0	0.99	92,677	0.23	468,997	0.79	220,040	211,248	829.4
RC204	100	1574.6	0.00	5153.1	0.94	115,341	0.60	2,776,477	0.80	1,710,953	1,538,783	3930.7
RC205	100	1732.6	0.31	10800.3	1.78	88,727	1.02	9,843,946	1.19	3,437,063	3,430,023	7831.4
RC206	100	1698.1	0.51	10800.5	1.56	83,694	0.14	820,918	1.34	388,183	386,530	10612.2
RC207	100	1664.0	2.90	2607.9	2.90	85,112	0.00	—	—	—	—	—
RC208	100	1570.8	0.38	10800.5	0.99	126,026	1.10	14,549,998	0.79	8,831,413	8,350,806	3268.4

EC.5.2. Detailed Results for the CMTVRPTW-LT on Machine 2

Table EC.7: Detailed Results for the CMTVRPTW-LT on Machine 2.

Name	n	UB	Gap%	CPU	Step1		Step2	Step3	Step4	Step5	Step6	Step7
					LB_1%	$\lvert\mathcal{S}_1\rvert$	UB_1%	$\lvert\mathcal{S}_2\rvert$	LB_2%	$\lvert\mathcal{S}_3\rvert$	$\lvert\mathcal{U}_3\rvert$	CPU_7
C201	70	1063.2	0.00	1763.9	1.32	73,100	0.00	193,245	1.23	126,068	126,068	1709.1
C202	70	1053.4	0.00	1055.0	1.01	80,492	0.49	358,813	0.97	276,759	276,728	989.0
C203	70	1045.2	0.00	6320.7	1.36	74,881	0.11	527,949	1.23	304,353	301,363	6241.2
C204	70	1038.4	0.00	5062.3	1.23	99,533	0.36	1,202,977	1.14	739,544	699,670	4907.4
C205	70	1048.2	0.00	1592.8	1.32	90,134	0.14	460,554	1.26	305,412	305,407	1545.9
C206	70	1044.1	0.00	7794.4	1.39	98,334	0.21	637,799	1.33	490,576	490,554	7701.0
C207	70	1040.3	0.00	3927.9	1.27	79,955	0.11	348,838	1.19	261,048	260,847	3876.7
C208	70	1040.3	0.00	4624.2	1.23	103,225	0.21	437,840	1.17	339,511	339,466	4562.7
R201	70	1118.4	0.00	25.5	0.87	46,359	0.48	25,963	0.57	6,918	6,913	3.7
R202	70	1041.1	0.00	300.3	1.58	43,544	0.31	201,182	1.34	107,136	106,552	214.0
R203	70	959.5	0.00	108.3	0.93	48,480	0.58	144,231	0.77	79,149	77,280	28.8
R204	70	921.8	0.00	156.4	1.04	55,664	0.35	205,710	0.87	104,360	92,268	79.0
R205	70	1033.4	0.00	396.8	1.43	53,155	0.76	442,093	1.18	271,289	270,593	314.6
R206	70	985.9	0.00	490.3	1.40	46,994	0.43	303,276	1.21	178,267	175,953	392.2
R207	70	942.0	0.00	154.6	0.99	50,905	0.35	112,706	0.89	64,598	61,999	103.5
R208	70	917.5	0.00	289.1	1.09	57,615	0.49	369,567	1.00	229,453	191,736	175.1
R209	70	955.9	0.00	161.3	1.21	47,464	0.86	297,899	0.98	171,354	169,539	84.7
R210	70	983.4	0.00	605.1	1.36	49,087	0.62	455,564	1.08	240,281	237,893	397.1
R211	70	914.8	0.00	102.7	0.79	47,537	0.89	273,397	0.63	154,017	148,983	19.7
RC201	70	1367.5	0.00	49.7	1.48	34,378	0.93	60,653	1.26	39,866	39,843	15.7
RC202	70	1284.6	0.00	38.0	1.11	34,975	0.97	55,394	1.05	43,518	43,167	10.0
RC203	70	1230.5	0.00	136.4	0.83	43,143	1.89	263,988	0.59	189,537	179,703	11.6
RC204	70	1206.6	0.00	224.6	1.35	60,300	0.37	110,285	1.16	78,262	64,582	182.1
RC205	70	1340.4	0.00	70.7	1.57	42,950	0.25	41,690	1.28	27,274	27,124	39.8
RC206	70	1290.2	0.00	505.4	1.77	52,079	0.40	84,813	1.62	62,714	62,385	468.5
RC207	70	1241.1	0.00	2632.9	1.89	43,328	0.70	268,515	1.58	190,033	186,740	2562.3
RC208	70	1209.4	0.00	3849.1	1.79	55,744	2.17	3,418,724	1.55	2,600,727	2,457,134	2255.3
C201	80	1185.7	0.00	2986.2	1.90	77,383	1.18	5,201,862	1.07	1,709,777	1,709,777	2678.8
C202	80	1180.2	0.54	10819.7	2.14	93,954	0.11	2,990,658	1.34	505,504	505,390	10649.0
C203	80	1172.9	0.77	10800.6	1.77	97,780	0.12	2,420,682	1.34	672,903	663,411	10456.7
C204	80	1166.6	1.86	10802.6	1.86	137,321	0.00	2,631,140	1.86	—	—	—
C205	80	1172.8	0.00	3978.6	1.32	122,476	0.24	721,239	1.04	334,464	334,456	3842.9
C206	80	1171.1	0.00	7627.1	1.43	111,942	0.09	947,314	1.12	322,467	322,443	7510.6
C207	80	1167.2	0.00	6798.3	1.57	103,184	0.34	2,212,347	1.15	708,382	708,077	6597.4
C208	80	1167.2	0.00	4583.5	1.36	113,796	0.50	1,583,179	1.18	942,403	942,289	4346.1
R201	80	1205.6	0.00	213.9	1.32	58,184	0.51	219,463	1.10	113,873	113,850	144.1
R202	80	1121.2	0.00	959.8	1.21	61,000	1.16	2,727,978	1.05	1,694,726	1,690,912	464.7
R203	80	1035.4	0.00	342.0	1.06	63,178	0.14	131,127	0.93	71,170	69,937	250.1
R204	80	1002.1	0.00	1002.0	1.06	73,415	0.57	1,270,848	0.94	765,387	687,112	708.0
R205	80	1105.7	0.00	1823.7	1.46	67,339	0.82	1,427,352	1.24	856,246	854,563	1435.0
R206	80	1055.7	0.00	2645.7	1.41	62,520	1.31	7,132,878	1.06	3,817,155	3,792,555	1469.0
R207	80	1011.4	0.00	174.9	0.49	64,222	1.04	603,276	0.36	328,075	320,715	12.3
R208	80	993.5	0.00	299.6	0.71	76,140	0.62	525,157	0.63	300,981	254,373	41.1
R209	80	1038.4	0.00	1769.1	1.55	64,921	0.23	549,278	1.22	245,275	242,552	1555.0
R210	80	1053.7	0.00	620.1	1.09	63,966	0.73	780,240	0.98	531,827	528,038	397.5
R211	80	999.0	0.00	452.1	1.07	66,980	0.00	137,488	0.94	67,862	65,223	378.4
RC201	80	1554.1	0.00	48.4	1.22	46,918	0.30	38,434	1.18	27,659	27,643	23.8

Continued on next page

Table EC.7 – *Continued from previous page*

Name	n	UB	Gap%	T_{tol}	Step1		Step2	Step3	Step4	Step5	Step6	Step7
					LB_1%	$\lvert\mathcal{S}_1\rvert$	UB_1%	$\lvert\mathcal{S}_2\rvert$	LB_2%	$\lvert\mathcal{S}_3\rvert$	$\lvert\mathcal{U}_3\rvert$	CPU_7
RC202	80	1459.9	0.00	157.4	1.30	50,054	0.57	118,480	1.24	91,214	90,591	114.9
RC203	80	1392.3	0.00	38.8	0.36	57,989	0.09	4,464	0.19	1,450	1,351	0.3
RC204	80	1366.5	0.00	121.3	0.40	76,469	1.21	298,790	0.27	193,960	161,538	6.1
RC205	80	1519.8	0.00	145.0	1.32	52,936	0.36	92,537	1.09	51,743	51,566	97.2
RC206	80	1457.5	0.00	703.9	1.49	58,334	1.86	1,716,842	1.28	1,046,941	1,044,317	154.1
RC207	80	1402.9	0.00	276.3	1.19	52,610	0.63	216,250	0.98	128,042	125,412	163.4
RC208	80	1365.6	0.00	2357.5	0.63	67,344	2.44	3,874,716	0.48	2,827,665	2,689,894	39.8
C201	100	1509.5	3.62	712.7	3.62	139,594	0.00	—	—	—	—	—
C202	100	1465.5	0.24	10885.0	1.22	138,193	0.08	1,044,966	1.04	583,926	583,258	10772.2
C203	100	1459.8	0.96	10803.1	1.53	156,408	0.14	3,647,094	1.26	2,112,198	2,080,358	10431.9
C204	100	1448.7	0.00	10783.9	1.28	194,422	0.30	4,697,236	1.00	2,199,415	2,072,281	10168.5
C205	100	1464.6	0.59	10801.1	1.51	163,114	0.74	6,053,521	1.28	4,528,781	4,528,767	9939.6
C206	100	1460.1	0.78	10801.2	1.55	159,357	0.13	3,028,539	1.40	2,236,889	2,236,830	10559.2
C207	100	1454.8	0.00	3097.7	0.99	143,319	0.41	1,703,054	0.77	937,848	937,523	2902.3
C208	100	1451.9	0.00	1850.8	1.15	154,756	0.56	3,529,928	0.98	2,355,649	2,355,438	1505.3
R201	100	1403.1	0.00	1384.2	1.33	111,549	0.29	704,475	1.07	298,169	298,071	1216.0
R202	100	1318.0	2.27	2365.2	2.27	103,173	0.00	—	—	—	—	—
R203	100	1216.4	2.06	1833.3	2.06	118,157	0.00	—	—	—	—	—
R204	100	1162.2	0.00	3975.7	0.98	132,844	0.51	7,070,401	0.78	3,786,501	3,451,375	2658.4
R205	100	1267.7	0.00	1575.8	1.29	111,750	0.27	1,173,186	0.99	376,087	374,704	1262.9
R206	100	1222.9	0.99	10803.1	1.38	101,050	0.65	16,335,694	1.18	9,854,870	9,747,971	7552.7
R207	100	1182.5	0.21	10800.9	1.13	116,480	0.63	12,994,502	0.92	6,978,108	6,682,569	8378.7
R208	100	1157.5	0.00	2439.3	0.92	140,534	0.55	7,427,231	0.70	3,661,269	3,222,293	956.2
R209	100	1207.8	0.00	1810.4	0.91	107,332	0.88	5,374,640	0.72	3,302,742	3,283,149	717.9
R210	100	1215.8	0.21	10802.6	1.18	101,760	0.60	7,227,850	0.93	3,438,665	3,397,981	9614.2
R211	100	1178.4	2.64	2325.7	2.64	130,207	0.00	—	—	—	—	—
RC201	100	1809.5	0.00	95.6	0.87	86,817	0.67	264,662	0.59	104,368	104,323	20.1
RC202	100	1689.2	0.72	10800.8	1.61	78,276	0.85	5,241,171	1.48	3,852,418	3,835,769	9177.8
RC203	100	1601.0	0.00	1932.9	0.96	96,968	0.68	1,809,271	0.73	922,127	887,566	1484.7
RC204	100	1574.6	0.00	4949.1	0.96	123,626	0.80	5,022,289	0.80	3,099,659	2,788,374	3225.6
RC205	100	1737.7	0.00	8263.9	1.68	82,548	0.31	1,516,683	1.20	491,548	489,944	7976.3
RC206	100	1702.5	0.88	10803.2	1.69	87,516	0.60	3,856,317	1.44	1,830,614	1,826,110	10095.3
RC207	100	1641.7	0.88	10800.8	1.40	90,209	1.24	16,810,631	1.15	10,326,206	10,244,663	5709.7
RC208	100	1572.7	0.59	10800.4	1.13	126,184	0.71	6,838,161	0.91	3,510,589	3,299,010	8025.7

EC.5.3. Detailed Results for the CMTVRPTW-LD on Machine 2

Table EC.8: Detailed Results for the CMTVRPTW-LD on Machine 2.

Name	n	$\bar{d}$	UB	Gap%	CPU	Step1		Step2	Step3	Step4	Step5	Step6	Step7
						LB_1%	$\lvert\mathcal{S}_1\rvert$	UB_1%	$\lvert\mathcal{S}_2\rvert$	LB_2%	$\lvert\mathcal{S}_3\rvert$	$\lvert\mathcal{U}_3\rvert$	CPU_7
C201	70	220	1918.7	0.00	0.3	0.00	477	0.00	0	0.00	0	0	0.0
C201	70	250	1587.5	0.00	0.1	0.00	756	0.00	0	0.00	0	0	0.0
C202	70	220	1896.6	0.00	12.2	0.30	1,264	0.13	349	0.30	287	250	0.5
C202	70	250	1582.7	0.00	8.5	0.03	2,800	0.00	123	0.03	97	92	0.0
C203	70	220	1835.9	0.00	26.3	0.28	2,155	0.00	426	0.28	364	305	0.0
C203	70	250	1571.6	0.00	19.3	0.77	5,713	0.18	4,720	0.77	3,934	3,464	0.5
C204	70	220	1774.3	0.00	66.4	0.43	3,002	0.00	677	0.43	611	574	0.1
C204	70	250	1557.8	0.00	44.3	1.02	9,547	0.00	5,819	1.02	5,275	4,768	0.8
C205	70	220	1846.3	0.00	9.5	0.98	895	0.03	494	0.98	413	409	0.2
C205	70	250	1580.5	0.00	4.2	0.26	1,701	0.54	736	0.26	649	642	0.0
C206	70	220	1842.3	0.00	9.8	1.37	1,185	0.01	854	1.37	779	761	0.1
C206	70	250	1573.3	0.00	6.6	0.28	2,526	0.13	656	0.28	577	550	1.5
C207	70	220	1798.6	0.00	11.7	0.46	1,565	0.00	518	0.46	484	455	0.0
C207	70	250	1568.6	0.00	7.7	0.16	4,060	0.03	415	0.16	340	301	0.1
C208	70	220	1815.5	0.00	6.7	0.43	1,515	0.00	441	0.43	383	372	0.0
C208	70	250	1568.6	0.00	6.8	0.16	3,104	0.00	321	0.16	261	240	0.0
R201	70	75	1838.1	0.00	2.5	0.06	866	0.00	105	0.06	70	69	0.0
R201	70	100	1597.0	0.00	0.1	0.00	2,009	0.00	0	0.00	0	0	0.0
R202	70	75	1708.5	0.00	7.2	0.05	1,854	0.00	125	0.05	101	98	0.0
R202	70	100	1469.4	0.00	1.4	0.00	4,621	0.00	0	0.00	0	0	0.0

Continued on next page

Table EC.8 – *Continued from previous page*

Name	n	$\bar{d}$	UB	Gap%	T_{tol}	Step1		Step2	Step3	Step4	Step5	Step6	Step7
						LB_1%	$\lvert\mathcal{S}_1\rvert$	UB_1%	$\lvert\mathcal{S}_2\rvert$	LB_2%	$\lvert\mathcal{S}_3\rvert$	$\lvert\mathcal{U}_3\rvert$	CPU_7
R203	70	75	1559.1	0.00	14.4	0.18	2,828	0.00	259	0.18	225	214	0.0
R203	70	100	1305.6	0.00	5.2	0.00	5,959	0.00	0	0.00	0	0	0.0
R204	70	75	1390.4	0.00	26.4	0.46	3,572	0.00	824	0.46	658	611	0.1
R204	70	100	1110.3	0.00	87.4	0.15	8,708	0.00	367	0.11	250	235	0.0
R205	70	75	1608.9	0.00	5.5	0.71	1,707	0.00	868	0.71	711	701	0.0
R205	70	100	1358.8	0.00	8.9	0.22	4,041	0.00	307	0.22	246	241	0.0
R206	70	75	1531.3	0.00	10.3	0.22	2,771	0.18	401	0.22	292	282	0.0
R206	70	100	1278.6	0.00	26.5	0.52	5,842	0.34	3,532	0.52	2,914	2,814	0.4
R207	70	75	1454.8	0.00	17.2	0.21	3,271	0.00	292	0.21	218	208	0.0
R207	70	100	1186.1	0.00	51.0	0.70	7,817	0.26	5,235	0.70	4,588	4,253	0.5
R208	70	75	1376.1	0.00	27.9	0.44	3,636	0.00	958	0.44	738	667	0.1
R208	70	100	1087.6	0.00	105.6	0.21	8,021	0.31	1,912	0.14	1,213	1,130	0.1
R209	70	75	1476.4	0.00	8.7	0.55	2,864	0.00	830	0.55	700	669	0.1
R209	70	100	1211.5	0.00	23.8	0.65	5,557	0.31	3,954	0.62	2,935	2,866	0.4
R210	70	75	1543.5	0.00	9.3	0.83	2,732	0.14	2,036	0.83	1,852	1,718	0.2
R210	70	100	1299.0	0.00	22.5	0.48	5,949	0.00	1,294	0.48	1,105	1,070	0.2
R211	70	75	1375.4	0.00	16.2	0.81	4,024	0.04	3,208	0.81	2,824	2,721	0.5
R211	70	100	1082.0	0.00	79.5	0.10	9,719	0.00	254	0.10	191	186	0.0
RC201	70	75	2392.0	0.00	3.2	0.09	525	0.00	123	0.09	97	96	0.0
RC201	70	100	1798.5	0.00	0.1	0.00	1,088	0.00	0	0.00	0	0	0.0
RC202	70	75	2167.3	0.00	7.3	0.51	1,030	0.00	311	0.51	240	230	0.0
RC202	70	100	1664.8	0.00	10.0	0.62	2,772	0.00	747	0.62	568	546	0.1
RC203	70	75	1986.1	0.00	34.0	0.52	2,017	0.00	500	0.51	357	314	0.0
RC203	70	100	1482.0	0.00	12.1	0.00	5,301	0.00	0	0.00	0	0	0.0
RC204	70	75	1843.6	0.00	41.4	0.55	2,979	0.00	1,057	0.55	892	787	0.0
RC204	70	100	1290.9	0.00	102.7	1.03	12,800	0.00	5,616	0.94	3,697	3,398	0.9
RC205	70	75	2197.3	0.00	5.3	0.26	895	0.00	211	0.26	164	151	0.0
RC205	70	100	1723.5	0.00	6.7	0.11	2,507	0.00	177	0.11	120	117	0.0
RC206	70	75	2095.4	0.00	6.1	0.79	1,175	0.00	437	0.79	357	344	0.0
RC206	70	100	1582.4	0.00	14.6	1.20	3,408	0.00	2,626	1.13	2,048	2,002	0.9
RC207	70	75	1924.7	0.00	11.6	1.56	2,097	0.00	2,205	1.56	2,044	1,899	0.1
RC207	70	100	1367.3	0.00	24.6	1.45	7,100	0.01	6,069	1.45	3,719	3,599	0.2
RC208	70	75	1818.1	0.00	95.6	1.32	2,967	0.76	4,456	1.32	4,361	4,149	2.1
RC208	70	100	1249.3	0.00	155.2	1.73	14,495	0.14	21,001	1.62	16,346	15,696	16.9
C201	80	220	2283.6	0.00	14.9	0.10	573	0.00	150	0.10	128	128	0.0
C201	80	250	1859.1	0.00	2.8	0.10	953	0.00	157	0.10	122	122	0.0
C202	80	220	2230.9	0.00	16.4	0.05	1,639	0.00	163	0.05	133	122	0.0
C202	80	250	1838.7	0.00	11.6	0.59	3,877	0.00	1,297	0.59	1,144	1,069	0.2
C203	80	220	2183.4	0.00	27.7	0.25	2,653	0.00	512	0.25	438	377	0.0
C203	80	250	1823.0	0.00	27.3	0.90	6,555	0.00	5,606	0.90	5,100	4,476	0.8
C204	80	220	2139.2	0.00	272.4	0.85	3,439	0.00	2,505	0.85	2,327	2,178	0.2
C204	80	250	1817.6	0.00	67.5	0.84	9,576	0.00	6,240	0.84	5,926	5,346	1.2
C205	80	220	2210.8	0.00	11.0	0.73	1,099	0.03	580	0.73	494	488	0.7
C205	80	250	1846.8	0.00	4.5	0.42	2,156	0.00	643	0.42	582	570	0.0
C206	80	220	2203.8	0.00	147.8	0.98	1,524	0.00	930	0.98	868	847	0.0
C206	80	250	1835.2	0.00	7.3	0.46	2,964	0.00	1,016	0.46	890	853	0.0
C207	80	220	2160.8	0.00	25.0	0.53	1,917	0.00	733	0.53	701	668	0.0
C207	80	250	1832.1	0.00	9.8	0.34	4,430	0.00	1,031	0.34	857	789	0.0
C208	80	220	2184.1	0.00	26.0	0.50	1,873	0.00	717	0.50	633	622	0.0
C208	80	250	1830.8	0.00	9.5	0.81	3,859	0.00	2,255	0.81	2,097	2,036	0.1
R201	80	75	2017.9	0.00	3.2	0.45	1,164	0.00	325	0.45	235	232	0.0
R201	80	100	1714.1	0.00	0.2	0.00	2,911	0.00	0	0.00	0	0	0.0
R202	80	75	1882.4	0.00	10.3	0.42	2,711	0.04	894	0.42	720	686	0.1
R202	80	100	1580.8	0.00	2.4	0.00	7,099	0.00	0	0.00	0	0	0.0
R203	80	75	1662.5	0.00	20.5	0.15	3,741	0.22	658	0.15	526	498	0.1
R203	80	100	1385.4	0.00	54.2	0.25	9,167	0.05	851	0.25	654	625	0.2
R204	80	75	1521.4	0.00	41.3	0.39	5,618	0.00	1,085	0.39	927	868	0.2
R204	80	100	1196.2	0.00	210.9	0.30	15,660	0.39	5,657	0.28	4,191	3,935	0.6
R205	80	75	1731.2	0.00	8.2	0.68	2,415	0.16	1,896	0.68	1,636	1,593	0.1
R205	80	100	1427.2	0.00	13.7	0.13	6,018	0.00	253	0.13	167	163	0.0
R206	80	75	1634.6	0.00	1.8	0.00	3,689	0.00	0	0.00	0	0	0.0
R206	80	100	1350.6	0.00	20.7	0.00	9,608	0.00	0	0.00	0	0	0.0
R207	80	75	1569.6	0.00	26.0	0.29	4,643	0.04	707	0.29	562	533	0.1
R207	80	100	1262.7	0.00	93.6	0.51	12,573	0.00	2,255	0.51	1,538	1,464	0.3

Continued on next page

Table EC.8 – *Continued from previous page*

Name	n	$\bar{d}$	UB	Gap%	T_{tol}	Step1		Step2	Step3	Step4	Step5	Step6	Step7
						LB_1%	$\lvert\mathcal{S}_1\rvert$	UB_1%	$\lvert\mathcal{S}_2\rvert$	LB_2%	$\lvert\mathcal{S}_3\rvert$	$\lvert\mathcal{U}_3\rvert$	CPU_7
R208	80	75	1499.6	0.00	48.8	0.65	5,817	0.05	3,558	0.65	2,891	2,656	0.5
R208	80	100	1170.5	0.00	253.7	0.62	15,003	0.18	8,237	0.62	6,332	5,870	1.3
R209	80	75	1604.3	0.00	15.6	0.50	4,007	0.07	1,779	0.50	1,527	1,464	0.2
R209	80	100	1304.6	0.00	53.3	0.77	10,513	0.08	6,007	0.69	4,044	3,930	1.0
R210	80	75	1643.8	0.00	14.1	0.29	3,473	0.13	695	0.29	575	550	0.1
R210	80	100	1372.3	0.00	50.2	0.52	8,631	0.00	2,149	0.51	1,707	1,660	0.6
R211	80	75	1496.8	0.00	39.8	0.99	6,288	0.03	8,827	0.97	7,774	7,493	3.7
R211	80	100	1166.1	0.00	238.1	0.57	17,621	0.31	10,954	0.47	5,593	5,452	1.8
RC201	80	75	2757.4	0.00	4.4	0.64	620	0.12	347	0.64	285	277	0.2
RC201	80	100	2034.0	0.00	4.5	0.17	1,606	0.00	169	0.17	112	111	0.0
RC202	80	75	2466.4	0.00	9.9	0.46	1,092	0.00	377	0.46	311	280	0.0
RC202	80	100	1869.7	0.00	0.9	0.00	3,258	0.00	0	0.00	0	0	0.0
RC203	80	75	2280.8	0.00	20.1	0.11	2,102	0.00	205	0.11	148	134	0.0
RC203	80	100	1695.5	0.00	48.8	0.52	6,695	0.04	1,620	0.49	1,282	1,200	0.3
RC204	80	75	2157.2	0.00	40.7	0.43	3,666	0.02	905	0.43	758	684	0.1
RC204	80	100	1501.1	0.00	161.0	1.01	13,791	0.00	9,189	0.98	6,231	5,540	1.7
RC205	80	75	2519.3	0.00	7.0	0.38	1,015	0.00	314	0.38	249	221	0.0
RC205	80	100	1932.9	0.00	1.3	0.00	3,016	0.00	0	0.00	0	0	0.0
RC206	80	75	2416.6	0.00	8.7	0.07	1,339	0.07	204	0.07	172	164	0.2
RC206	80	100	1775.2	0.00	12.8	0.33	4,677	0.02	651	0.31	412	406	0.0
RC207	80	75	2253.2	0.00	16.0	0.70	2,459	0.00	1,199	0.70	937	871	0.0
RC207	80	100	1609.2	0.00	48.7	0.82	9,594	0.00	3,753	0.81	3,080	2,969	0.2
RC208	80	75	2123.0	0.00	84.9	0.72	3,744	0.80	4,896	0.72	4,673	4,444	4.1
RC208	80	100	1467.9	0.00	306.5	1.48	15,818	0.30	31,299	1.38	23,434	22,562	40.0
C201	100	220	2902.4	0.00	532.2	0.50	837	0.00	400	0.50	360	360	0.0
C201	100	250	2335.4	0.00	13.4	0.34	1,261	0.00	381	0.34	359	359	0.0
C202	100	220	2830.8	0.00	392.4	0.51	2,145	0.04	1,084	0.51	968	850	25.2
C202	100	250	2311.8	0.00	22.8	0.57	5,576	0.03	3,075	0.57	2,797	2,549	0.8
C203	100	220	2763.0	0.00	249.6	0.52	3,345	0.01	1,749	0.52	1,574	1,376	14.7
C203	100	250	2292.2	0.00	66.6	0.78	10,120	0.08	11,049	0.78	10,379	9,155	3.0
C204	100	220	2704.4	0.00	1049.8	0.56	4,445	0.00	2,480	0.56	2,278	2,117	0.2
C204	100	250	2283.6	0.00	305.9	0.79	13,972	0.02	11,071	0.79	10,305	9,310	37.2
C205	100	220	2793.2	0.00	68.5	0.99	1,459	0.02	1,035	0.99	989	983	4.3
C205	100	250	2320.4	0.00	23.1	0.95	2,657	0.08	1,835	0.95	1,746	1,732	2.6
C206	100	220	2770.6	0.00	159.0	1.04	2,029	0.02	1,410	1.04	1,358	1,328	7.6
C206	100	250	2308.8	0.00	13.5	1.03	4,373	0.00	3,071	1.03	2,854	2,775	0.5
C207	100	220	2743.2	0.00	364.3	0.67	2,226	0.12	1,428	0.67	1,384	1,334	3.3
C207	100	250	2305.7	0.00	26.1	0.83	5,641	0.00	3,451	0.83	3,248	3,054	0.2
C208	100	220	2738.9	0.00	68.7	0.40	2,350	0.00	878	0.40	790	778	0.0
C208	100	250	2302.2	0.00	20.6	0.99	5,790	0.00	4,070	0.99	3,898	3,817	0.6
R201	100	75	2273.4	0.00	6.0	0.28	1,959	0.00	428	0.28	321	314	0.1
R201	100	100	1916.9	0.00	8.4	0.00	5,227	0.00	159	0.00	114	114	0.0
R202	100	75	2100.3	0.00	35.1	0.34	7,118	0.00	1,782	0.34	1,480	1,446	0.1
R202	100	100	1756.3	0.00	333.2	0.11	18,409	0.00	573	0.10	378	368	0.0
R203	100	75	1869.9	0.00	142.1	0.45	11,725	0.18	14,684	0.45	13,846	12,850	2.2
R203	100	100	1548.9	0.00	1754.6	0.57	29,792	0.02	18,465	0.53	13,317	12,852	9.0
R204	100	75	1712.0	0.00	111.4	0.00	16,618	0.00	0	0.00	0	0	0.0
R204	100	100	—	—	1385.1	—	—	—	—	—	—	—	—
R205	100	75	1961.7	0.00	17.2	0.14	5,132	0.08	650	0.14	581	568	0.1
R205	100	100	1604.5	0.00	56.5	0.41	13,773	0.01	2,407	0.39	1,820	1,794	0.6
R206	100	75	1854.1	0.00	69.7	0.50	10,265	0.11	6,341	0.50	5,657	5,391	0.7
R206	100	100	1518.9	0.00	1039.6	0.36	25,794	0.20	15,627	0.29	9,427	9,028	2.4
R207	100	75	1771.5	0.00	149.3	0.59	14,334	0.19	19,875	0.59	18,127	16,769	2.5
R207	100	100	1416.3	1.12	2779.7	1.12	34,547	0.00	134,296	1.12	0	0	0.0
R208	100	75	1687.7	0.00	255.1	0.40	16,068	0.04	6,045	0.40	5,055	4,496	0.5
R208	100	100	—	—	1648.8	—	—	—	—	—	—	—	—
R209	100	75	1833.2	0.00	48.5	0.57	9,413	0.02	5,864	0.57	5,304	5,137	1.5
R209	100	100	1462.5	0.00	457.2	0.40	27,109	0.00	3,408	0.36	2,033	2,012	0.5
R210	100	75	1841.6	0.00	60.1	0.18	10,169	0.00	770	0.18	656	634	0.1
R210	100	100	1532.4	0.00	825.0	0.71	27,692	0.04	30,379	0.66	22,444	21,447	10.0
R211	100	75	1678.9	0.00	272.7	0.45	17,127	0.17	17,622	0.44	15,392	14,695	1.7
R211	100	100	—	—	3065.5	—	—	—	—	—	—	—	—
RC201	100	75	3120.3	0.00	7.9	0.11	1,180	0.00	207	0.11	154	149	0.0
RC201	100	100	2370.2	0.00	7.8	0.02	3,478	0.00	151	0.02	96	96	0.0

Continued on next page

Table EC.8 – *Continued from previous page*

Name	n	$\bar{d}$	UB	Gap%	T_{tol}	Step1		Step2	Step3	Step4	Step5	Step6	Step7
						LB_1%	$\lvert\mathcal{S}_1\rvert$	UB_1%	$\lvert\mathcal{S}_2\rvert$	LB_2%	$\lvert\mathcal{S}_3\rvert$	$\lvert\mathcal{U}_3\rvert$	CPU_7
RC202	100	75	2819.5	0.00	24.3	0.67	2,998	0.01	1,658	0.67	1,342	1,222	0.3
RC202	100	100	2148.6	0.00	37.4	0.48	9,120	0.10	2,291	0.48	1,921	1,895	0.2
RC203	100	75	2550.5	0.00	41.3	0.22	4,752	0.00	531	0.22	422	392	0.0
RC203	100	100	1896.4	0.00	122.0	0.25	16,820	0.00	986	0.24	654	644	0.1
RC204	100	75	2430.3	0.00	82.9	0.54	7,170	0.07	3,863	0.54	3,253	2,975	0.6
RC204	100	100	1725.8	0.00	415.8	0.74	28,861	0.24	24,501	0.58	14,171	13,099	2.4
RC205	100	75	2874.8	0.00	14.1	0.15	2,531	0.00	334	0.15	260	239	0.0
RC205	100	100	2206.2	0.00	23.9	0.19	7,426	0.00	546	0.19	391	382	0.0
RC206	100	75	2724.7	0.00	16.6	0.15	3,108	0.12	459	0.15	300	288	0.2
RC206	100	100	2064.1	0.00	32.9	0.42	9,932	0.15	3,274	0.36	1,710	1,688	0.4
RC207	100	75	2612.7	0.00	30.0	0.70	5,324	0.00	3,771	0.70	3,450	3,268	0.4
RC207	100	100	1876.2	0.00	134.9	0.75	15,379	0.10	10,980	0.75	7,901	7,714	0.5
RC208	100	75	2381.3	0.00	716.3	0.23	8,376	0.36	4,070	0.23	3,656	3,467	545.9
RC208	100	100	1667.7	0.00	929.5	1.12	28,870	0.43	96,836	0.91	59,488	57,269	212.0

EC.5.4. Detailed Results for the CMTVRPTW-R on Machine 2

Table EC.9: Detailed Results for the CMTVRPTW-R on Machine 2.

Name	n	UB	Gap%	CPU	Step1		Step2	Step3	Step4	Step5	Step6	Step7
					LB_1%	$\lvert\mathcal{S}_1\rvert$	UB_1%	$\lvert\mathcal{S}_2\rvert$	LB_2%	$\lvert\mathcal{S}_3\rvert$	$\lvert\mathcal{U}_3\rvert$	CPU_7
C201R0.25	70	1068.7	0.00	242.6	1.61	26,707	0.13	67,130	1.52	54,705	54,705	207.0
C201R0.5	70	1072.0	0.00	37.6	1.35	22,922	0.10	29,021	1.29	20,730	20,730	22.4
C201R0.75	70	1080.9	0.00	11.8	0.43	20,711	0.61	12,820	0.43	8,475	8,475	0.2
C202R0.25	70	1121.0	0.00	12.2	0.53	30,210	0.02	4,134	0.52	3,166	3,165	0.4
C202R0.5	70	1121.0	0.00	9.7	0.52	28,775	0.00	2,933	0.52	2,060	2,060	0.1
C202R0.75	70	1121.0	0.00	8.8	0.52	31,069	0.00	2,203	0.52	1,667	1,666	0.1
C203R0.25	70	1156.3	0.00	143.2	0.30	35,364	0.16	5,951	0.25	2,337	2,263	0.4
C203R0.5	70	1156.3	0.00	46.5	0.35	37,000	0.16	6,468	0.24	2,348	2,267	0.5
C203R0.75	70	1156.3	0.00	37.0	0.24	38,003	0.00	1,151	0.22	502	491	0.1
C204R0.25	70	1145.6	0.00	115.4	0.28	83,449	0.00	1,996	0.27	1,155	1,142	0.2
C204R0.5	70	1145.6	0.00	143.4	0.27	87,259	0.00	2,349	0.27	1,374	1,355	0.4
C204R0.75	70	1145.6	0.00	150.8	0.22	90,878	0.00	1,717	0.22	798	792	0.2
C205R0.25	70	1063.2	0.00	169.8	1.54	40,812	0.28	78,505	1.50	69,049	69,041	144.2
C205R0.5	70	1066.6	0.00	17.3	0.87	39,002	0.05	12,372	0.83	7,883	7,881	1.6
C205R0.75	70	1075.9	0.00	20.9	0.92	33,685	0.52	33,647	0.91	27,270	27,261	4.4
C206R0.25	70	1053.4	0.00	270.6	1.45	50,183	0.45	115,024	1.45	99,348	99,282	237.6
C206R0.5	70	1062.3	0.00	277.6	1.58	48,754	0.13	69,204	1.51	47,081	46,980	247.8
C206R0.75	70	1072.5	0.00	48.4	1.22	38,127	0.21	48,531	1.20	32,128	32,041	25.2
C207R0.25	70	1047.2	0.00	71.7	1.04	50,802	0.80	108,618	1.03	89,719	89,310	43.2
C207R0.5	70	1051.9	0.00	30.7	0.91	47,196	0.30	25,947	0.84	20,924	20,746	7.8
C207R0.75	70	1060.6	0.00	16.5	0.46	41,394	0.13	4,879	0.31	2,188	2,142	0.6
C208R0.25	70	1050.6	0.00	306.1	1.48	57,101	0.38	121,272	1.45	92,151	92,048	274.4
C208R0.5	70	1055.9	0.00	103.4	1.36	43,646	0.31	65,057	1.34	47,134	47,028	74.5
C208R0.75	70	1058.5	0.00	21.7	0.73	42,289	0.00	8,530	0.65	4,631	4,614	1.4
R201R0.25	70	1159.1	0.00	8.5	0.72	19,893	0.17	4,201	0.69	2,446	2,443	0.7
R201R0.5	70	1173.9	0.00	9.6	0.66	19,492	0.18	4,337	0.65	2,531	2,529	0.6
R201R0.75	70	1214.4	0.00	18.9	0.59	17,043	0.03	3,162	0.58	1,787	1,784	0.7
R202R0.25	70	1115.4	0.00	10.2	0.00	26,764	0.00	0	0.00	0	0	0.0
R202R0.5	70	1125.5	0.00	5.0	0.00	22,469	0.00	0	0.00	0	0	0.0
R202R0.75	70	1125.5	0.00	3.5	0.00	24,033	0.00	0	0.00	0	0	0.0
R203R0.25	70	1113.0	0.00	419.2	0.13	28,763	0.00	316	0.13	214	201	0.0
R203R0.5	70	1123.8	0.00	229.0	0.10	28,499	0.00	281	0.08	184	172	0.0
R203R0.75	70	1148.4	0.66	10800.3	0.66	29,121	0.00	3,557	0.66	0	0	0.0
R204R0.25	70	1057.7	0.00	1677.2	0.74	49,087	0.12	22,912	0.68	12,507	11,600	5.6
R204R0.5	70	1057.7	0.00	512.9	0.72	41,467	0.12	20,824	0.68	11,825	11,008	5.6
R204R0.75	70	1079.8	0.00	702.7	0.88	41,922	0.31	87,319	0.83	50,066	45,444	33.9
R205R0.25	70	1073.5	0.00	24.2	0.74	28,431	0.20	11,908	0.64	5,374	5,304	2.0
R205R0.5	70	1083.0	0.00	20.9	0.37	30,505	0.30	3,880	0.33	2,070	2,034	0.9
R205R0.75	70	1084.6	0.00	17.8	0.11	23,401	0.00	301	0.00	0	0	0.0
R206R0.25	70	1039.6	0.00	47.6	0.01	33,632	0.00	168	0.00	0	0	0.0

Continued on next page

Table EC.9 – *Continued from previous page*

Name	n	UB	Gap%	T_{tol}	Step1		Step2	Step3	Step4	Step5	Step6	Step7
					LB_1%	$\lvert\mathcal{S}_1\rvert$	UB_1%	$\lvert\mathcal{S}_2\rvert$	LB_2%	$\lvert\mathcal{S}_3\rvert$	$\lvert\mathcal{U}_3\rvert$	CPU_7
R206R0.5	70	1059.3	0.00	238.5	0.85	36,100	0.00	11,200	0.56	2,699	2,641	1.8
R206R0.75	70	1070.6	0.00	171.0	0.70	33,834	0.53	46,722	0.45	15,976	15,611	3.4
R207R0.25	70	1049.3	0.00	82.6	0.65	35,212	0.12	10,736	0.65	6,864	6,427	1.6
R207R0.5	70	1056.5	0.00	217.1	0.47	35,277	0.38	21,784	0.35	7,720	7,313	2.1
R207R0.75	70	1056.5	0.00	62.5	0.38	34,529	0.00	2,337	0.33	1,038	976	0.3
R208R0.25	70	997.4	0.00	66.2	0.00	46,207	0.00	0	0.00	0	0	0.0
R208R0.5	70	997.4	0.00	74.0	0.00	43,645	0.00	0	0.00	0	0	0.0
R208R0.75	70	997.4	0.00	72.3	0.00	47,517	0.00	0	0.00	0	0	0.0
R209R0.25	70	995.4	0.00	120.9	1.10	30,179	0.26	50,548	0.93	27,600	27,184	20.3
R209R0.5	70	997.4	0.00	100.3	1.02	26,600	0.41	54,456	0.83	28,538	28,218	11.9
R209R0.75	70	1033.8	0.00	71.5	0.85	24,623	0.29	14,828	0.83	8,387	8,298	3.7
R210R0.25	70	1026.5	0.00	29.3	0.62	32,481	0.00	3,746	0.57	1,998	1,975	0.8
R210R0.5	70	1032.7	0.00	172.9	0.20	30,432	0.09	882	0.11	303	300	0.0
R210R0.75	70	1094.5	0.00	102.3	0.46	30,565	0.09	3,374	0.35	1,289	1,272	0.7
R211R0.25	70	930.4	0.00	243.0	1.14	34,847	0.31	80,974	0.91	36,353	35,218	33.8
R211R0.5	70	930.4	0.00	283.7	0.99	31,549	0.13	30,740	0.85	15,223	14,814	24.1
R211R0.75	70	958.8	0.00	648.8	1.40	28,133	0.49	216,734	1.22	135,839	134,198	223.3
RC201R0.25	70	1367.5	0.00	4.7	0.22	16,887	0.00	390	0.13	153	153	0.0
RC201R0.5	70	1397.6	0.00	10.9	1.26	15,756	0.47	10,496	1.20	7,706	7,691	1.8
RC201R0.75	70	1434.6	0.00	10.2	1.16	13,228	0.16	5,635	1.00	3,167	3,156	0.8
RC202R0.25	70	1409.8	0.00	25.4	1.70	18,489	0.72	41,183	1.70	34,952	34,460	9.3
RC202R0.5	70	1413.9	0.00	22.1	1.99	17,052	0.01	19,865	1.99	16,036	15,788	9.8
RC202R0.75	70	1438.3	0.00	7.9	0.23	16,077	0.00	362	0.23	243	231	0.0
RC203R0.25	70	1397.9	0.00	21.1	0.35	25,588	0.00	1,061	0.29	440	405	0.1
RC203R0.5	70	1407.7	0.00	23.0	0.92	24,145	0.00	6,756	0.88	3,170	2,916	1.0
RC203R0.75	70	1483.9	0.00	19.2	0.00	27,745	0.00	0	0.00	0	0	0.0
RC204R0.25	70	1354.0	0.00	467.3	1.42	42,663	0.92	197,032	1.10	111,538	101,583	46.7
RC204R0.5	70	1354.0	0.00	383.2	1.41	46,836	1.35	401,433	1.10	267,935	243,749	42.3
RC204R0.75	70	1409.5	0.00	545.5	1.44	42,899	0.38	74,835	0.95	25,649	24,405	10.5
RC205R0.25	70	1361.5	0.00	16.2	0.86	22,544	0.54	11,874	0.61	6,084	6,032	1.0
RC205R0.5	70	1433.0	0.00	22.0	0.81	21,769	0.13	4,861	0.66	2,864	2,838	1.0
RC205R0.75	70	1474.6	0.00	10.2	0.42	18,995	0.00	1,040	0.42	589	571	0.1
RC206R0.25	70	1309.1	0.00	21.6	0.77	30,403	0.13	5,211	0.65	2,608	2,559	0.7
RC206R0.5	70	1309.9	0.00	12.0	0.67	25,340	0.28	4,301	0.54	2,492	2,441	0.7
RC206R0.75	70	1347.7	0.00	11.2	0.25	25,117	0.26	1,378	0.20	707	692	0.1
RC207R0.25	70	1281.8	0.00	253.4	2.01	30,298	1.00	236,362	1.86	166,364	162,632	186.9
RC207R0.5	70	1281.8	0.00	349.5	2.00	27,296	1.21	283,283	1.86	212,493	208,614	277.7
RC207R0.75	70	1382.5	0.00	74.7	1.09	22,721	0.32	19,665	0.77	10,138	9,962	3.9
RC208R0.25	70	1216.4	0.00	2271.4	1.84	40,048	0.74	222,098	1.69	169,796	166,554	2160.3
RC208R0.5	70	1216.4	0.00	2040.1	1.81	39,711	1.16	367,092	1.60	275,298	272,838	1839.6
RC208R0.75	70	1235.3	0.00	242.9	1.48	34,701	0.82	106,166	1.25	78,136	77,593	98.9
C201R0.25	80	1213.4	0.00	11.6	0.93	32,941	0.00	19,800	0.53	4,603	4,603	1.3
C201R0.5	80	1216.1	0.00	18.6	2.02	27,182	0.00	73,280	0.51	3,274	3,274	0.7
C201R0.75	80	1226.8	0.00	12.4	1.97	23,088	0.03	56,159	0.25	901	901	0.1
C202R0.25	80	1249.5	0.00	31.6	1.08	33,262	0.20	37,658	0.77	19,891	19,868	6.5
C202R0.5	80	1249.5	0.00	24.7	0.85	35,556	0.04	13,510	0.58	5,347	5,344	1.3
C202R0.75	80	1251.7	0.00	20.6	1.37	33,280	0.12	45,136	0.62	6,261	6,256	1.1
C203R0.25	80	1283.0	0.00	684.0	1.24	61,575	0.30	282,939	1.00	118,138	113,143	398.4
C203R0.5	80	1283.0	0.00	350.4	1.29	58,000	0.04	175,440	0.99	45,398	43,770	125.4
C203R0.75	80	1287.1	0.00	1942.3	2.00	60,097	0.01	831,777	1.24	99,909	96,264	1664.5
C204R0.25	80	1269.0	0.00	8905.2	0.88	135,150	0.24	272,191	0.79	124,621	123,116	226.1
C204R0.5	80	1269.0	0.00	7151.8	0.87	128,833	0.25	272,193	0.79	129,912	128,158	199.5
C204R0.75	80	1274.4	0.00	2957.2	0.76	133,551	0.00	61,420	0.62	25,196	24,008	30.9
C205R0.25	80	1202.3	0.00	16.7	0.78	47,464	0.29	37,048	0.18	4,390	4,388	0.4
C205R0.5	80	1210.1	0.00	19.0	1.74	47,453	0.02	86,268	0.50	4,287	4,285	1.3
C205R0.75	80	1213.6	0.00	19.2	0.53	43,020	0.00	3,992	0.50	2,070	2,069	0.4
C206R0.25	80	1195.6	0.00	52.0	1.58	59,841	0.64	244,974	0.55	38,291	38,254	2.7
C206R0.5	80	1201.3	0.00	50.9	0.93	55,737	0.47	53,642	0.77	31,014	30,969	8.4
C206R0.75	80	1206.6	0.00	36.7	1.98	46,061	0.18	128,524	0.57	7,170	7,154	1.1
C207R0.25	80	1192.3	0.00	126.4	1.14	59,604	0.81	180,420	0.54	68,504	68,171	9.0
C207R0.5	80	1193.9	0.00	100.1	1.52	62,417	0.92	268,983	0.58	61,092	60,683	3.9
C207R0.75	80	1199.9	0.00	111.2	1.10	60,771	0.30	53,114	0.71	19,639	19,441	7.8
C208R0.25	80	1192.7	0.00	81.9	1.68	71,066	0.29	216,447	0.60	25,170	25,112	8.1
C208R0.5	80	1198.3	0.00	88.7	1.51	56,473	0.24	103,794	0.91	21,892	21,817	13.0

Continued on next page

Table EC.9 – *Continued from previous page*

Name	n	UB	Gap%	T_{tol}	Step1		Step2	Step3	Step4	Step5	Step6	Step7
					LB_1%	$\lvert\mathcal{S}_1\rvert$	UB_1%	$\lvert\mathcal{S}_2\rvert$	LB_2%	$\lvert\mathcal{S}_3\rvert$	$\lvert\mathcal{U}_3\rvert$	CPU_7
C208R0.75	80	1198.3	0.00	152.3	2.63	55,398	1.30	1,607,974	0.47	71,906	71,553	1.4
R201R0.25	80	1244.7	0.00	16.2	0.59	26,849	0.38	15,431	0.50	8,440	8,437	2.1
R201R0.5	80	1261.8	0.00	23.4	0.82	24,387	0.33	23,110	0.77	13,794	13,785	3.2
R201R0.75	80	1284.3	0.00	12.6	0.21	22,200	0.00	592	0.20	306	306	0.0
R202R0.25	80	1185.2	0.00	28.5	0.00	34,627	0.00	0	0.00	0	0	0.0
R202R0.5	80	1203.4	0.00	43.1	0.33	31,116	0.07	1,797	0.31	998	989	0.5
R202R0.75	80	1212.6	0.00	70.1	0.30	30,435	0.00	1,251	0.21	509	506	0.1
R203R0.25	80	1196.1	0.00	573.6	0.11	38,442	0.03	526	0.08	218	206	0.0
R203R0.5	80	1205.1	0.00	460.6	0.60	40,710	0.00	6,458	0.54	2,774	2,549	0.7
R203R0.75	80	1227.4	0.00	5040.1	0.76	39,438	0.08	33,018	0.68	14,807	13,587	13.3
R204R0.25	80	1152.7	0.00	1620.0	0.42	58,458	0.05	10,937	0.36	5,295	4,660	1.8
R204R0.5	80	1152.7	0.00	715.8	0.44	57,971	0.23	30,253	0.36	15,045	13,125	4.3
R204R0.75	80	1162.3	0.00	1686.5	0.86	57,201	0.75	1,597,405	0.80	924,719	814,696	247.5
R205R0.25	80	1147.0	0.00	62.8	0.53	34,826	0.27	13,191	0.51	7,972	7,878	2.0
R205R0.5	80	1159.7	0.00	24.5	0.25	35,413	0.00	851	0.22	510	503	0.1
R205R0.75	80	1185.5	0.00	69.5	0.71	31,508	0.08	10,971	0.56	3,837	3,739	1.5
R206R0.25	80	1111.5	0.00	65.1	0.14	40,750	0.00	575	0.09	222	215	0.0
R206R0.5	80	1122.4	0.00	68.3	0.00	34,416	0.00	0	0.00	0	0	0.0
R206R0.75	80	1149.1	0.00	303.8	0.64	32,772	0.05	16,468	0.44	4,313	4,232	2.1
R207R0.25	80	1113.7	0.00	181.6	0.14	45,546	0.00	537	0.00	0	0	0.0
R207R0.5	80	1128.7	0.00	350.0	0.53	49,272	0.31	46,736	0.42	22,006	21,293	7.3
R207R0.75	80	1128.7	0.00	617.1	0.48	40,774	0.25	41,221	0.37	13,749	13,315	5.0
R208R0.25	80	1083.2	0.00	1999.0	0.13	64,367	0.00	781	0.00	0	0	0.0
R208R0.5	80	1083.2	0.00	230.7	0.11	58,742	0.00	641	0.00	0	0	0.0
R208R0.75	80	1086.2	0.00	128.0	0.34	56,138	0.07	6,419	0.24	2,212	1,979	1.1
R209R0.25	80	1079.1	0.00	253.4	0.85	43,473	0.34	78,711	0.73	43,093	42,424	18.8
R209R0.5	80	1083.5	0.00	158.8	0.90	42,941	0.42	119,192	0.73	60,783	60,061	19.7
R209R0.75	80	1109.9	0.00	40.2	0.09	36,985	0.00	331	0.00	0	0	0.0
R210R0.25	80	1098.9	0.00	70.2	0.60	41,133	0.16	18,481	0.50	7,906	7,879	3.2
R210R0.5	80	1111.1	0.00	90.8	0.54	39,999	0.07	9,132	0.47	4,416	4,406	2.1
R210R0.75	80	1165.0	0.00	99.8	0.11	36,435	0.15	1,392	0.01	325	325	0.1
R211R0.25	80	1012.3	0.00	696.8	1.17	47,885	0.42	361,789	1.03	221,453	215,928	327.9
R211R0.5	80	1013.1	0.00	1456.6	1.18	45,886	0.60	660,708	1.04	405,276	398,267	349.9
R211R0.75	80	1039.0	0.00	1692.4	1.20	45,737	0.55	606,198	0.92	264,710	261,104	361.0
RC201R0.25	80	1573.3	0.00	12.0	0.88	26,774	0.09	5,165	0.75	3,208	3,203	1.3
RC201R0.5	80	1596.6	0.00	10.5	0.78	21,550	0.27	7,172	0.67	4,432	4,424	1.2
RC201R0.75	80	1625.1	0.00	6.7	0.61	20,934	0.53	7,612	0.41	3,886	3,876	0.4
RC202R0.25	80	1558.6	0.00	18.6	0.62	24,654	0.14	4,176	0.61	2,925	2,854	0.6
RC202R0.5	80	1565.2	0.00	28.2	0.68	24,878	0.26	6,098	0.68	3,656	3,588	1.5
RC202R0.75	80	1609.3	0.00	11.5	0.23	21,244	0.00	592	0.20	312	301	0.0
RC203R0.25	80	1579.8	0.00	247.2	0.88	37,528	0.21	30,073	0.63	7,339	6,995	1.9
RC203R0.5	80	1606.7	0.00	65.7	1.00	39,406	0.03	26,917	0.74	7,975	7,645	2.8
RC203R0.75	80	1665.2	0.00	130.4	0.86	37,381	0.12	26,227	0.80	13,385	12,611	9.9
RC204R0.25	80	1540.4	0.00	122.9	0.34	62,857	0.24	7,609	0.27	4,618	4,183	0.9
RC204R0.5	80	1540.4	0.00	119.9	0.32	62,851	0.24	7,155	0.25	3,958	3,612	0.9
RC204R0.75	80	1567.1	0.00	84.5	0.26	51,668	0.00	1,849	0.16	585	523	0.1
RC205R0.25	80	1537.3	0.00	16.2	0.37	32,018	0.00	1,222	0.37	1,104	1,092	0.3
RC205R0.5	80	1610.2	0.00	31.6	0.60	25,048	0.00	2,770	0.50	1,612	1,599	0.5
RC205R0.75	80	1661.1	0.00	10.2	0.28	22,959	0.01	718	0.23	339	332	0.0
RC206R0.25	80	1500.8	0.00	12.3	0.72	34,492	0.26	10,230	0.58	5,559	5,464	0.9
RC206R0.5	80	1502.0	0.00	13.0	0.45	32,828	0.27	4,945	0.39	3,152	3,093	0.5
RC206R0.75	80	1539.0	0.00	12.5	0.55	24,387	0.00	2,381	0.47	1,383	1,352	0.1
RC207R0.25	80	1461.2	0.00	64.8	1.14	34,512	0.42	69,996	1.01	44,880	43,459	24.2
RC207R0.5	80	1461.2	0.00	96.4	1.13	32,452	1.01	206,437	1.01	136,113	132,807	43.4
RC207R0.75	80	1550.4	0.00	53.2	0.87	29,788	0.12	14,718	0.68	8,244	8,089	2.2
RC208R0.25	80	1382.9	0.00	149.5	1.00	46,636	0.26	62,156	0.85	37,444	36,447	41.6
RC208R0.5	80	1386.4	0.00	503.8	1.14	47,248	0.29	90,395	1.04	58,405	57,564	232.1
RC208R0.75	80	1419.0	0.00	63.3	0.81	43,478	0.09	18,254	0.66	10,013	9,936	7.5
C201R0.25	100	1500.6	0.00	3414.1	2.25	58,756	0.53	509,337	1.92	376,546	376,545	3317.5
C201R0.5	100	1500.6	0.00	1595.5	2.20	43,009	0.63	433,397	1.91	310,723	310,722	1523.9
C201R0.75	100	1504.0	0.00	264.5	1.58	36,538	0.77	209,161	1.28	139,334	139,333	237.8
C202R0.25	100	1545.4	0.00	988.5	1.61	60,990	0.93	1,160,944	1.32	606,638	604,419	858.5
C202R0.5	100	1547.3	0.00	116.5	1.27	62,290	0.20	118,118	1.00	66,856	66,720	65.5
C202R0.75	100	1552.9	0.00	332.2	1.55	53,836	0.21	227,279	1.30	141,279	140,903	278.5

Continued on next page

Table EC.9 – *Continued from previous page*

Name	n	UB	Gap%	T_{tol}	Step1		Step2	Step3	Step4	Step5	Step6	Step7
					LB_1%	$\lvert\mathcal{S}_1\rvert$	UB_1%	$\lvert\mathcal{S}_2\rvert$	LB_2%	$\lvert\mathcal{S}_3\rvert$	$\lvert\mathcal{U}_3\rvert$	CPU_7
C203R0.25	100	1577.7	0.00	3579.0	1.35	90,805	0.16	711,469	1.05	258,603	248,246	2706.1
C203R0.5	100	1578.7	0.00	8502.8	1.47	92,963	0.53	2,251,480	1.11	843,086	806,437	7544.2
C203R0.75	100	1579.6	0.00	9873.9	1.71	94,530	0.77	6,657,944	1.05	1,414,118	1,358,852	6976.8
C204R0.25	100	1560.5	0.00	1306.6	0.69	171,421	0.00	44,191	0.61	18,596	18,244	17.9
C204R0.5	100	1560.9	0.00	818.0	0.74	182,207	0.10	134,010	0.62	32,182	31,559	49.5
C204R0.75	100	1569.1	0.00	1273.9	0.74	173,840	0.27	325,786	0.62	150,382	143,213	119.1
C205R0.25	100	1492.9	0.90	10800.3	2.38	75,790	0.50	909,834	2.12	689,032	688,965	10678.5
C205R0.5	100	1490.0	0.00	1993.6	2.14	66,551	0.46	494,184	1.91	360,022	359,979	1761.4
C205R0.75	100	1491.7	0.00	1528.5	1.89	59,757	0.78	543,904	1.67	401,119	401,046	1474.4
C206R0.25	100	1476.0	0.00	6635.4	2.02	88,135	0.75	1,022,058	1.83	781,636	780,961	6515.1
C206R0.5	100	1481.7	0.00	3305.9	2.25	67,580	0.57	787,232	1.98	558,147	557,452	3224.3
C206R0.75	100	1490.5	0.00	405.3	1.74	68,002	0.95	762,682	1.22	349,292	348,810	323.2
C207R0.25	100	1472.8	0.00	6020.8	1.75	88,965	0.72	750,996	1.53	547,905	546,028	5877.3
C207R0.5	100	1474.4	0.00	1407.8	1.72	73,013	0.69	553,225	1.47	377,688	375,854	1316.2
C207R0.75	100	1496.8	2.64	10800.7	2.90	67,652	0.36	2,424,185	2.64	1,821,042	1,814,134	10480.1
C208R0.25	100	1471.2	0.00	7326.4	1.93	98,816	1.04	2,032,014	1.67	1,407,301	1,404,781	7124.6
C208R0.5	100	1477.4	0.00	5852.2	2.19	77,346	1.07	1,953,497	1.88	1,274,698	1,271,453	5639.4
C208R0.75	100	1493.8	2.47	10800.2	2.81	74,227	0.00	940,053	2.47	570,710	568,826	10686.5
R201R0.25	100	1435.6	0.00	60.1	0.72	53,751	0.44	111,440	0.66	71,377	71,329	15.2
R201R0.5	100	1442.6	0.00	58.2	0.70	45,774	0.52	111,341	0.65	74,462	74,417	12.1
R201R0.75	100	1483.6	0.00	41.3	0.74	38,239	0.31	50,830	0.74	39,153	39,134	6.3
R202R0.25	100	1401.4	0.00	328.1	0.66	49,297	0.53	271,750	0.55	164,924	159,657	19.9
R202R0.5	100	1413.8	0.00	717.3	0.80	46,843	0.48	509,339	0.70	287,036	276,312	97.7
R202R0.75	100	1429.0	0.00	536.7	0.65	46,577	0.08	47,777	0.42	11,045	10,702	5.5
R203R0.25	100	1370.9	0.00	3170.2	0.20	71,920	0.16	6,924	0.16	4,439	4,016	1.1
R203R0.5	100	1372.8	0.00	7325.6	0.18	74,404	0.19	8,732	0.16	6,110	5,562	1.3
R203R0.75	100	1394.7	0.00	4790.6	0.37	75,209	0.31	58,451	0.30	29,005	26,767	4.8
R204R0.25	100	1330.2	1.40	10802.7	1.40	97,487	0.00	1,322,661	1.40	—	—	—
R204R0.5	100	1329.8	1.34	10802.1	1.34	98,010	0.00	1,434,749	1.34	—	—	—
R204R0.75	100	1346.6	1.49	10804.5	1.49	96,181	0.00	2,747,467	1.49	—	—	—
R205R0.25	100	1314.4	0.00	131.5	0.72	66,261	0.40	156,201	0.63	92,286	91,573	29.8
R205R0.5	100	1332.3	0.00	252.3	0.80	60,800	0.37	166,241	0.73	103,299	101,978	46.7
R205R0.75	100	1361.8	0.00	138.7	0.90	50,194	0.35	191,646	0.57	62,685	61,674	22.3
R206R0.25	100	1274.8	0.00	389.2	0.29	51,263	0.53	94,558	0.09	27,643	26,794	1.9
R206R0.5	100	1298.1	0.00	1729.6	0.63	52,354	0.14	77,991	0.38	20,258	19,740	8.4
R206R0.75	100	1323.5	0.00	2692.7	0.85	52,981	0.44	737,644	0.54	218,660	214,909	39.2
R207R0.25	100	1286.7	0.00	1065.8	0.74	75,247	0.04	151,917	0.71	87,358	83,256	147.7
R207R0.5	100	1297.3	0.00	1043.9	0.57	76,309	0.25	176,044	0.52	73,174	69,851	30.7
R207R0.75	100	1304.7	0.00	1318.6	0.46	75,193	0.00	21,376	0.32	5,367	5,066	2.4
R208R0.25	100	1253.1	0.00	3353.6	0.61	109,524	0.41	785,560	0.50	433,671	409,150	108.1
R208R0.5	100	1253.1	0.00	1350.9	0.67	95,356	0.17	341,918	0.50	107,435	100,799	96.1
R208R0.75	100	1254.4	0.65	10800.7	0.65	93,317	0.00	54,533	0.65	—	—	—
R209R0.25	100	1255.8	0.00	4755.0	1.22	74,961	0.56	3,171,692	1.01	1,887,015	1,869,963	3659.0
R209R0.5	100	1258.8	0.27	10800.5	1.35	65,820	0.51	3,728,123	1.12	2,149,937	2,132,452	9654.0
R209R0.75	100	1288.6	0.00	283.1	0.34	64,899	0.00	4,381	0.15	796	784	0.2
R210R0.25	100	1290.7	2.27	10816.4	2.27	69,147	0.00	10,671,062	2.27	—	—	—
R210R0.5	100	1283.7	0.00	1919.4	0.89	65,917	0.66	2,072,395	0.64	861,177	856,658	166.7
R210R0.75	100	1341.5	0.00	475.5	0.55	67,039	0.43	249,901	0.45	117,433	116,443	19.5
R211R0.25	100	1171.4	0.00	3008.6	0.77	88,733	1.14	8,066,475	0.47	3,915,814	3,822,646	70.8
R211R0.5	100	1189.9	2.19	5576.3	2.19	85,861	0.00	—	—	—	—	—
R211R0.75	100	1208.0	1.93	10807.7	1.93	73,930	0.00	5,421,206	1.93	—	—	—
RC201R0.25	100	1839.1	0.00	64.2	1.18	40,814	0.14	77,927	0.99	36,744	36,720	42.8
RC201R0.5	100	1849.6	0.00	22.7	0.62	35,505	0.57	45,825	0.47	25,465	25,447	2.7
RC201R0.75	100	1871.2	0.00	14.2	0.57	31,802	0.00	4,964	0.44	2,135	2,127	0.2
RC202R0.25	100	1790.8	0.00	36.9	0.58	45,940	0.25	21,160	0.53	15,939	15,712	3.2
RC202R0.5	100	1813.4	0.00	42.1	0.52	41,595	0.45	47,984	0.48	32,238	31,719	3.5
RC202R0.75	100	1841.7	0.00	97.1	1.00	43,995	0.36	117,829	0.90	72,484	71,107	37.1
RC203R0.25	100	1808.2	0.00	1569.4	0.64	64,977	0.00	34,893	0.38	7,830	7,391	2.1
RC203R0.5	100	1831.1	0.00	1757.8	0.73	60,133	0.31	242,962	0.49	103,747	97,792	27.9
RC203R0.75	100	1880.7	0.00	3743.4	0.89	65,187	0.41	761,811	0.60	264,045	249,054	89.9
RC204R0.25	100	1749.4	0.00	303.5	0.66	94,989	0.00	43,646	0.48	13,494	12,566	6.1
RC204R0.5	100	1749.4	0.00	212.8	0.71	94,916	0.00	54,750	0.48	12,747	11,875	5.9
RC204R0.75	100	1780.4	0.00	280.1	0.39	92,347	0.07	13,456	0.23	4,191	3,773	1.5
RC205R0.25	100	1760.4	0.00	67.5	0.90	54,942	0.49	168,679	0.69	76,214	75,702	17.9

Continued on next page

Table EC.9 – *Continued from previous page*

Name	n	UB	Gap%	T_{tol}	Step1		Step2	Step3	Step4	Step5	Step6	Step7
					LB_1%	$\|\mathcal{S}_1\|$	UB_1%	$\|\mathcal{S}_2\|$	LB_2%	$\|\mathcal{S}_3\|$	$\|\mathcal{U}_3\|$	CPU_7
RC205R0.5	100	1819.0	0.00	214.1	0.98	44,770	0.48	180,116	0.86	119,062	118,223	73.5
RC205R0.75	100	1877.8	0.00	43.6	0.81	39,477	0.24	43,644	0.62	19,924	19,591	11.6
RC206R0.25	100	1734.1	0.00	31.9	0.64	46,013	0.09	22,631	0.48	9,150	9,043	2.7
RC206R0.5	100	1746.9	0.00	45.7	0.80	44,664	0.27	64,752	0.61	29,537	29,102	9.2
RC206R0.75	100	1793.6	0.00	45.8	0.42	36,286	0.22	11,870	0.35	6,920	6,744	1.2
RC207R0.25	100	1694.4	0.00	9404.7	1.48	53,009	0.76	2,629,088	1.22	1,723,538	1,702,377	9013.7
RC207R0.5	100	1694.4	0.00	5561.5	1.44	57,294	0.81	2,626,179	1.21	1,698,146	1,682,745	4813.3
RC207R0.75	100	1780.4	0.00	235.0	0.57	50,920	0.38	56,757	0.42	31,779	31,399	5.5
RC208R0.25	100	1628.5	3.35	3788.0	3.35	89,134	0.00	—	—	—	—	—
RC208R0.5	100	1604.9	1.66	10802.0	1.85	89,052	0.29	5,145,328	1.66	3,398,663	3,338,812	7334.2
RC208R0.75	100	1620.1	0.16	10800.4	1.49	72,567	1.02	6,673,378	1.16	3,654,532	3,633,587	8324.2

EC.5.5. Detailed Results for the DRP on Machine 2

Table EC.10: Detailed Results for the DRP on Machine 2.

Name	n	UB	Gap%	CPU	Step1		Step2	Step3	Step4	Step5	Step6	Step7
					LB_1%	$\|\mathcal{S}_1\|$	UB_1%	$\|\mathcal{S}_2\|$	LB_2%	$\|\mathcal{S}_3\|$	$\|\mathcal{U}_3\|$	CPU_7
C201	70	1862.8	0.00	2.1	0.50	11,277	0.09	3,311	0.50	2,647	2,647	0.3
C202	70	1856.9	0.00	3.6	0.29	14,354	0.32	3,731	0.29	3,063	3,059	0.2
C203	70	1852.1	0.00	7.9	0.35	15,132	0.24	3,626	0.35	2,897	2,875	0.4
C204	70	1851.6	0.00	24.2	0.35	23,122	0.34	8,347	0.35	6,234	6,189	0.6
C205	70	1853.0	0.00	2.5	0.31	13,702	0.28	3,278	0.31	2,516	2,516	0.2
C206	70	1851.9	0.00	2.4	0.30	16,063	0.07	1,080	0.30	918	918	0.0
C207	70	1851.9	0.00	3.4	0.37	13,268	0.28	4,107	0.37	3,205	3,199	0.4
C208	70	1851.9	0.00	2.8	0.37	15,607	0.07	1,491	0.37	1,258	1,257	0.1
R201	70	1531.5	0.00	8.4	0.67	9,626	0.00	2,095	0.66	1,462	1,462	0.6
R202	70	1462.2	0.00	2.6	0.13	10,054	0.00	346	0.13	265	265	0.0
R203	70	1413.3	0.00	9.6	0.42	11,914	0.03	2,308	0.42	1,849	1,835	0.4
R204	70	1393.1	0.00	21.6	0.55	14,229	0.03	4,778	0.55	4,150	4,082	0.7
R205	70	1458.7	0.00	2.8	0.39	10,296	0.00	1,063	0.39	698	697	0.2
R206	70	1429.2	0.00	49.0	0.39	10,361	0.01	1,704	0.38	1,375	1,370	34.4
R207	70	1403.0	0.00	12.1	0.71	12,911	0.10	10,625	0.71	9,553	9,500	1.5
R208	70	1390.4	0.00	28.1	0.73	13,209	0.03	10,283	0.73	9,742	9,601	2.0
R209	70	1417.8	0.00	12.6	0.97	10,446	0.15	15,377	0.97	13,562	13,535	4.6
R210	70	1433.9	0.00	6.4	0.51	11,910	0.02	2,979	0.50	2,546	2,531	0.8
R211	70	1390.2	0.00	12.3	0.72	14,040	0.04	8,505	0.71	7,662	7,620	1.5
RC201	70	2328.5	0.00	52.7	1.28	4,405	0.00	3,292	1.28	3,237	3,236	34.4
RC202	70	2253.2	0.94	10802.4	0.94	5,292	0.16	3,961	0.94	3,669	3,645	10762.9
RC203	70	2227.5	0.00	5.4	0.72	6,753	0.05	3,701	0.72	3,566	3,527	0.5
RC204	70	2225.4	0.00	14.0	0.79	8,219	0.05	3,937	0.79	3,825	3,773	3.1
RC205	70	2270.7	0.00	430.0	0.86	5,452	0.05	3,058	0.86	2,900	2,888	423.9
RC206	70	2259.0	0.00	99.2	0.67	5,025	0.48	4,316	0.67	4,226	4,221	45.1
RC207	70	2233.0	0.00	6.0	0.88	6,040	0.13	4,551	0.88	4,485	4,459	1.3
RC208	70	2225.4	0.00	6.5	0.79	9,009	0.05	4,915	0.79	4,676	4,639	1.0
C201	80	2143.0	0.00	20.5	1.44	12,996	0.25	55,359	1.44	52,525	52,525	15.4
C202	80	2142.7	0.00	68.3	1.47	15,302	0.11	85,568	1.47	76,937	76,875	59.1
C203	80	2138.6	0.00	280.9	1.45	18,539	0.24	187,650	1.45	164,810	164,183	270.4
C204	80	2133.7	0.00	232.4	1.47	29,418	0.14	192,202	1.47	166,327	165,085	101.7
C205	80	2139.7	0.00	36.3	1.58	17,107	0.13	70,178	1.58	65,768	65,767	30.2
C206	80	2135.1	0.00	42.6	1.42	16,714	0.13	64,825	1.42	61,495	61,487	35.6
C207	80	2133.7	0.00	25.2	1.42	17,807	0.13	68,368	1.42	62,756	62,726	19.8
C208	80	2133.7	0.00	35.7	1.43	17,909	0.13	67,827	1.43	63,095	63,080	27.9
R201	80	1662.9	0.00	24.6	0.57	13,305	0.17	5,765	0.51	3,451	3,451	1.1
R202	80	1612.0	0.00	15.6	0.70	14,291	0.20	19,284	0.69	14,288	14,256	6.9
R203	80	1552.3	0.00	94.0	0.84	17,791	0.51	100,956	0.80	74,369	74,042	58.0
R204	80	1528.1	0.00	15.0	0.60	21,176	0.10	16,733	0.60	14,449	14,247	5.8
R205	80	1583.7	0.00	8.3	0.47	13,813	0.00	2,731	0.43	1,877	1,876	0.5
R206	80	1565.8	0.00	380.8	1.09	16,987	0.23	73,358	1.07	54,795	54,687	344.2
R207	80	1538.1	0.00	47.2	0.85	18,756	0.09	33,216	0.84	26,048	25,920	30.2
R208	80	1526.5	0.00	75.8	0.78	22,474	0.03	28,214	0.78	22,390	22,063	53.9

Continued on next page

Table EC.10 – *Continued from previous page*

Name	n	UB	Gap%	T_{tol}	Step1		Step2	Step3	Step4	Step5	Step6	Step7
					LB_1%	$\lvert\mathcal{S}_1\rvert$	UB_1%	$\lvert\mathcal{S}_2\rvert$	LB_2%	$\lvert\mathcal{S}_3\rvert$	$\lvert\mathcal{U}_3\rvert$	CPU_7
R209	80	1544.5	0.00	19.3	0.57	17,620	0.07	7,765	0.55	6,132	6,114	1.6
R210	80	1565.6	0.00	126.1	0.90	16,603	0.48	96,401	0.89	69,320	69,170	93.4
R211	80	1526.6	0.00	52.7	0.80	20,396	0.05	26,774	0.80	22,835	22,710	38.4
RC201	80	2610.4	0.00	37.3	1.16	5,863	0.29	9,218	1.16	8,753	8,751	7.5
RC202	80	2526.6	0.77	10802.2	0.77	6,599	0.11	5,053	0.77	4,187	4,164	10798.8
RC203	80	2505.5	0.00	9.8	0.74	9,880	0.10	7,042	0.74	5,626	5,569	1.6
RC204	80	2499.1	0.00	21.2	0.72	10,544	0.16	8,589	0.72	7,027	6,908	1.5
RC205	80	2549.9	0.00	48.9	1.23	6,497	0.27	12,813	1.23	11,476	11,443	5.0
RC206	80	2542.0	0.00	33.4	0.97	6,918	0.46	14,257	0.97	12,622	12,605	22.8
RC207	80	2511.0	0.00	113.2	0.87	8,405	0.25	13,435	0.87	10,533	10,484	30.7
RC208	80	2499.1	0.00	13.4	0.72	10,471	0.16	9,392	0.72	7,516	7,461	1.5
C201	100	2733.4	0.00	167.5	0.97	19,276	0.12	41,367	0.97	37,516	37,516	152.1
C202	100	2729.1	0.00	323.7	0.90	22,807	0.10	56,303	0.90	49,505	49,428	297.1
C203	100	2725.8	0.00	1471.7	0.92	29,514	0.07	91,041	0.92	77,389	76,963	1386.0
C204	100	2720.8	0.00	875.2	0.86	40,125	0.12	100,533	0.86	91,464	90,699	424.7
C205	100	2726.9	0.00	187.3	0.96	22,335	0.10	49,998	0.96	47,277	47,275	164.1
C206	100	2722.3	0.00	81.3	0.83	23,126	0.11	43,139	0.83	41,175	41,167	66.4
C207	100	2720.9	0.00	77.4	0.83	23,407	0.22	56,062	0.83	51,702	51,679	59.7
C208	100	2720.7	0.00	94.6	0.84	23,441	0.12	44,414	0.84	41,650	41,640	80.9
R201	100	1974.3	0.00	12.7	0.35	22,580	0.13	4,804	0.34	3,477	3,477	1.0
R202	100	1919.0	0.81	10802.1	0.82	27,670	0.50	266,325	0.81	223,279	222,936	10476.2
R203	100	1845.7	0.00	83.3	0.59	31,876	0.00	30,637	0.59	25,770	25,566	61.1
R204	100	1819.2	0.00	22.1	0.18	35,415	0.07	4,818	0.18	3,862	3,799	2.4
R205	100	1884.4	0.00	38.8	0.45	25,467	0.00	6,440	0.44	4,879	4,875	1.6
R206	100	1852.8	0.00	17.7	0.45	32,984	0.01	10,720	0.43	8,606	8,566	2.5
R207	100	1831.5	0.00	22.7	0.35	37,813	0.03	10,462	0.37	9,148	9,059	1.7
R208	100	1815.5	0.00	91.5	0.15	38,860	0.01	2,563	0.15	1,878	1,841	0.9
R209	100	1846.0	0.00	37.2	0.59	30,544	0.18	47,365	0.58	41,570	41,470	14.2
R210	100	1853.6	0.00	171.5	0.54	34,505	0.21	53,216	0.56	44,311	44,123	91.1
R211	100	1815.5	0.00	30.3	0.22	44,252	0.15	13,386	0.21	11,071	10,945	1.5
RC201	100	2961.9	0.81	10801.6	0.81	11,982	0.00	12,912	0.81	11,777	11,771	10688.0
RC202	100	2870.7	0.00	10321.1	0.44	14,349	0.42	31,575	0.44	27,327	27,205	10304.5
RC203	100	2853.0	0.00	13.8	0.48	19,787	0.01	10,644	0.48	9,326	9,224	3.5
RC204	100	2847.0	0.00	259.4	0.46	21,760	0.13	18,864	0.46	16,572	16,333	2.3
RC205	100	2898.2	0.00	60.6	0.55	15,302	0.09	10,700	0.56	9,640	9,604	12.0
RC206	100	2886.3	0.00	5427.7	0.42	15,346	0.21	11,046	0.41	9,554	9,543	5337.4
RC207	100	2854.6	0.00	101.5	0.46	16,473	0.13	11,154	0.46	9,438	9,390	2.6
RC208	100	2846.7	0.00	13.9	0.45	25,110	0.20	28,899	0.45	26,158	25,975	4.5